AMPK-Dependent Regulation of Lipid Metabolism in the *C. elegans* Dauer Larva

Meng Xie

Department of Biology, McGill University, Montréal

December 2013

A thesis submitted to McGill University in partial fulfilment of the requirements of the degree of PhD in Biology

Table of Contents

List of Tables and Figures

Chapter 1

Chapter 2

Abstract

Caenorhabditis elegans can enter an alternative dormant state called “dauer” to circumvent harsh environmental conditions. During this stage they cease their reproductive developmental program and food intake, while remaining fully viable and motile. During this stage increased levels of AMP-activated kinase (AMPK) blocks the exhaustion of the cellular energy depot by directly inhibiting a critical triglyceride lipase called ATGL-1. By performing a whole genome RNAi survey for genes that, when compromised, enhance the survival of AMPK mutant dauers I revealed that catalase genes were somehow involved in dauer survival in the mutants. I showed that increased hydrogen peroxide, to an optimal level, can alter both the abundance and the nature of the fatty acid content through HIF-1 transcription factor-dependent expression of several fatty acid biosynthetic enzymes. In addition, I showed that the AMPK-dependent phosphorylation of ATGL-1 not only signals its polyubiquitylation and subsequent proteasome-dependent degradation, but also generates a 14-3-3 binding site, which is recognized by PAR-5, the *C. elegans* 14-3-3 protein homologue. This association sequesters ATGL-1 away from cellular lipid droplets thereby reducing its accessibility to substrate. By studying the *C. elegans* CGI-58 protein, I provide evidence that in addition to its previously characterised role as a co-activator of ATGL in mammals, it also functions to maintain lipid droplet structure and prevents lipid exchange and fusion events among the lipid droplets. In summary, my work characterizes several regulators of the lipolysis pathway that can shed light on development of novel therapeutic treatments for diseases associated with abnormal lipid storage, hydrolysis or general homeostasis.

Résumé

Les *Caenorhabditis elegans* ont la capacité d'entrer dans une phase de dormance alternative appelée 'dauer', afin d'échapper à des conditions environnementales difficiles, pendant laquelle ils cessent de se développer et de se nourrir, tout en restant mobile, et accroissent leur capacité de résistance au stress, si bien qu'ils sont capables de vivre quatre fois plus longtemps que les animaux adultes normaux. Les animaux dont la signalisation des insuline est en danger entrent dans une phase 'dauer' à une température restrictive, où la proteine AMPK agit comme un interrupteur qui limite la délivrance du dépôt d'énergie en ralentissant directement l'ATGL, l'enzyme restraignant le taux de tout le processus de lipolyse. En uitlisant des RNA interférants pour realiser une étude du génome, à la recherche de gènes, qui, lorsqu'ils sont compromis, améliorent la survie des AMPK mutantes dormantes, je révèle que le péroxyde d'hydrogène, lorsqu'il est augmenté à un niveau optimal, peut modifier à la fois l'abondance et la nature de la teneur en acide gras, à travers l'expression de facteur de transcription HIF-1 dépendant de plusieurs enzymes clés impliquées dans la biosynthèse des acides gras. De plus, je démontre que la phosphorylation catalysée par l'AMPK de l'ATGL-1 signale non seulement sa poly-ubiquitination, suivie de sa dégradation liée aux protéasomes, mais génère également un site de liaison 14-3-3. Ce dernier est reconnu par PAR-5, la protéine homologue de 14-3-3 des *C. elegans*, qui éloigne l'ATGL-1 des goutelettes lipidiques cellulaires, et donc décroit sa possibilité de former un substrat. En étudiant la protéine CGI-58 des *C. elegans*, j'apporte la preuve qu'en plus de son rôle de co-activateur de la protéine ATGL, observé chez les mammifères, elle agit également pour maintenir une structure de gouttelettes lipidiques normale et empêcher tout échange de lipides et toute fusion entre les gouttelettes lipidiques. En résumé, mon travail met en lumière plusieurs régulateurs de l'action de lypolyse qui peuvent avoir des conséquences sur le développement de traitements thérapeutiques novateurs pour les maladies associées aux lipides.

Acknowledgements

First of all, I would like to thank my supervisor Dr. Richard Roy for bringing me from UK to Canada and guiding me into the world of worm biology. I not only learned a variety of experimental techniques, but also more importantly, the way to construct a scientific project, from initial proposal to final publication. I also really appreciate the opportunities he provided for me to participate into all kinds of scientific conferences and teaching activities, both of which potentiate my step forward into the world of science. Next, I would like to thank our lab manager Shaolin Li, who conducted most of my technical trainings and provided many useful suggestions to my projects. My PhD study would be 100 times harder without his support. Also, thanks to Dr. Patrick Narbonne who set up a solid base for my work so that I can further proceed smoothly. In addition, I would like to thank for the support from present and former lab members Dr. Yu Lu, Dr. Julie Mantovani, Dr. Emilie Demoinet, Christopher St-Francois, Abbas Ghazi and Emily Wendland. Thanks for the discussions and useful suggestions during the lab meetings with the Zetka lab members, especially Dr. Monique Zetka. Thanks to my supervisor committee members Dr. Christian Rocheleau and Dr. Russell Jones for the support and critiques during committee meetings and PhD qualify exam. Thanks to Dr. Elke Küster-Schöck for all the microscopy trainings. Thanks to Dr. Tamara Western for the usage of the GCMS instrument. Thanks to Julie Degans for the French translation of my abstract. Finally, I would like to express my sincere appreciation to all my family members who are always there, brothers and sisters who back me up all the time. Special thank to my girlfriend Wenwen Xu who will soon become family, without her I would not write this thesis at all.

Preface

This thesis is presented in accordance with the manuscript-based thesis guidelines. It consists of 4 chapters: a literature review (Chapter 1) that is divided into 5 subchapters to provide a thorough review of the relevant literature and states the rationale and objectives of the thesis; 2 chapters of research manuscripts (Chapter 2 and 3); and a discussion (Chapter 4). Chapter 2 has been published and Chapter 3 has been prepared for submission.

This thesis has been entirely written by the candidate in collaboration with the candidate's thesis supervisor.

This thesis has been written according to the "Guidelines for thesis preparation" from the Faculty of Graduate Studies and Research.

Contributions of Co-Authors

Chapter 2: This chapter has been accepted for publication in *Cell Metabolism* as follows:

Xie, M., and Roy, R. (2012). Increased levels of hydrogen peroxide induce a HIF-1-dependent modification of lipid metabolism in AMPK compromised C. elegans dauer larvae. Cell Metab. 16, 322-35.

I performed all the experiments and wrote the research article in collaboration with Dr. Richard Roy.

Chapter 3: This chapter is prepared to submit for publication to *Cell Metabolism* as follows:

Xie, M and Roy, R. CGI-58 Regulates Lipolysis in an ATGL-dependent and independent Manner in *C. elegans* Dauer Larvae

I performed all the experiments and wrote the research article in collaboration with Dr. Richard Roy.

Chapter 1: Literature Review

Chapter 1.1 General Introduction

Organisms have exploited almost every possible niche on the surface of the planet, ranging from lush tropical jungles and the main-land deserts to the depths of the oceans. To adapt to these diverse environments, many of which are severe and/or constantly changing, animals have had to evolve various means of ensuring that essential cellular processes so that growth and reproduction can proceed unhindered. One way to better understand how animals adjust these processes to adapt to environmental change is to use genetic analysis to interrogate gene function and their role(s) in regulating pathways required for any observed adaptation.

The genetic pathways that are involved in the various modes of adaptation to environmental stress can be dissected by characterizing the genes that are affected in mutants that arise in simple unicellular microorganisms such as yeast, to complex multicellular organisms like mammals. It is the identification and characterization of these gene activities that can provide a framework to better comprehend how genes work together to mediate environmental adaptation at the molecular and genetic level.

Environmental Changes and Metabolic Adaptation

Most organisms have little to no control over the environments into which they are born. Therefore they need to adjust their behaviour and physiology accordingly in response to the challenges posed by their surroundings. When vital environmental parameters like food, water and oxygen availability, sunlight exposure, population density and temperature range are altered to the extreme, failure of adaptation can result in species extinction. To avoid being eliminated, organisms have evolved changes in behaviour and physiology adjusted to compensate for these extremes.

Many animals have evolved an extended dormant state such as hibernation characterized by both behavioral and metabolic changes that provide a means to circumvent periods of dramatic temperature fluctuation. To prepare for this period of dormancy, they stimulate their feeding behaviour to consume a large amount of food, which is subsequently converted to the form of fat deposits via a series of metabolic

reactions. During hibernation, animals reduce their movements and metabolic activities to a minimum level, accompanied by a number of energy-conserving physiological responses including blood vessel constriction, reduced respiratory rate and core body temperature cooling. It is worth mentioning that the hibernation period is not employed by all animals to accommodate to environmental temperature fluctuations, possibly due to more evolved adaptative strategies that leave animals less vulnerable to temperature variations and predation (Geiser, 2013).

In the desert, food and water sources are only available occasionally. To overcome such long-term nutrient scarcity, desert animals like camels have evolved both behavioural and anatomical adaptations to be able to consume large amounts of food and water at one time. In addition, they metabolically convert the extra nutrients into triglyceride molecules that are subsequently packed into reservoir fatty tissues to provide them with a long-term energy supply.

In some species of nematodes, dramatic increases in population density after hatching can cause the animals to liberate a pheromone that induces them to enter a hibernation-like dormant state called the dauer larvae to preserve their energy for long-term usage. To escape from certain predators some species of the Cicada family have developed an extended 17-year life cycle, most of which is spent in the form of underground nymph diapauses only to emerge after this cycle to reproduce and die shortly thereafter.

Most metabolic readjustments that occur in response to food/nutrient deprivation are associated with an increase of fat/lipid stores, while the evolution of adipose tissue was probably provided a selective advantage to organisms that experience these types of environmental challenges on a cycle basis. Therefore, lipids and the enzymes that regulate biosynthesis and storage have evolved as key molecules that provide animals with some metabolic flexibility, allowing animals to respond to an environmental challenge such as nutrient deprivation by mobilizing these stores of energy in an attempt to adjust to the environmental stress. Their regulation has become the primary targets of several studies to better understand metabolic adaptation through our

analysis of how these energy storage molecules can be stockpiled and mobilized and, of particular importance, how they are controlled.

C. elegans as a Model Organism for Metabolic Adaptation to Environmental Changes

Caenorhabditis elegans is a free-living and transparent multicellular eukaryotic organism that can be easily and economically cultured and frozen for long term storage under laboratory conditions. *C. elegans* possesses a transparent cuticle which facilitates the visualization of various cellular processes and cellular structures both with and without chemical and/or antibody staining (Horvitz and Sulston, 1980; Sulston et al., 1983). In addition, the relatively short generation time and easily amenable genome make it an excellent model organism for unbiased large-scale screening and genetic analysis. Genetic mapping has identified a number of key regulatory genes involved in various cellular processes, including numerous signal transduction pathways, the RNAi and mRNA pathways and even the neurobiological basis of certain behaviours and aging (Greenwald, 1998; Khavaria and Rinn, 2007). Moreover, gene function can be disrupted using RNA interference (RNAi) providing an efficient means of performing reverse genetic analyses (Fire et al., 1998). Finally, the use of various fluorescent tags enables the labelling of specific proteins, cellular organelles or cell types to facilitate cell biological and biochemical analysis of various cellular processes (Chalfie et al., 1994).

C. elegans has been used efficiently to study lipid metabolism and it offers a number of advantages that complement the studies performed with other model organisms in several important ways. There is growing evidence that demonstrates that many signaling pathways that are important in regulating lipid metabolism in mammals are also critical in *C. elegans*, particularly the insulin signaling pathway which controls numerous physiological processes in both mammals and *C. elegans* (Kimura et al., 1997). In addition, many of the proteins that are involved in the process of lipogenesis, lipolysis and lipid transport are conserved among all eukaryotes from *C. elegans* to mammals. *C. elegans* use the same set of lipases to initiate the breakdown of

triglyceride molecules trapped in lipid droplets, which are the major storage form and site for surplus energy (Wang et al., 2008; Narbonne and Roy, 2009). Regulation of lipid storage and usage is also dependent on conserved pathways and key proteins, including regulation by the AMP-activated kinase (AMPK), target of rapamycin (TOR) kinase, sterol response element binding protein (SREBP) and CCAAT/enhancer binding protein (C/EBP) transcription factors (Long et al., 2002; McKay et al., 2003; Apfeld et al., 2004; Jia et al., 2004; Yang et al., 2006). Despite a much simpler body structure, *C. elegans* possesses its own lipid transport machinery. One well-characterized example of this machinery is the low-density lipoprotein (LDL) family receptor responsible for lipid shuffling between intestinal cells and oocytes (Grant and Hirsh, 1999). Other behaviors like feeding rate, progeny production rate and locomotion are all altered in response to food availability. These could be used as standard phenotypes to investigate gene functions that mediate feeding behavior (Tecott et al., 1995; Sawin et al., 2000). In addition, the relatively simple nervous system of *C. elegans* with only 302 neurons allows researchers to functionally dissect the neural circuits that are responsible for the maintenance of energy homeostasis. The roles of serotonin and TGF-β signals on the neuronal regulation of fat storage, fat metabolism and feeding rates have been extensively studied in *C. elegans* to complement their known functions in mammals and to establish a broader understanding of energy homeostasis (Greer et al., 2008; Srinivasan et al., 2008).

Methods for examining fat storage and metabolism have evolved rapidly in the last decade. Sudan Black, a lipophilic dye, was among the first stains used to label intracellular fat, initially in bacteria (Burdon et al., 1942). It was employed in *C. elegans* studies to aid visual assessment of body fat in fixed animals expressing a defective insulin receptor ortholog DAF-2 (Kimura et al., 1997). Sudan Black staining was mainly localized to the intestine and hypodermis, indicating the major fat storage organs in *C. elegans*. One major drawback of Sudan Black staining is that the requirement of the fixation step makes it unsuitable for high-throughput screening of novel genes (Kimura et al., 1997; Ogg et al., 1997; Jia et al., 2004). Some attempts to stain fat stores with fluorescent dyes like LipidTOX were subject to the similar limitations due to the obligatory fixation process. To assess fat storage in live intact animals, dyes like Nile

Red and fatty acid-conjugated BODIPY were introduced as alternatives (Ashrafi et al., 2003). Nile Red and BODIPY were initially used in mammalian cells to label intracellular lipid droplets and monitor fatty acid intake respectively (Greenspan et al., 1985; Schaffer and Lodish, 1994). In *C. elegans*, both dyes can be incorporated in the *E. coli* diet and ingested by the animals while feeding. The dyes are eventually absorbed through the intestinal epithelium and accumulate in intestinal cells. Nile Red was initially used in a genome-wide RNAi screen for genes involved in regulation of fat storage in *C. elegans* (Ashrafi et al., 2003). A recent study revealed that Nile Red also stained acidified cellular compartments or lysosome-related organelles (LROs), which are distinct from the major fat storage compartments in *C. elegans* (O'Rourke et al., 2009). Since then, Oil Red O staining has become the method of choice to assess major fat stores using biochemical assays (O'Rourke et al., 2009). BODIPY-conjugated fatty acids have also been shown to share a similar staining pattern as Nile Red in *C. elegans* by the same group (O'Rourke et al., 2009), while a later study demonstrated that BODIPY labelled both lipid droplets and LROs, where the former demonstrated a weaker fluorescence intensity (Zhang et al., 2010). Development of label-free lipid imaging techniques is also progressing to meet the continual demand for identification of fat storage compartments in live animals. Coherent anti-Strokes Raman Scattering (CARS) and Stimulated Raman Scattering (SRS) microscopy techniques were initially developed in mammalian cells to detect lipid droplets based on C-H bond vibration in lipids (Nan et al., 2003; Freudiger et al., 2008), and was subsequently used in *C. elegans* to visualize fat storage compartments (Yen et al., 2010; Hellerer et al., 2007; Le et al., 2010; Wang et al., 2011). With the aid of SRS microscopy, 9 new regulators of fat content in *C. elegans* were identified in an RNAi survey (Wang et al., 2011). In addition, CARS has also been used to detect the abundance of unsaturated fatty acids in *C. elegans* by monitoring the vibrations of C=C double bonds (Le et al., 2010; Rinia et al., 2008). Despite of all these practical applications of CARS and SRS, a verification step with fluorescent markers is still necessary to confirm that the structures detected by these label-free techniques are indeed lipid droplets in *C. elegans*.

Metabolic Adaptation to Environmental Stress in *C. elegans*

Temperature: *C. elegans* belongs to the family of ectotherms, whose body temperature is largely dependent on external heat sources to accomplish an optimal metabolic rate. Within an acceptable physiological temperature range, their metabolic rate is proportional to the environmental temperature, owing to increased enzyme activity that leads to elevated reaction rates (Klass, 1977; Van Voorhies and Ward, 1999). This is illustrated by the increased activity of lactate dehydrogenase and production of lactate, when shifting the animals from 10°C to 20°C (Paul et al., 2000; Föll et al., 1999). More complex processes such as embryonic development and feeding behaviours are determined also affected by the environmental temperature. *Clk* mutants exhibit slowed development and behaviour and fail to coordinate these processes with environmental temperature variation, suggesting that deviation from the live biological clock phase, developmental and behavioural processes might be maintained independent of external temperature, possibly due to the existence of some compensating mechanisms (Wong et al., 1995; Branicky et al., 2001). Temperature has also been shown to be a critical environmental cue that influences dauer decision at L1 larva stage. Temperature-upshift at the L1 molt enhanced the percentage of dauer larvae formation in response to pheromone induction, possibly due to the elevated enzyme activity (Golden and Riddle, 1984a; Golden and Riddle, 1984b).

Food Restriction: Like in many organisms, dietary restriction can substantially increase the life span of *C. elegans* by reducing metabolic rate and consequently decreasing the generation of reactive oxygen species (ROS) (Sohal and Weindruch, 1996). At the molecular level, the transcription factors PHA-4 and SKN-1 were shown to be responsible for this lifespan-extension. PHA-4 stimulates the expression of several superoxide dismutase genes that clear up the excessive ROS produced mainly by the mitochondrial electron transport chain in a dietary restriction specific manner (Panowski et al., 2007). Although the TOR signaling and autophagy pathways were shown to be active downstream of PHA-4, the exact underlying mechanism is still largely unknown (Vellai et al., 2003; Jia and Levine, 2007; Hansen et al., 2008). SKN-1 expressed in the two ASI head neurons was shown to detect dietary restriction and propagate the signals

to the peripheral tissues to increase metabolic rate in a cell non-autonomous fashion (Bishop and Guarente, 2007). Food restriction can also affect the developmental program of *C. elegans* larvae. When hatching in the absence or in limited food source, *C .elegans* arrest at L1 larva stage and are able to survive for two weeks accompanied with a lowered metabolism rate (Lee et al., 2012).

Oxygen Level: Unlike most organisms that expire during hyperoxic conditions, *C. elegans* can tolerate up to a 100% oxygen level with minimal changes in metabolic rate for at least 50 generations (Van Voorhies and Ward, 2000). Genes encoding complexes in the mitochondrial electron transport chain were shown to affect the animals' sensitivity to hyperoxic conditions (Senoo-Matsuda et al., 2001; Kondo et al., 2005). Moreover, *C. elegans* can also develop increased tolerance to anoxic conditions. In the absence of oxygen, 90% of *C. elegans* can survive by consuming most of their carbohydrate stocks (Föll et al., 1999). The transcription factor hypoxia inducing factor-1 (HIF-1) was found to be critical for the survival of *C. elegans* at low oxygen conditions, as *hif-1* mutants failed to adapt to 0.5-1% oxygen level (Shen and Powell-Coffman, 2003). At normoxic condition, HIF-1 proteins are hydroxylated by HIF prolyl-hydroxylases, ubiquitinated by the Von Hippel-Lindau (VHL) tumor suppressor protein and targeted for rapid proteasomal degradation. When environmental oxygen is low, HIF prolyl-hydroxylase activity is inhibited due to loss of its co-substrate, oxygen. Without the hydroxylation, HIF-1 can accumulate and stimulate expression of several genes required to enhance survival during low oxygen conditions, including glycolytic enzymes and vascular endothelial growth factors (Shen and Powell-Coffman, 2003).

Osmotic Stress: The excretory system of *C. elegans* consists of pore cells, duct cells, excretory cells and excretory gland cells. One major function of the system is to maintain osmoregulation in the animal, more or less like a kidney (Nelson and Riddle, 1984). Normally, wild type animals can adapt up to 0.5M NaCl media by switching on the glycerol 3-phosphate dehydrogenase gene to accumulate cellular glycerol level with a yet unknown biochemical mechanism (Lamitina et al., 2004; Lamitina et al., 2006; Lamitina and Strange, 2005). Genetic inhibition of genes involved in the insulin-like signaling pathway, like *daf-2*, *age-1* and *daf-16*, was shown to significantly improve the

animals' resistance to hypertonic solutions up to 400mM (Lamitina and Strange, 2005). Similarly, the osmotic resistance in *daf-2* mutant dauer larvae is further increased compared to adults with the same genetic background (Narbonne and Roy, 2009). The α2 subunit of AMPK was shown to have a unique role in maintaining osmoregulation of older dauers by protecting their lipid storage from depletion (Narbonne and Roy, 2009). In the absence of AMPK, rapid exhaustion of the triglyceride resources leads to failure of the osmoregulatory organ functions reflected by lower survival rate at high molarity solutions. Such failure is considered as the ultimate cause of the early expiration of AMPK mutant dauer larvae.

Dauer Metabolism

The dauer stage of *C. elegans* was described in 1975 by Cassada and Russell, describing an alternative developmental stage, in parallel to the third stage larva. The dauer decision is triggered by crowding and potentiated by environmental stresses, such as high heat and nutrient scarcity, where the larval development arrests before sexual maturity (Cassada and Russell, 1975). These modified L3 stage larvae have a number of distinct characters: they stop feeding; they are completely sealed both at the mouth and the anus; their cuticle is thickened rendering them resistant to some harsh chemicals; they are motionless most of the time, while the mechanosensory system is still functional enabling rapid movement upon touching; and they are more resistant to environmental stresses than normal L3 animals (Cassada and Russell, 1975; Riddle and Albert, 1997). These distinct characteristics are associated with or responsible for an extended dauer larvae lifespan of several months, compared to the normal adult lifespan of 14 days. Since the animals stop feeding once they enter the dauer stage, they rely solely on internal energy stores, mainly in the form of triglycerides, which accumulate in their intestinal and hypodermal cells during the prolonged L2d stage (Riddle and Albert, 1997). To limit energy expenditure, their metabolic and energy-consuming activities are suppressed, which would explain why they remain motionless most of the time. Experimental evidence demonstrated that dauer larvae consumed less oxygen and produced less heat as a result of reduced activities of the enzymes involved

in various metabolic processes (O'Riordan and Burnell, 1989; Vanfleteren and De Vreese, 1996; Houthoofd et al., 2002). However, transcription of enzymes involved in fatty acid β-oxidation, glycolysis and the glyoxylate cycle was shown to be enhanced in dauer larvae indicating that these larvae have a more active conversion process of triglyceride to glucose, which further establishes the role of triglyceride as the main energy storage molecule in the dauer (Wang and Kim, 2003; McElwee et al., 2004; McElwee et al., 2006; Jones et al., 2001; Holt and Riddle, 2003). Such a lipid to sugar conversion process may also facilitate the transfer of energy from lipid-containing cells, mainly the intestinal and hypodermal cells, into other tissues (Ogg et al., 1997). *C. elegans* dauer larvae have a functional glyoxylate cycle, which is commonly present in plants and bacteria, but not in animals. It provides an alternative anabolic pathway to the citric acid cycle that utilizes similar enzymes as the citric acid cycle to convert the 2-carbon acetyl-CoA derived from the fatty acid β-oxidation process into 4-carbon succinate and malate molecules for the biosynthesis of carbohydrates (Kondrashov et al., 2006). Therefore, the net production of the glyoxylate cycle is from fatty acids to glucose, which correlates well with the energy supply mechanism of the dauer larvae. The level of the enzyme phosphoenolpyruvate-carboxykinase (PEPCK) that catalyzes the rate-limiting step of the gluconeogenesis process was also found to be elevated in dauers, indicating that the starved dauer larvae uses gluconeogenic like pathways to obtain glucose from the non-carbohydrate carbon substrates, such as pyruvate and glycerol, in addition to using lipid as the major source (O'Riordan and Burnell, 1989).

Serial analysis of gene expression (SAGE) and DNA microarray assays also showed that expression of genes involved in several anaerobic processes were upregulated, including malate dismutation and fermentation pathways (Jones et al., 2001; Holt and Riddle, 2003; Wang and Kim, 2003). The malate dismutation process provides the mitochondria with an anaerobic means of generating energy using a specialised electron transport chain. It has been postulated that the access to available oxygen is limited within the interior of the dauer intestine, very likely due to the sealed alimentary canal and relatively impermeable cuticle (Holt and Riddle, 2003). To accommodate such oxygen limitation, mitochondria of the inner intestine may switch from aerobic metabolism to anaerobic metabolic processes such as malate dismutation, and

transport the resulting products to the peripheral tissues for aerobic metabolism. Although dauer larvae are more resistant to hypoxic stress than adults or any other larva stages, they require a certain amount of absolute oxidative metabolism to efficiently utilize the energy store as they were unable to survive for more than 24 hours in the complete absence of oxygen (Burnell et al., 2005).

In dauer larvae, the enzymes that are involved in protecting the organism from reactive oxygen species (ROS), like superoxide dismutases (SOD) and catalases, were found to be elevated at both the transcriptional and protein activity levels (Vanfleteren and De Vreese, 1996, Houthoofd et al., 2002, Jones et al., 2001, Wang and Kim, 2003). ROS are produced from complexes I and III of the electron transport chain of aerobically functioning mitochondria during ATP generation. It has been postulated that low aerobic metabolism and increased SOD and catalase level are combined to protect the dauer larvae from ROS damage and contribute to their long-term survival (Burnell et al., 2005).

Other *C. elegans* Diapauses

C. elegans larvae can undergo at least two other types of diapause to adjust to nutrient deprivation. When hatched under conditions of starvation, instead of executing the postembryonic development program, emergent L1 larvae arrest their development at the L1 stage where they can survive for about 2 weeks in a quiescent state. Animals exit this quiescent state and resume their regular developmental program as soon as an appropriate food source becomes available. Nutrient ingestion activates an ATPase called ASNA-1 to induce insulin secretion in insulin-producing intestinal cells which in turn activates the insulin-like signaling pathway, resulting in suppression of the DAF-16/FOXO transcription factor activity (Kao et al., 2007; Baugh and Sternberg, 2006). When DAF-16 is in the nucleus, it activates the transcription of a cyclin-dependant kinase inhibitor called *cki-1* that leads to cell cycle arrest (Hong et al., 1998; Baugh and Sternberg, 2006).

Another instance of diapause-like behaviour occurs when *C. elegans* are isolated from their food source at the L4 larval stage. These animals will execute the adult

reproductive diapause, where they halt their somatic and germline development, while leaving the proliferative zone cells in complete arrest. Once placed onto food, the animals are able to resume germ cell proliferation, meiotic development, oogenesis and become fertile without obvious consequences (Pazdernik and Schedl, 2013).

Chapter 1.2 Signaling Pathways that Regulate Dauer Arrest

Past studies on genes that regulate Dauer formation revealed two classes of mutations: dauer-constitutive (Daf-c) and dauer-defective (Daf-d) genes. Characterization of these genes have revealed three distinct and evolutionarily conserved pathways that regulate this developmental decision. These include insulin/IGF-1 signaling (IIS), TGFβ-like, and guanylyl cyclase signaling pathways, all of which converge on a steroid hormone pathway where the decision to execute dauer is made (Gerisch et al., 2001; Gottlieb and Ruvkun, 1994; Jia et al., 2002; Riddle et al., 1981; Thomas et al., 1993; Vowels and Thomas, 1992; Birnby et al., 2000; Kimura et al., 1997).

Insulin/IGF-1 Signaling Pathway

Influence of the IIS pathway on dauer formation was originally defined by the Daf-c genes *daf-2* and *daf-23*/*age-1* and the Daf-d gene *daf-16* (Gottlieb and Ruvkun, 1994; Murphy et al., 2003). Unlike other Daf-c mutations, strong mutant alleles of *daf-2* exhibit irreversible non-conditional dauer arrest coupled with uncoordinated fat storage, extended reproductive periods and reduced brood size (Ogg et al., 1997; Gems et al., 1998; Morris et al., 1996). Under favorable conditions, a conserved IIS pathway that prevent the animals from dauer entry was defined through activation of the DAF-2/insulin receptor (InR) homolog by binding of the secreted insulin-like peptides that leads to sequential activation of several kinases, including AGE-1/phosphoinositide 3-kinase (PI3K), 3-phosphoinositide-dependent kinase 1 (PDK-1), AKT-1 and AKT-2 (Kimura et al., 1997; Morris et al., 1996; Paradis et al., 1999; Paradis and Ruvkun, 1998). The activated AKT-1 protein kinase inhibits the FOXO transcription factor DAF-16 through direct phosphorylation, preventing it from entering the nucleus to activate the transcription of certain genes that signal dauer entry (Hertweck et al., 2004; Lee et al., 2001; Lin et al., 1997; Lin et al., 2001; Ogg et al., 1997). Such cytoplasmic retention of DAF-16 was also regulated by the two 14-3-3 proteins PAR-5 and FTT-2 in *C. elegans* to establish reproductive growth and a normal life span (Berdichevsky et al., 2006; Li et al., 2007a). Conversely, under unfavorable conditions, the IIS pathway is not activated,

leading to import of DAF-16 into the nucleus where it activates the transcription of genes that affect stress resistance, dauer formation and longevity. In addition, regulation of DAF-16 by the insulin-like pathway is affected by DAF-18, the *C. elegans* ortholog of the phosphoinositide 3-phosphatase PTEN, by antagonizing AGE-1/PI3K (Gil et al., 1999; Mihaylova et al., 1999; Ogg and Ruvkun, 1998; Rouault et al., 1999). The DAF-16 proteins that remain in the cytoplasm are ubiquitinated by the E3 ubiquitin ligase RLE-1 and targeted for proteasomal degradation (Li et al., 2007b).

In addition to the IIS pathway, other inputs may impinge upon DAF-16. These include c-Jun N-terminal kinase (JNK) (Oh et al., 2005), mitogen-activated protein kinase (MAPK) (Nanji et al., 2005; Troemel et al., 2006) and AMP-activated protein kinase (AMPK) (Apfeld et al., 2004; Greer et al., 2007). These kinases exert their input on DAF-16 via various mechanisms: JNK modulates DAF-16 nuclear translocation; MAPK does not act on DAF-16 directly but mediates expression of secreted immune response genes to promote immunity in parallel to the IIS pathway; AMPK regulates DAF-16 through direct phosphorylation (Apfeld et al., 2004; Greer et al., 2007). Moreover, various nuclear complexes were also shown to modulate distinct aspects of DAF-16 function, including heat shock factor (HSF-1) (Hsu et al., 2003), β-catenin (BAR-1) (Essers et al., 2005), the Sirtuin protein deacetylase (SIR-2.1) (Berdichevsky et al., 2006), SMK-1 nuclear co-regulator (Wolff et al., 2006) and the DAF-12 nuclear receptor (Berman and Kenyon, 2006).

In addition to the Daf-c phenotype, the IIS pathway is also well-known for its influence on life span in *C. elegans*. Mutants of the insulin/IGF receptor homolog *daf-2* live twice as long as the wild type adults (Kenyon et al., 1993), accompanied with increased resistance to all forms of stress (Lithgow and Walker 2002; Garsin et al., 2003). Life span extension was also observed in *Drosophila* mutated for the insulin receptor ortholog or its substrate protein (Clancy et al., 2001; Tatar et al., 2001) and in mice with compromised IGF-1 receptor (Holzenberger et al., 2003), indicating that the impact of IIS on life span is evolutionarily conserved. Both phenotypes were initially suggested to be regulated primarily in the neuron by DAF-2 (Apfeld and Kenyon, 1998; Wolkow et al., 2000). However, similar studies on the major target of the insulin-like pathway, DAF-16,

suggested that the two phenotypes were differentially regulated in distinct tissues. In neurons, DAF-16 is more involved in the regulation of the Daf-c phenotype (Apfeld and Kenyon, 1998; Alcedo and Kenyon, 2004), while expression of DAF-16 in the intestine could fully rescue the reduced longevity seen in *daf-16(-)* germline-efficient animals and increase the life span of insulin-like pathway mutants (Libina et al., 2003). In addition to the spatial specificity, the insulin-like signaling also exhibits temporal specificity as it was shown to regulate dauer arrest with minimal impact on life span during larval development, while it mainly regulates longevity during adulthood (Dillin et al., 2002).

Bioinformatic analysis predicted 37 insulin-like peptides (ILPs) in the *C. elegans* genome (Pierce et al., 2001), although only a subset have been assigned for distinct functional roles. Some act as receptor agonists, such as INS-7; while others act as receptor antagonists, like INS-1. Despite the potential functional redundancy, there is evidence showing that the *ins* genes are involved in regulating dauer arrest. Overexpression of the gene that most resembles human insulin, *ins-1*, in either wild-type or *daf-2* mutant animals results in an enhancement of the dauer arrest phenotype, indicating a potential antagonizing mechanism between *ins-1* and *daf-2* signaling. Although the exact mechanism is still unclear, not all INS family members are involved in regulating dauer arrest. Overexpression of *ins-18* enhanced dauer arrest, but not *ins-9*, *ins-19*, *ins-22* or *ins-31*. This could be explained structurally as INS-1 and INS-18 are the only INS family members that contain C-peptides that are derived from normal insulin release from the β cells. Many of the INS family proteins are expressed in the largest chemosensory organs, the amphid neurons, indicating that the external dauer inducing factors could regulate the expression and/or secretion of insulins (Pierce et al., 2001). Importantly, one of the antagonizing ILPs, DAF-28 was shown to be transcriptionally inhibited by dauer pheromone and food deprivation, indicating regulation by neuronal sensing of environmental cues (Li et al., 2003). In addition, synaptic proteins such as UNC-64/syntaxin, UNC-31/CAPS and ASNA-1/ATPase were also shown to be involved in modulating ILP release, which further impinges on neuronal regulation on the IIS pathway (Ailion et al., 1999; Munoz and Riddle, 2003; Kao et al., 2007).

External stress was shown to induce nuclear translocation of DAF-16 in wild-type adults to adapt to changing environmental conditions (Henderson and Johnson, 2001; Lee et al., 2001; Lin et al., 2001). Microarray analysis of *daf-2* and *daf-2; daf-16* double mutants revealed that DAF-16 promotes the expression of genes involved in a wide range of physiological responses, including metabolism, energy generation and cellular stress responses (McElwee et al., 2003). On the other hand, genes involved in growth and reproduction, such as Target-of-rapamycin (TOR) serine/threonine protein kinase pathway components, are repressed presumably to conserve energy (Jia et al., 2004). TOR is also a downstream target of the insulin/DAF-2 signaling pathway, which has been shown to be involved in promoting reproductive development in *C. elegans* by regulating mRNA translation (Jia et al., 2004). *let-363* and *daf-15* encode TOR and its binding partner Raptor respectively in *C. elegans*. Unlike mutants in components of the insulin-like signaling pathway that arrest as complete dauers, *let-363* and *daf-15* mutants arrest as dauer-like larvae without complete dauer morphogenesis (Jia et al., 2004). These phenotypes are epistatic to *daf-16* loss-of-function Daf-d mutations, indicating that *let-363* and *daf-15* most likely act downstream of *daf-16* to regulate dauer arrest.

There is genetic evidence that suggests that AGE-1/PI3K is not the only output of the IIS pathway. Gain-of-function mutations of *akt-1* and *pdk-1* and loss-of–function mutations of *daf-18* were shown to only suppress the dauer arrest phenotype in *age-1* mutant, but not in *daf-2* mutants (Inoue and Thomas, 2000a; Paradis et al., 1999; Paradis and Ruvkun, 1998; Gil et al., 1999; Gottlieb and Ruvkun, 1994; Ogg and Ruvkun, 1998; Vowels and Thomas, 1992). Moreover, nuclear localization of DAF-16 by inactivation of either the upstream AKT-1 or the 14-3-3 protein homolog FTT-2 was not sufficient to improve stress response or extend life span unless *daf-2* was also compromised (Berdichevsky et al., 2006; Hertweck et al., 2004; Lin et al., 2001). These results suggest the existence of alternative outputs independent of the AKT pathway from DAF-2 to DAF-16. For example, three enhancers of the *akt*-1 mutant (*ea*k) genes were identified in a genetic screen designed to identify mutants that enhance the dauer arrest phenotype in an *akt-1* null mutant background, which function in parallel to AKT-1 to inhibit DAF-16 action (Hu et al., 2006).

TGF-β-like Signaling Pathway

The TGF-β-like pathway is one of the major paracrine pathways that regulate dauer formation and is defined by the Daf-c genes *daf-1*, *daf-4*, *daf-7*, *daf-8* and *daf-14*; and the Daf-d genes *daf-3* and *daf-5* (Patterson and Padgett, 2000; Thomas et al., 1993). These genes comprise the core components of the TGF-β pathway: TGF-β ligand/DAF-7 binds and activates heteromeric type I and II serine/threonine kinase TGF-β receptors/DAF-1 and DAF-4 at the cell surface, leading to the phosphorylation activation of SMAD transcription factors/DAF-3, DAF-8 and DAF-14 that translocate into the nucleus to regulate gene transcription (Ren et al., 1996; Georgi et al., 1990; Estevez et al., 1993; Inoue and Thomas, 2000b; Patterson et al., 1997). *daf-5* encodes a SNO/SKI transcription factor that physically interacts with DAF-3/SMAD in the neuron to regulate dauer development (Da Graca et al., 2004; Tewari et al., 2004). Similar to the role of SMADs in mammal as downstream effectors of the TGF-β pathway, DAF-8 and DAF-14 are required for DAF-7-mediated dauer arrest (Inoue and Thomas, 2000b). Conversely, initial genetic analysis of the other SMAD family member, DAF-3 suggested an antagonistic effect of DAF-3 on the TGF-β signaling pathway (Patterson et al., 1997). DAF-3 activity is also affected by temperature as *daf-3* loss-of-function mutants are dauer defective at 25°C, while they enter dauer constitutively at 27°C (Thomas et al., 1993; Ailion and Thomas, 2000). In addition, DAF-3 exerts differential regulation of Daf-c genes: *daf-3* mutation suppressed dauer arrest in *daf-1*, *daf-4*, *daf-7*, *daf-8* and *daf-14* mutants (Thomas et al., 1993), while it enhances the weak dauer arrest phenotype of *sdf-9* mutants (Ohkura et al., 2003). Therefore DAF-3 can either induce or block dauer arrest depending on the environment and the genetic background, although the exact mechanism through which it exerts these effects is still unclear.

A GFP reporter driven by the *daf-7* promoter was expressed solely in the ASI neurosensory cells (Ren et al., 1996), while the downstream TGF-β receptors and SMAD transcription factors are ubiquitously expressed (Patterson et al. 1997; Gunther et al., 2000; Inoue and Thomas, 2000b; Da Graca et al., 2004), indicating a signal cascade of the TGF-β pathway propagating from the ASI neuron to the entire animal. Consistent with the expression pattern of DAF-7, genetic studies showed that DAF-7

regulation of reproductive growth is dependent on external cues such as food availability, temperature and dauer pheromone, indicating clear coupling between neurons and environmental signals (Ren et al., 1996; Schackwitz et al., 1996). Data from *C. elegans* and other systems are consistent with a model of DAF-7 expression being controlled by distinct environmental cues that couple the signal from the ASI neurons to alter metabolism and larval development (Da Graca et al., 2004). In favorable conditions, high levels of DAF-7 are secreted from the ASI neuron to peripheral tissues and activate DAF-1/4 receptor kinases to phosphorylate DAF-8/14 SMAD transcription factors, resulting in inhibition of DAF-3/SMAD and promote the transcription of genes involved in energy utilization and reproductive growth. In unfavorable conditions, less DAF-7 is produced in the ASI neuron; and the inhibition on DAF-3/SMAD is relieved, leading to transcriptional activation of genes for energy storage and dauer specification (Da Graca et al., 2004; reviewed by Fielenbach and Antebi, 2008).

Microarray analysis of gene expression profiles of L2/L3 wild-type larvae and *daf-7* mutants at similar developmental stages that were about to form dauer revealed that many of the IIS pathway genes and ILPs exhibit altered levels of expression, indicating a potential feedback mechanism of the TGF-β pathway on the IIS pathway (Liu et al., 2004). In addition, transcription of many DAF-16-regulated genes was altered in *daf-7* adult mutants, and a motif associated with DAF-16-regulated transcription was commonly found to be present in the promoters of many TGF-β regulated genes (Shaw et al., 2007). Many of the TGF-β pathway Daf-c mutants also exhibited longer life span in a DAF-16-dependent manner (Shaw et al., 2007). This evidence suggests that the cross-talk between TGF-β and IIS pathways is not only limited to dauer formation, but may also converge on regulating survival states in diverse developmental and physiological contents.

cGMP Signaling Pathway

The cGMP signaling pathway is defined by the Daf-c gene, *daf-11*, which encodes a transmembrane guanylyl cyclase (GCY) that is expressed in a number of chemosensory neurons to catalyze the conversion of GTP to cGMP in response to G-protein signaling or external ligand binding (Birnby et al., 2000). The cGMP-gated ion channel proteins TAX-2 and TAX-4 are potential downstream effectors of the cGMP pathway and have been shown to be involved in sensory and neuronal development (Coburn and Bargmann, 1996; Coburn et al., 1998; Komatsu et al., 1996). GFP fusion constructs of DAF-11 and TAX-4 share an overlapping expression pattern, suggesting a potential spatial functional cooperation between the two proteins (Komatsu et al., 1996; Birnby et al., 2000). The order of interaction was further suspected by the fact that exogenous cGMP was able to rescue the Daf-c phenotype of *daf-11* mutant but not that of *tax-4* mutants, since DAF-11 is responsible for producing cGMP that acts on TAX-4 (Birnby et al., 2000). In contrast to the *daf-11* mutant, *tax-2* and *tax-4* mutants exhibited weaker Daf-c phenotypes (Coburn et al., 1998). Genetic analysis also revealed that functional TAX-4 was not the only determinant of the strong Daf-c phenotype typical of *daf-11* mutants. Other factors such as the sensory cilium structure genes and presence of a functional ASJ neuron are also critical (Schackwitz et al., 1996, Vowels and Thomas, 1992; Coburn et al., 1998). Taken together, these data suggest that DAF-11 prevents dauer formation partially by activating TAX-2 and TAX-4 via cGMP production, while other downstream effectors also likely contribute to this decision.

Another important gene that seems to be involved in the cGMP pathway is *daf-21*, which encodes a HSP90 homologue (Birnby et al., 2000). Animals with gain-of-function mutations in *daf-21* share the same defects in chemosensory responses as *daf-11* mutants including dauer formation which can be rescued by exogenous supplementation of cGMP analogue, indicating closely related functional roles of the two genes in a similar chemosensory pathway. Nonetheless, null *daf-21* mutants do not arrest as dauer and are larval lethal, suggesting a more complicated role of *daf-21* in dauer formation.

cGMP signaling seems to act upstream of the IIS and TGF-β pathways according to experimental evidence. Mutation of the downstream effectors of either the IIS pathway (DAF-16/FOXO) or the TGF-β pathway (DAF-5/SNO-SKI) can partially suppress the Daf-c phenotype of *daf-11* mutant (Vowels and Thomas, 1992; Thomas et al., 1993). In addition, cilium structure mutants can only suppress dauer arrest in *daf-11* mutants, but not in *daf-2*/InR and *daf-7*/TGF-β mutants. Moreover, rescue of the Daf-c phenotype with exogenous cGMP was only observed in *daf-11* mutants, but not in mutants deficient in the other two signaling pathways. Finally, expression of DAF-7 in the ASI neuron and DAF-28/ILP in the ASI and ASJ neurons was shown to be controlled by DAF-11 (Murakami et al., 2001).

Steroid Hormone Signaling Pathway

Genetic epistasis experiments revealed the Daf-c gene *daf-9* and the Daf-d gene *daf-12* function downstream of cGMP, IIS and TGF-β pathways with unique pleiotropies in gonadal migration among all Daf mutants (Albert and Riddle, 1988; Gerisch et al., 2001; Jia et al., 2002; Riddle et al., 1981; Thomas et al., 1993; Antebi et al., 1998). *daf-12* encodes 1 of the 284 nuclear hormone receptors (NHR) identified in *C. elegans*, which are transcription factors that often respond to lipid hormones (Robinson-Rechavi et al., 2005). It has been shown to be involved in a number of cellular processes including dauer formation, fat metabolism, developmental timing, gonadal maturation and longevity (Antebi et al., 2000; Snow and Larsen, 2000). Structurally, DAF-12/NHR contains a DNA-binding domain at the N-terminus similar to vertebrate pregnane X and vitamin D receptors, null mutations of which result in a Daf-d phenotype; and a ligand-binding domain at the C-terminus similar to vertebrate thyroid hormone receptor, mutations in which give rise to Daf-c phenotypes (Antebi et al., 2000; Riddle et al., 1981; Vowels and Thomas, 1992; Thomas et al., 1993). The latter indicates that loss of hormone binding is critical for dauer arrest. *daf-9* encodes a cytochrome P450 related steroid hydroxylase. Null mutants of *daf-9* form dauer larvae unconditionally and can recover as sterile and long-lived adults (Gerisch et al., 2001; Jia et al., 2002). The Daf-c

phenotype can be suppressed by null mutation of *daf-12*, suggesting that DAF-9 inhibits DAF-12 in its regulation of dauer arrest.

Several lines of evidence suggest that DAF-9 and DAF-12 regulate dauer arrest hormonally. Wild-type, *daf-3*/SMAD and *daf-16*/FOXO animals grown on cholesterol-deficient media phenocopied the gonadal cell migration defect and Daf-c phenotypes typical of *daf-9* mutants, whereas *daf-12* mutants cultured on similar media did not produce the same phenotype (Gerisch et al., 2001). In addition, cholesterol deprivation also enhanced the Daf-c phenotypes of *daf-12* mutants. Two conclusions could be made from the above experimental evidence: first, sterols could be a potential substrate and ligand of DAF-9/CYP450 and DAF-12/NHR respectively; second, the cholesterol sensitivity is consistent with the genetic position of *daf-9* observed in the epistasis experiments, which is downstream of *daf-3* and *daf-16* and upstream of *daf-12* in the dauer pathway. Furthermore, chemical identification of the endogenous ligands for DAF-12/NHR revealed two bile acid-like steroids, named Δ-4 and Δ-7 dafachronic acid (DA) that can activate DAF-12-mediated transcription in the nanomolar range (Motola et al., 2006). Moreover, with the aid of various GFP-tagged DAF-9 protein constructs, Mak and Ruvkun demonstrated that DAF-9 functions non-autonomously to suppress dauer arrest, resembling a hormone-mediated mechanism (Mak and Ruvkun, 2004).

Conclusion

Taken together, a model of dauer formation from the initial detection of environmental signals to an eventual hormone-based alteration in development and physiology is established (Figure 1.1). During favorable conditions, environmental cues are sensed by the G-protein coupled receptors (GPCRs) in the neuronal tissue, which in turn activates the cGMP pathway resulting in membrane depolarization and release of DAF-28/ILPs and DAF-7/ TGF-β to activate the downstream IIS and TGF-β pathways in the endocrine cells. The final output of the two pathways converges on transcriptional activation of the hormone biosynthetic genes, like DAF-9/CYP450 that catalyze the production of DA molecules; the ligands for DAF-12/NHR. DAs are transported to target

tissues and thereby activate DAF-12/NHR to instruct animals to execute the normal reproductive program and inhibit dauer arrest. During unfavorable conditions, the cGMP and downstream IIS and TGF-β pathways are not activated, consequently leading to a shutdown of hormone synthesis. The unbound DAF-12/NHRs associate with certain co-repressor proteins to specify dauer formation for long-term survival instead of continuous energy-consuming processes typical of the reproductive program.

Figure 1.1. Regulatory Pathways for Dauer Arrest in *C. elegans*

Under favorable growth conditions, the amphid neurons in the head of the *C. elegans* detect environmental cues to stimulate the production of cGMP molecules. These signals open cGMP-gated ion channels resulting in membrane depolarization and subsequent release of DAF-7/TGFβ and DAF-28/insulin ligands. Binding of DAF-7/TGFβ to its cognate receptor(s) leads to activation of the TGFβ receptor signaling proteins DAF-8 and DAF-14, which translocate from the cytoplasm into the nucleus to inhibit the action of DAF-3 and DAF-5, and promote the transcription of hormone biosynthetic enzymes like DAF-9. DAF-9 catalyzes the production of dafachronic acids that activate the DAF-12 nuclear receptors in target tissue to promote the reproductive program. Binding of the DAF-28/insulin to its receptors activates a series of protein kinases including AGE-1/PI3K, PDK-1 and AKT1/2, which eventually antagonize the translocation of DAF-16/FOXO transcription factors into the nucleus where they inhibit the transcription of DAF-9. Under unfavorable growth conditions, the DAF-7 and DAF-28 ligands are not released and the DAF-9 transcription is inhibited by DAF-16 leading to inactivation of the DAF-12 nuclear receptors and promotion of dauer arrest.

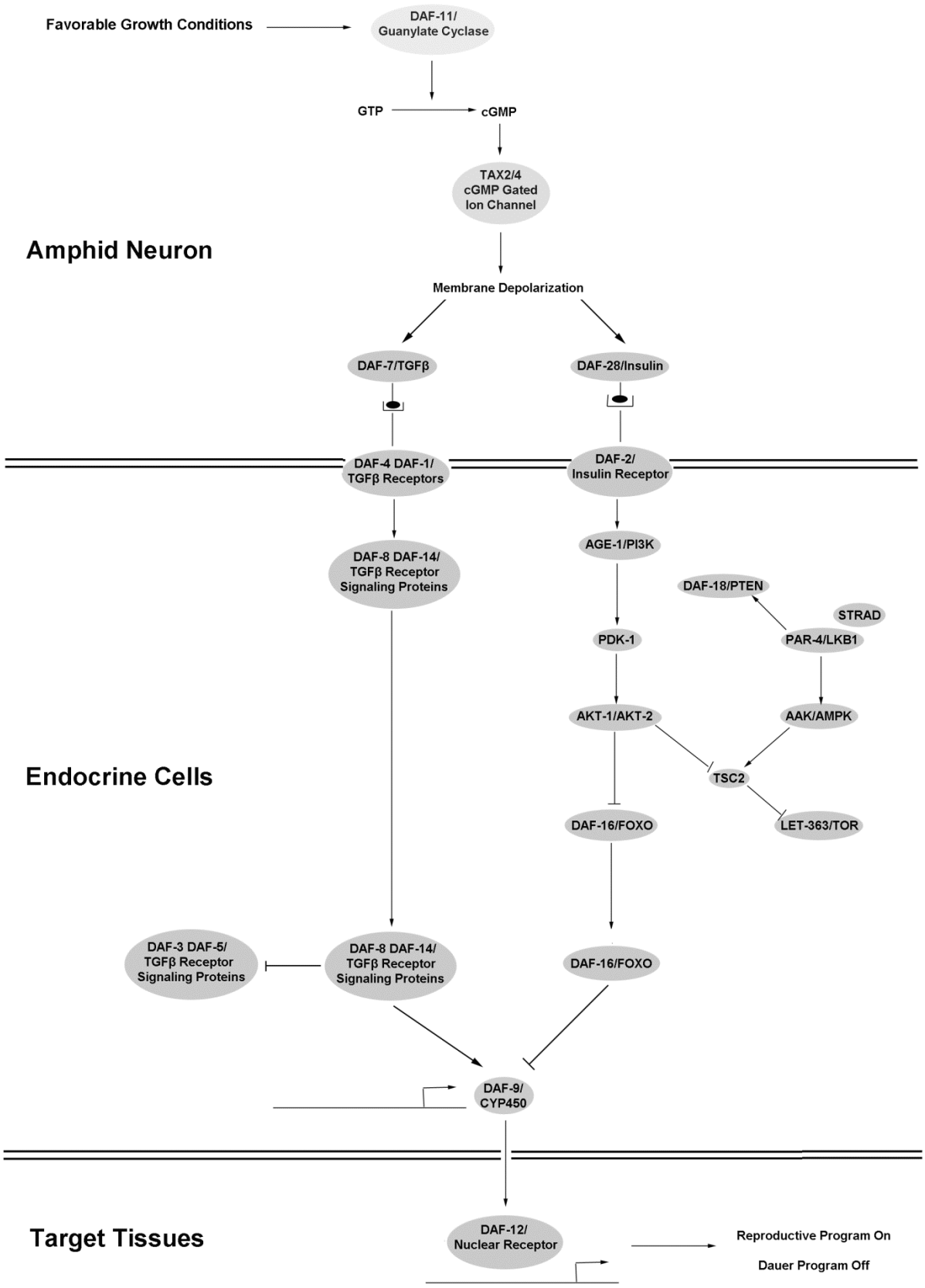
Favorable Growth Conditions
DAF-11/
Guanylate Cyclase
GTP
cGMP
TAX2/4
cGMP Gated
Ion Channel
Amphid Neuron
Membrane Depolarization
DAF-7/TGFβ
DAF-28/Insulin
DAF-4 DAF-1/
TGFβ Receptors
DAF-2/
Insulin Receptor
AGE-1/PI3K
DAF-8 DAF-14/
TGFβ Receptor
Signaling Proteins
DAF-18/PTEN
STRAD
PDK-1
PAR-4/LKB1
AKT-1/AKT-2
AAK/AMPK
TSC2
Endocrine Cells
DAF-16/FOXO
LET-363/TOR
DAF-3 DAF-5/
TGFβ Receptor
Signaling Proteins
DAF-8 DAF-14/
TGFβ Receptor
Signaling Proteins
DAF-16/FOXO
DAF-9/
CYP450
Target Tissues
DAF-12/
Nuclear Receptor
Reproductive Program On
Dauer Program Off

Chapter 1.3 AMP-activated Protein Kinase (AMPK)

Structure and Regulation

AMPK is a critical regulator of cellular energy homeostasis. The enzyme was initially identified as a regulator of 3-hydroxy-3-methylglutaryl coenzyme A (HMG-CoA) reductase and acetyl coenzyme A (Acetyl Co-A) carboxylase in two independent studies (Beg et al., 1973; Carlson and Kim, 1973). Later studies on the two enzymes found that the kinase responsible for their phosphorylation and inactivation required AMP as a cofactor for self activation and thus was named AMPK (Ferrer et al., 1985; Carling et al., 1987).

AMPK exists universally as a hetero-trimeric complex composed of a catalytic (α) subunit and two regulatory (β and γ) subunits in all organisms. Each subunit has at least two isoforms and appears to form functional complexes in random combination resulting in differential tissue expression and its final subcellular localization (Cheung et al., 2000; Salt et al., 1998). The catalytic subunit contains a Ser/Thr kinase domain at the N-terminus and a binding domain for the β regulatory subunit at the C-terminus (Hardie et al., 2012). The C-terminal region of the β regulatory subunit comprises the core component of the complex by binding the C-terminus of α subunit and the N-terminus of γ subunit. The β subunit also contains a carbohydrate-binding domain that was shown to interact with oligosaccharide components of glycogen for inhibition of AMPK activity (McBride et al., 2009). The γ subunit contains four cystathionine-β-synthase (CBS) domains in two tandem repeats, each of which is referred to as a Bateman domain (Carling et al., 2012). Three out of the four CBS domains were revealed to be occupied by adenine nucleotides in the crystal structure of the AMPK core, whereby one of them was tightly bound by AMP while the other two bind AMP, ADP or ATP in a competitive manner (Xiao et al., 2007).

Two conditions need to be met for AMPK activation: AMP and ADP act as activators of the AMPK complex from yeast to human. Addition of AMP into purified recombinant AMPK preparation *in vitro* resulted in as much as a ten-fold increase in AMPK kinase activity assessed by high performance liquid chromatography (Suter et al., 2006).

Binding of AMP or ADP to the Bateman domains led to a conformational change in the γ subunit exposing the activation loop centered by a conserved Thr residue, which was named as Thr172 according to its position in the original rat sequence (Hawley et al., 1996). Such exposure makes the protein complex available for phosphorylation by upstream activating kinases. On the other hand, binding of ATP competitively antagonized the allosteric activation of AMPK and subsequent exposure of Thr172 by AMP and ADP (Carling et al., 2012; Hardie et al., 2012). It appears that different γ subunit isoforms possess different sensitivities to AMP, ADP and ATP molecules, which may provide implications for tissue-specific AMPK regulation. As a result of such allosteric regulation, AMPK can sense changes in cellular AMP/ATP and ADP/ATP ratios and adjust metabolic conditions accordingly by phosphorylating key substrates.

The major upstream kinase of AMPK is Liver Kinase B1 (LKB1), which was originally identified as a tumor suppressor protein (Ylikorkala et al., 1999; Shaw et al., 2004). LKB1 is associated with two accessory proteins, Ste20-related adaptor protein-α (STRADα) and mouse protein 25-α (MO25α), both of which were shown to activate its kinase activity and affect its cytoplasmic localization (Baas et al., 2003; Boudeau et al., 2003). The LKB-1- STRADα- MO25α complex phosphorylates AMPK at Thr172 that is exposed upon binding of AMP or ADP to the γ subunit. Given that AMP, ADP and ATP have similar binding affinity to the γ subunits (Xiao et al., 2011) and ADP is normally maintained at a higher level in cells compared to AMP, ADP may act as the major activator to promote Thr172 phosphorylation under moderate energy stress (Hardie et al., 2012). However, as energy levels decrease, AMP levels will increase as more phosphate groups are released from ATP and ADP molecules for energy production and thus further amplify the activation signal on AMPK. Such a graded response of AMPK activity allows organism to accommodate to a wide range of energy stress levels. Another kinase that has been identified to phosphorylate AMPK at Thr172 is the Ca^{2+}/calmodulin-dependent protein kinase kinase β (CaMKKβ), which responds to increased intracellular Ca^{2+} level independent of AMP/ATP ratio (Hardie et al., 2012). Increases in AMP and ADP levels in tumor cells that lack LKB1 failed to activate AMPK due to low basal CaMKKβ activity, which could be reversed by increasing intracellular Ca^{2+} level (Hawley et al., 2003; Fogarty et al., 2010). AMP activation of AMPK is also

dependent on myristylation of the N-terminus of the β subunit, given that loss of the myristoyl group resulted in failure of AMPK to respond to AMP activation and reduced extent of Thr172 phosphorylation (Oakhill et al., 2010). Moreover, lysine residues of the α subunit of AMPK were acetylated by p300 acetyltransferase and deacetylation of these residues enhanced the physical interaction of AMPK with LKB1 and its subsequent phosphorylation and activation (Lin et al., 2012). It is worth mentioning that hydrogen peroxide (H_2O_2) was shown to activate AMPK in mammalian cells by oxidatively modifying the cysteine residues of the α subunit, indicating that AMPK is not only an indicator of the intracellular metabolic status, but is also able to respond to the cellular redox status (Zmijewski et al., 2010).

Physiological Role

In general, AMPK is activated under energy-demanding conditions or in nutrient scarced environments, where intracellular ATPs are rapidly converted to AMP for energy production resulting in a steep increase of the AMP/ATP ratio (Figure 1.2). Physiological stimuli that have been shown to activate AMPK include intense muscular exercise, ischaemia, glucose deprivation, heat shock and hypoxia (Carling et al., 2012; Hardie et al., 2012; Zhang et al., 2009). Activated AMPK in turn phosphorylates and modulates activities of key proteins such as acetyl-CoA carboxylase 1 (ACC1), HMG-CoA reductase and glycogen synthase kinase 3β (GSK-3β) which are involved in carbohydrate and lipid metabolism. This results in suppression of the ATP-consuming anabolic events like fatty acid (FA) synthesis, cholesterol synthesis and gluconeogenesis. It also stimulates ATP-producing catabolic events such as FA oxidation, and glucose transport into the muscle tissue. Despite of the general view of AMPK as a catabolism promoter while inhibiting anabolism, it has been shown to directly phosphorylate and inhibit a catabolism enzyme adipose triglyceride lipase (ATGL), the enzyme that catalyzes the rate limiting step of lipolysis process during *C. elegans* dauer larva stage, indicating a catabolism suppressing role of AMPK during energy deprivation (Narbonne and Roy, 2009). The critical role of AMPK as a “master switch” of body energy balance makes it an ideal drug target for treatment of metabolic

disorders such as obesity, insulin resistance and Type 2 diabetes (Zhang et al., 2009). Consistent with this, the widely used anti-diabetic drug metformin has been shown to activate AMPK regardless of AMP/ATP ratio in muscle cells, although its beneficial effects on diabetes are not mediated exclusively through AMPK (Fryer et al., 2002).

Several lines of evidence suggest that certain cellular stresses can activate AMPK independent of AMP, ADP or Ca^{2+} levels. In mammalian cell culture, H_2O_2 has been shown to activate AMPK via multiple mechanisms. At high concentration, AMPK activation seemed to be a result of increased ATP/AMP ratio owing to inhibition of mitochondrial ATP synthesis by H_2O_2 (Hawley et al., 2010). A more direct regulatory mechanism of H_2O_2 on AMPK involves oxidation of two conserved Cys residues in the AMPK catalytic subunit (Zmijewski et al., 2010). Gene expression and structure analysis demonstrated that AMPK regulated the expression of catalase genes via DAF-16/FOXO to control cellular H_2O_2 level, suggesting a potential two-way feedback regulation mechanism between AMPK and H_2O_2 (Murphy et al., 2003; Greer et al., 2007; Petriv and Rachubinski, 2004). Another type of stress that could activate AMPK is genotoxicity. Ionizing radiation induced DNA damage triggered a robust phosphorylation and activation of AMPK independent of LKB1, which was initially activated in the nucleus and subsequently propagated into the cytoplasm (Sanli et al., 2010).

Carbohydrate Metabolism Regulation

One of the catabolic processes that AMPK mediates is glucose uptake in skeletal muscle and adipose tissue. The type 4 glucose transporter (GLUT4) is one of the 13 carbohydrate transporter proteins in the human genome that is highly expressed in muscle cells and adipocytes (Joost and Thorens, 2001; Wood and Trayhurn, 2003). It catalyzes glucose transport from intracellular storage vesicles to the plasma membrane via an ATP-independent, facilitative diffusion mechanism (Hruz and Mueckler, 2001). The translocation process of GLUT4 involves intracellular sorting, vesicular transport to the cell membrane followed by the eventual fusion of the GLUT4 storage vesicles with the plasma membrane mediated by RAB G-protein family members (Huang and Czech,

2007). Under basal conditions, RABs are maintained in an inactive GDP-bound state by binding to the RAB-GTPase activating protein (RAB-GAP) family members such as TBC1 domain family member 1 (TBC1D1) and AKT substrate of 160kDa (AS160, also known as TBC1D4) that are associated with GLUT4 storage vesicles (Sakamoto and Holman, 2008). During muscle contraction, AMPK phosphorylates TBC1D1, promoting its interaction with 14-3-3 proteins to release RABs triggering the conversion of RABs to an active GTP-bound state and thereby stimulating fusion of the GLUT4 carrying vesicles with the plasma membrane in muscle cells (Chen et al., 2008; Pehmøller et al., 2009). AS160 is phosphorylated by protein kinase B (PKB/AKt), resulting in a similar stimulation mechanism of GLUT4 trafficking (Sakamoto and Holman, 2008). In contrast, AS160 appears to be the major regulator of GLUT4 transport in adipocytes since TBC1D1 expression is extremely low in 3T3-L1 adipocytes and even undetectable in the white adipose tissue (WAT) of the mouse (Chavez et al., 2008), indicating a differential regulatory role of AMPK in the two tissues. Indeed, AMPK seems to have a potential inhibiting role on AS160 in 3T3-L1 adipocytes through direct phosphorylation, given that treatment with known AMPK activators did not promote phosphorylation of AS160 at any of the insulin-stimulated phosphorylation sites or 14-3-3 binding sites (Chen et al., 2008; Chen et al., 2009). Several possible mechanisms could underlie this inhibitory role of AMPK in adipocytes. AMPK may prevent phosphorylation of AS160 by PKB or activate certain phosphatases to dephosphorylate AS160. Alternatively, phosphorylation of AS160 by AMPK may make it a less favorable substrate for PKB/AKt.

Loss of different AMPK catalytic subunit isoforms has been shown to result in varying degrees of compromise in glucose uptake in skeletal muscle. Knockout of the major catalytic subunit isoform AMPKα2 in mice failed to respond to AMPK activators upon glucose uptake, while elimination of AMPKα1 did not affect glucose uptake whatsoever (Jørgensen et al., 2004). Further evidence demonstrated that AMPK is indeed the primary mediator of contraction-induced glucose uptake in muscle cells. Loss of LKB1 abolished the contraction-induced AMPK activation and subsequent glucose uptake in mice (Sakamoto et al., 2005), indicating an underlying LKB1-dependent mechanism. In addition, muscle contraction in mice with muscle-specific loss-of-function mutations of AMPK was dramatically reduced when accompanied by impaired glucose uptake

(O'Neill et al., 2011). It is worth mentioning that TBC1D1 may not be the only downstream target of AMPK that mediates such an effect.

Multiple lines of evidence have also implicated certain long-term effects of AMPK activation on glucose trafficking. AMPK activation induced by various AMPK activators has been reported to stimulate GLUT4 expression in muscle cells (Holmes et al., 1999; Ojuka et al., 2000; Barnes et al., 2005; McGee et al., 2008) and increase GLUT4 mRNA levels in WAT of rainbow trout (Polakof et al., 2011). However, GLUT4 protein levels were unaffected in human adipose tissues treated with AMPK activators (Boyle et al., 2011). Therefore, more studies need to be conducted to fully understand the mechanism underlying the effect of AMPK on glucose uptake, especially its differential regulatory role in various organisms.

Lipolysis Regulation

Lipolysis describes the process of lipid breakdown involving stepwise hydrolysis of triglyceride (TG) molecules. Energy that is not required for immediate expenditure is mainly stored in the form of TG for long term usage. During nutrient scarcity or energy demanding periods, TG molecules are hydrolysed to diglyceride (DG), monoglyceride (MG) and glycerols in three sequential reactions catalyzed by adipose triglyceride lipase (ATGL), hormone sensitive lipase (HSL) and monoglyceride lipase (MGL) respectively, resulting in release of FAs at each step.

Studies on lipolysis revealed that AMPK can have either a stimulating role or suppressing role in mammalian cells. In cultured 3T3-L1 preadipocytes, activation of AMPK by cAMP is required for maximal activation of lipolysis (Yin et al., 2003). AMPK is also necessary for adrenaline-induced lipolysis in isolated rat adipocytes (Koh et al., 2007). On the other hand, some anti-lipolytic effects of AMPK were also observed in isolated rat, visceral and subcutaneous adipocytes (Sullivan et al., 1994; Anthony et al., 2009). There is also evidence showing that an increase in lipolysis caused by elevated cAMP levels was able to activate AMPK, partially due to FA acylation (Gauthier et al., 2008). Multiple studies have shown that AMPK directly phosphorylates HSL to suppress

both its role in PKA-dependent activation and translocation to the lipid droplets (Garton and Yeaman, 1990; Sullivan et al., 1994; Anthony et al., 2009). Conversely, controversial evidence was also published showing that mutation of the potential AMPK phosphorylation site on HSL prevented its localization to lipid droplets, however this phosphorylation event was unaffected in AMPK-deficient adipose cells (Su et al., 2003; Chakrabarti et al., 2011). In terms of ATGL, multiple lines of evidence have shown that ATGL is a direct phosphorylation target of AMPK, although the outcome can be either stimulating or repressing, depending on the context and/or the organism (Narbonne and Roy, 2009; Pagnon et al., 2012; Ahmadian et al., 2011). Taken together, many studies have suggested that both HSL and ATGL can be directly phosphorylated by AMPK, resulting in diverse consequent regulation of lipid hydrolysis. This differential regulation of lipolysis by AMPK likely reflects both the metabolic state of the animal as well as the nature of the environmental cues involved.

Lipogenesis and FA Oxidation Regulation

Acetyl-CoA carboxylase (ACC), the enzyme that catalyzes the production of a key substrate for FAs biosynthesis, malonyl-CoA, has been shown to be a direct phosphorylation target of AMPK in rat adipocytes (Sullivan et al., 1994) and the phosphorylation site was confirmed by combined treatment of dominant-negative AMPK and its pharmacological activator (Daval et al., 2005). Further evidence showed that AMPK activation during an energy-demanding period led to reduced production of malonyl-CoA, consistent with inhibition of ACC by AMPK (Takekoshi et al., 2006; Peng et al., 2012). In addition to the direct inhibition of ACC by AMPK, several studies also revealed that long-term activation of AMPK with either hormonal or other pharmacological treatments resulted in transcriptional repression of ACC gene expression in both rat adipocytes and human adipose tissues, likely through direct phosphorylation and inhibition of sterol-regulatory-element-binding protein-1c (SREBP-1c) transcription factor (Gaidhu et al., 2009; Orci et al., 2004; Boyle et al., 2011; Li et al., 2011). Specifically, the β1 subunit of AMPK appears to have a unique role in suppressing lipogenesis, as loss of this particular subunit resulted in increased

lipogenesis in mice adipose explants (Dzamko et al., 2010). Besides its role in FAs biosynthesis, malonyl-CoA also regulates FA oxidation by inhibiting carnitine palmitoyltransferase 1 (CPT1), a rate-limiting enzyme embedded in the outer membrane of mitochondria that mediates the transport of FAs into the mitochondria where FA oxidation takes place. Therefore, AMPK inhibition of ACC to reduce the production of malonyl-CoA affects FA oxidation by relieving the inhibition of CPT1 and thereby promoting the FA breakdown and energy production.

Role of AMPK on the *C. elegans* Dauer Larvae

The appropriate storage of lipid, osmoregulatory homeostasis and germline stem cell are largely dependent on the action of AMPK during the dauer progression. In the absence of AMPK, the germline stem cells exit quiescence and proliferate extensively to give rise to a germline hyperplasia phenotype in dauer animals with compromised insulin-like signaling (Narbonne and Roy, 2006). In addition, the same AMPK mutant dauers also expire prematurely at early dauer stage due to rapid exhaustion of their lipid reserves (Narbonne and Roy, 2009). Both of these AMPK actions are regulated by its upstream regulator LKB1. Curiously, although hormone sensitive lipase (HSL) has been shown to be a direct phosphorylation target of AMPK in muscle cells, loss of HSL does not affect the rapid depletion of lipid stores observed in *C. elegans* dauer larvae (Donsmark et al., 2004; Narbonne and Roy ,2009). Alternatively, another recently identified lipase that catalyzes the initial step of the lipolysis process, the adipose triglyceride lipase (ATGL) was found to be a direct phosphorylation target of AMPK at multiple residues (Narbonne and Roy, 2009). In *daf-2* mutant dauers, AMPK phosphorylates and inhibits ATGL to limit lipolysis, allowing the establishment of a lipid depot that provides the essential energy for the non-feeding nutrient-deprived dauer larva.

Figure 1.2: Physiological Role of AMPK.

Upon activation by upstream signals such as increased AMP/ATP ratio, intracellular Ca^{2+} and H_2O_2 level, AMPK can activate various metabolic processes via different downstream protein targets.

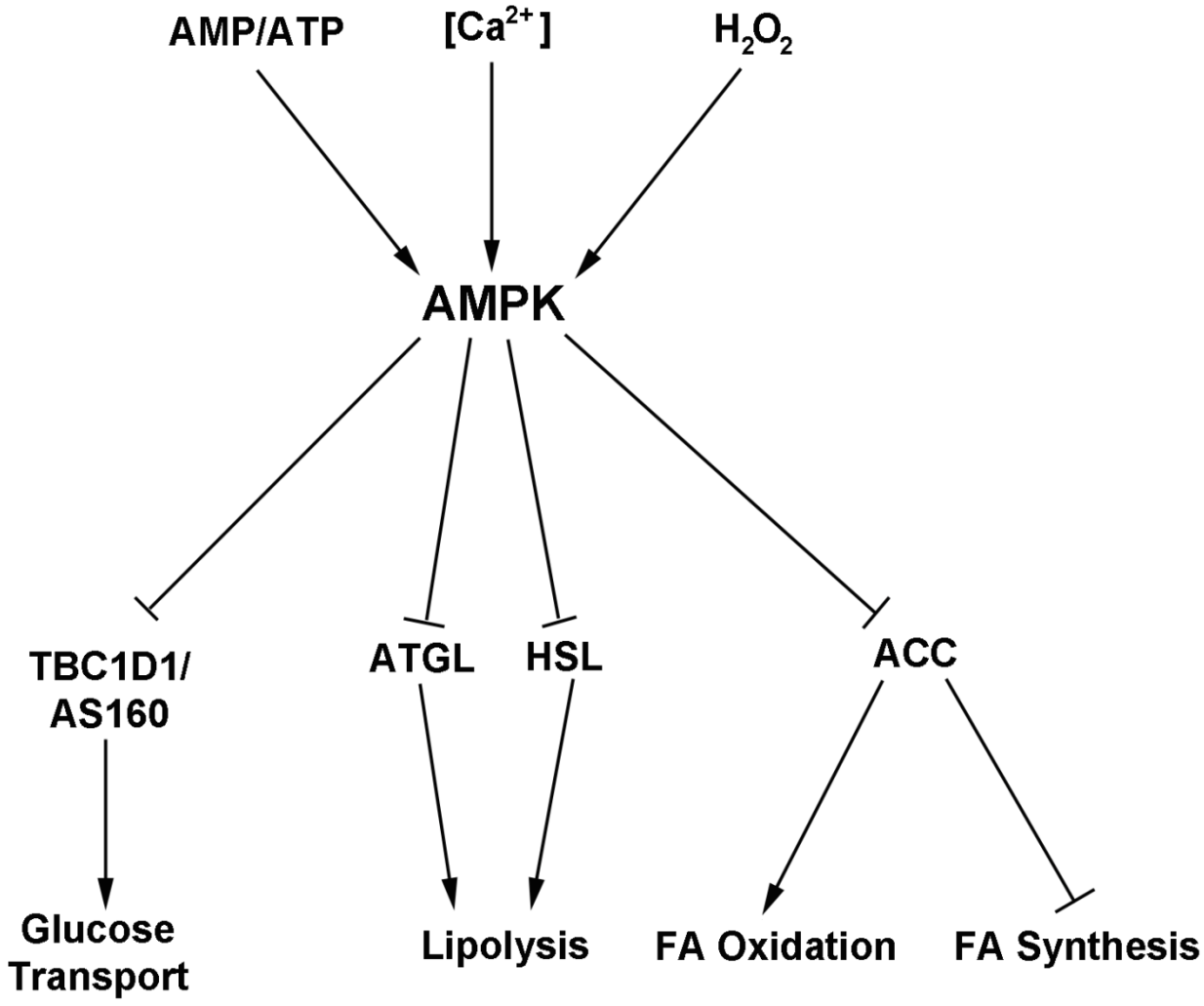

Chapter 1.4 Regulation of Lipolysis

Organisms store excess intake energy mainly in the form of triglyceride for long term usage. Fat synthesis is initiated by adding carbon units to an intermediate metabolite of carbohydrate metabolism, acetyl-CoA to form fatty acids (FAs) and subsequent esterification with glycerol to construct the triglyceride product. The entire process is referred to as lipogenesis and the final products are deposited in the cellular organelles, called lipid droplets. During energy demanding period, stored triglycerides are hydrolyzed into free FAs to provide energy substrates, the process of which is known as lipolysis.

Lipolytic enzymes

Lipolysis is the process of sequential lipid break down, each step of which is catalyzed by specific enzymes (Figure 1.3). The main function of adipose triglyceride lipase (ATGL) is to catalyze the first step of lipolysis for the generation of diglyceride and FAs by cleaving the ester bonds in triglyceride molecules. ATGL was identified independently by three groups in 2004 for its ability to hydrolyze triglyceride molecules (Zimmermann et al., 2004; Jenkins et al., 2004; Villena et al., 2004). ATGL is highly specific towards triglyceride, as it has been shown to exhibit little or no activity when exposed to other lipid intermediates such as diglyceride and monoglyceride (Zimmermann et al., 2004). Gene expression analysis revealed that ATGL mRNA was expressed in measurable amounts in all tissues, where the highest level was found in adipose tissue (Zimmermann et al., 2004; Villena et al., 2004). Structurally, ATGL contains a patatin-like phospholipase domain at the N-terminus that confers its enzymatic activity (Lass et al., 2006; Duncan et al., 2010), and a series of α-helical and loop domains at the C-terminus, including a hydrophobic stretch that corresponds to the substrate binding region and the major site of regulation for its catalytic activity (Schweiger et al., 2008; Kobayashi et al., 2008).

The second reaction in triglyceride breakdown is catalyzed by hormone sensitive lipase (HSL) to further release a FA molecule from diglyceride to generate monoglyceride.

HSL was initially identified as an enzyme that responded to fasting and catabolic hormones (Vaughan et al., 1964; Bjorntorp et al., 1962; Hollenberg et al., 1961). Later, HSL was found to hydrolyze a wide range of substrates with the highest maximal reaction rate attributed to diglycerides (Yeaman, 1990; Yeaman et al., 1994). The expression pattern of HSL mRNA and protein is similar to ATGL in various tissues, where the highest expression level was also observed in adipose tissue (Kraemer et al., 1993; Khoo et al., 1993). Human HSL protein contains 768 amino acids, much longer than ATGL's 504 amino acids. Based on protein domain architecture, two functional regions are predicted in HSL: the N-terminal domain, comprising the first 300 amino acids, mediates its interaction with substrates and protein partners (Osterlund et al., 1996; Shen et al., 1999); the C-terminal domain, comprising the rest of the protein, contains a common lipase α/β hydrolase fold that harbors the catalytic domain and all known phosphorylation sites of HSL (Osterlund et al., 1996; Anthonsen et al., 1998; Shen et al., 1998).

The last reaction of lipolysis is catalyzed by monoglyceride lipase (MGL) to free the final FA molecule from monoglyceride resulting in the production of the remaining glycerol molecules. MGL was initially discovered by its high specificity for monoglyceride in rat adipose tissue (Tornqvist and Belfrage, 1976). Like ATGL and HSL, MGL mRNA level was observed highest in adipose tissue (Karlsson et al., 1997). Human MGL is smaller in size than ATGL and HSL with only 303 residues, where the catalytic region spans almost the entire protein (Karlsson et al., 1997).

Although studies of lipolytic activities have shown that the majority of the lipase capacity is attributed to ATGL and HSL in *C. elegans* dauer larvae, *Drosophila* and murine adipose tissue (Narbonne and Roy, 2009; Grönke et al., 2005; Schweiger et al., 2006), it does not rule out the existence of other lipases that also contribute to lipolysis in other tissues or under particular physiological states. A recent study revealed that a number of patatin-like phospholipase domain-containing protein (PNPLA) family members act as alternative triglyceride hydrolases with high sequence homology to ATGL (Kienesberger et al., 2009). Among these proteins, PNPLA3 has drawn most attention due to its close relationship with various liver diseases, likely due to its suppression upon the

development of fatty liver (Romeo et al., 2010). In addition, two members of the carboxylesterase family have been demonstrated to preferentially hydrolyze short chain FAs in the lumen of the endoplasmic reticulum other than the cytoplasmic lipid droplets (Okazaki et al., 2006; Gilham et al., 2005).

Regulation of ATGL

CGI-58: Like some extracellular TG lipases, ATGL requires co-activator proteins to achieve maximal activity. CGI-58 is the best characterized co-activator of ATGL, where 1:1 molar ratio mixture of ATGL and CGI-58 *in vitro* gives rise to maximal stimulation of the former (Lass et al., 2006). CGI-58 protein was initially discovered in a proteomic approach designed to identify orthologous genes between *C. elegans* and human, and was given the name comparative gene identification-58. The activation potential of CGI-58 on ATGL was shown to exhibit species differences and domain specificity. Mouse ATGL was shown to better respond to both human and murine CGI-58 than human ATGL, despite the two proteins displaying 94% sequence identity (Lass et al., 2006). Mutation studies showed that the N-terminal portion of ATGL was required for CGI-58 activation (Lass et al., 2006). The C-terminal region of human ATGL was revealed to be important for the appropriate localization of the protein to the lipid droplets, as ATGL variants with truncated C-termini failed to bind the lipid droplets (Schweiger et al., 2008). In addition to its role in localization, the C-terminal region was also shown to suppress the enzyme activity *in vitro*, given that the same variants exhibited increased TG hydrolase activity by as much as 20-fold (Schweiger et al., 2008). Such a stimulation in enzyme activity is likely due to the interference of the C-terminal region on CGI-58 binding, as protein-protein interaction studies revealed that more CGI-58 proteins were recruited to the truncated ATGL than wild type ATGL (Schweiger et al., 2008).

The mechanism of how CGI-58 binding increases ATGL activity is currently unclear. Structural studies revealed that the N-terminal Trp-rich region of CGI-58 is crucial for both lipid droplet binding and ATGL activation (Gruber et al., 2010). The direct protein-protein interaction between ATGL and CGI-58 was shown to be essential for ATGL

activation but not sufficient, as some CGI-58 variants that are nonetheless capable of binding to ATGL failed to activate ATGL *in vitro* (Lass et al., 2006; Gruber et al., 2010; Granneman et al., 2007), indicating that additional interactions are required. Binding of CGI-58 to the lipid droplet is another essential interaction that is necessary for ATGL activation, given that CGI-58 variants that failed to localize to lipid droplet were not able to stimulate ATGL activity (Gruber et al., 2010).

Besides its role as the co-activator of ATGL, CGI-58 has also been reported to possess lysophosphatidic acid acyltransferase (LPAAT) activity to acylate lysophosphatidic acid to phosphatidic acid in an acyl-CoA dependant manner (Ghosh et al., 2008; Montero-Moran et al., 2010). Such LPAAT activity provides a channel to recycle the fatty acids released from TG hydrolysis for phospholipid synthesis, suggesting that CGI-58 may play a dual role in both lipid hydrolysis and synthesis depending on the metabolic requirement of the cell.

G0/G1 Switch Protein 2 (G0S2): Recently, G0S2 protein was identified as a selective regulator of ATGL (Yang et al., 2010). The protein was named because of the association of its mRNA expression pattern with G0 to G1 phase re-entry of mononuclear blood cells (Russell and Forsdyke, 1991). In mouse, G0S2 is predominantly expressed in white and brown adipose tissues and liver, where its overexpression led to accumulation of lipid (Yang et al., 2010). In human HeLa cells, overexpressed G0S2 was localized to lipid droplets and protected them from ATGL-mediated hydrolysis (Yang et al., 2010). Co-immunoprecipitation assays revealed that G0S2 directly interacted with the N-terminal region of ATGL without competing with the CGI-58 binding (Yang et al., 2010; Schweiger et al., 2008) and this interaction resulted in reduced ATGL hydrolase activity. G0S2 was only recruited to the lipid droplets when ATGL was present in significant abundance, suggesting that G0S2 itself is not capable of binding to the lipid droplets but requires ATGL as a bridge (Yang et al., 2010).

Regulation by lipid droplet-associated proteins: β-adrenergic activation of ATGL has been shown to be a crucial component for full hormone-activated lipolysis in white adipose tissue (Zimmermann et al., 2004; Haemmerle et al., 2006; Schweiger et al., 2006). Perilipin and CGI-58 are two important downstream effectors of the β-adrenergic

pathway. Perilipin is a family of proteins that coat lipid droplets, providing a structural and protective role. Perilipin-1 is the first identified Perilipin family member that is only expressed in cells that respond to β-adrenergic stimulation, such as adipocytes and steroidogenic cells; and its expression is essential for the.stimulation of lipid hydrolysis by β-adrenergic signals in these cells (Wolins et al., 2006a; Dalen et al., 2007). Under non-stimulated conditions, CGI-58 is sequestered by Perilipin-1 at the lipid droplet surface, making it unavailable for ATGL activation (Granneman et al., 2009a; Granneman et al., 2007; Subramanian et al., 2004). When the β-adrenergic signal pathway is activated, protein kinase A (PKA) phosphorylates Perilipin-1 causing it to dissociate from CGI-58 liberating the latter to activate ATGL (Granneman et al., 2007; Subramanian et al., 2004).

In non-adipose tissues, due to the absence of Perilipin-1, other mechanisms that regulate ATGL activity must exist, possibly involving other Perilipin family members. Indeed, all four of the other Perilipin family members have been implicated in ATGL function and lipid droplet homeostasis. In Perilipin-1-deficient mice, Perilipin-2 has been shown to compensate becoming the major protein that coats the lipid droplet, while it has also been shown to regulate the interaction between ATGL and the lipid droplet in a number of different cell lines (Listenberger et al., 2007; Bell et al., 2008; Tansey et al., 2001). Perilipin-3 is ubiquitously expressed, and its downregulation leads to less but larger lipid droplets, and an increased abundance of ATGL on the lipid droplets accompanied by increased lipolysis (Bell et al., 2008). Little evidence has been demonstrated to link Perlipin-4 with lipolysis besides that it is primarily expressed in the white adipose tissues (Wolins et al., 2003; Wolins et al., 2005). Perilipin-5 is mainly expressed in oxidative tissues, like the heart, skeletal muscle and liver, and induces lipolysis under fasting conditions (Wolins et al., 2006a). Perilipin-5 has been shown to recruit ATGL and CGI-58 to the surface of lipid droplet to promote their interaction and accelerate lipolysis (Granneman et al., 2009b).

Other than the Perilipin family, the fat-specific protein 27 (FSP27), also known as cell death-inducing DFFA-like effector c (CIDEC), is also a lipid droplet-associated protein that enhances lipid storage by inhibiting lipolysis (Puri et al., 2007; Keller et al., 2008).

Genetic screens designed to identify genes that affect lipid droplet size and morphology revealed that proteins involved in the ER-Golgi transport complex are necessary to maintain normal lipid droplet structure in an ATGL-dependant manner in *Drosophila* L2 cells (Guo et al., 2008; Beller et al., 2008). Phosphoprotein proteomic analysis revealed two phosphorylated serine residues on human ATGL but their cellular function was unknown (Bartz et al., 2007). These phosphorylation sites do not involve PKA and are not associated with its lipid droplet localization nor its catalytic capacity (Zimmermann et al., 2004; Duncan et al., 2010). In *C. elegans*, the ATGL ortholog ATGL-1 was shown to be directly phosphorylated by AMPK at several sites leading to decreased TG hydrolysis during the dauer stage (Narbonne and Roy, 2009). Whether a conserved mechanism exists in mammals is unknown and provides a novel direction to explore the regulation of ATGL activity and its effect in lipid homeostasis. ATGL has also been shown to be transcriptionally regulated by a number of factors and conditions, including insulin, mTOR, and fasting/feeding (reviewed by Lass et al., 2011). In general, activities that promote lipid storage would repress ATGL mRNA levels to reduce lipolysis, while during a nutrient-scarce period like fasting, ATGL mRNA transcription is commonly activated to promote lipolysis to meet the increased energy demand.

Regulation of Other Lipases

Regulation of HSL has been well characterized in adipocytes in the last a few decades. In response to β-adrenergic stimulation, HSL is phosphorylated by PKA at five distinct serine residues leading to doubled intrinsic enzyme activity (Kraemer and Shen, 2002; Krintel et al., 2008). In addition, PKA phosphorylation of HSL promotes its interaction with Perilipin-1, which is also a target of PKA (Miyoshi et al., 2007). The phosphorylated Perilipin-1 releases its binding partner CGI-58 under basal conditions, and exposes a docking site for phosphorylated HSL to localize to the lipid droplets and catalyze lipolysis. In non-adipose tissues, despite the absence of Perilipin-1, other Perilipin family members, such as Perilipin-2 and 5 may compensate for HSL (Wang et al., 2009). To date, regulation of MGL has not been well characterized. The mRNA levels of MGL have so far been found not to be affected by either hormones or the cellular energy

state, despite its high expression level in many tissues ranging from adipocytes to muscle cells. Although MGL has been shown to be required to completely breakdown TG molecules *in vitro* (Fredrikson et al., 1986), ATGL and HSL also exhibit MG hydrolase activity. Such functional redundancy might explain the reason why MGL is less affected at transcriptional level.

Figure 1.3. Lipolysis is comprised of sequential reactions, each of which is catalyzed by a specific enzyme resulting in the release of one free fatty acid molecule.

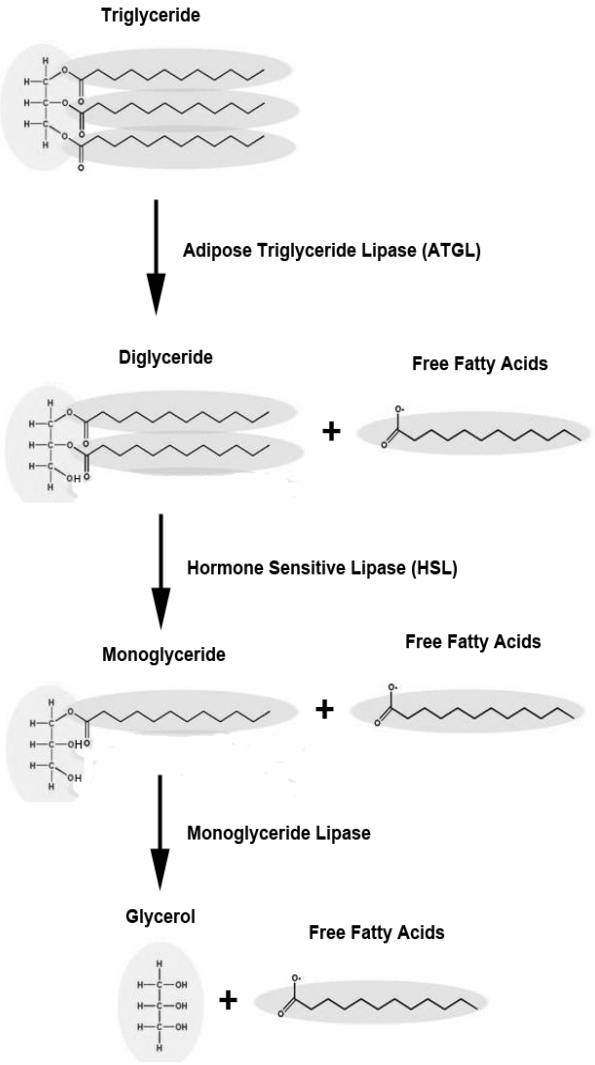

Chapter 1.5 Lipid Droplets

Lipid droplets were initially recognized in late 19th century due to their high diffraction properties making them easily recognizable by light microscopy (Wilson, 1896). Although, they were called by various names including liposomes, lipid/fat bodies, adiposomes and oil bodies in plant, as the research on them rapidly progresses, the name “lipid droplets” is now widely accepted by the field. Research interest on lipid droplets did not accelerate until the discovery of Perilipin, a hormonally regulated phosphoprotein closely associated with the periphery of lipid droplets (Greenberg et al., 1991). Since then, these organelles have been extensively studied in various aspects, ranging from oil production to disease-related examination.

Cellular Role of Lipid Droplets

Lipid droplets are ubiquitous organelles that are present in most eukaryotic cells. Each lipid droplet consists of a core of neutral lipids, surrounded by a phospholipid monolayer, ranging from 1 to 100 μm in diameter. Like plasma membranes, their surfaces are decorated by numerous proteins, providing functional and structural support to the organelle. The main function of lipid droplets is to provide a long-term storage depot for excess energy intake and to provide support to the organism during periods of high energy demand or nutrient scarcity. Excess energy is mainly stored in the form of triglyceride (TG), which is an ester derived from one glycerol molecule and three fatty acid molecules. It is chemically hydrophobic and highly reduced, making it an ideal molecule for energy storage. In mammals, the cells that are responsible for energy storage are the adipocytes, wherein lipid droplets often occupy most of the cytoplasmic space. Many of the products generated from lipolysis are involved in cell signaling pathways. For instance, free fatty acids, the final products of lipolysis, can act as ligands for certain nuclear receptors to influence gene expression (Ducharme and Bickel, 2008). Compartmentalization of the lipid molecules is also beneficial for the cells to buffer the toxic effects generated by excessive lipid molecules. In cultured human cell lines, excessive cholesterol present in the cytoplasm was recognized and taken up by

macrophages leading to ER stress and consequently cell death (Maxfield and Tabas, 2005). High levels of intracellular free fatty acids were shown to disrupt plasma membrane structure integrity and eventually induce cell apoptosis (Mishra and Simonson, 2005). On the other hand, excess lipid molecules, such as sterols and free fatty acids, can be esterified into esters and subsequently packed into lipid droplets for storage to prevent any potential toxic effects (Farese and Walther, 2009; Ducharme and Bickel, 2008). The loading of various lipid molecules into the lipid droplets may also aid the transport of these lipid cargos to other subcellular destinations or signaling pathways.

In addition to its lipid storage role, lipid droplets also serve as a warehouse to provide building blocks, such as phospholipids, sterols and eicosanoids, for the construction of plasma membranes. These building blocks can be generated during the process of lipid catabolism as needed and can be rapidly added to the growing membrane, sometimes coupled to cell division (Kurat et al., 2009). In *Drosophila*, a proteomic study revealed that massive amounts of various histone proteins were associated with lipid droplets during oogenesis and early embryo development, but disappeared in later stages, suggesting that these lipid droplets may not only act as energy depots for the ongoing cell division process, but also serve as a temporary platform to sequester maternally provided proteins (Cermelli et al., 2006). Similarly, in hepatitis C virus, the capsid core protein was found to be closely associated with the lipid droplets during viral replication in hepatocytes (Miyanari et al., 2007). It has also been shown in human hepatoma cells that the lipid droplets acted as a platform for proteasomal protein degradation (Ohsaki et al., 2006). To sum up, the lipid droplets not only act as energy storage organelles, but also participate in a number of other cellular processes to ensure sufficient energy supply.

Lipid Droplet Biogenesis

The growth of lipid droplets is accompanied by addition of polar lipid molecules to the surface to build the monolayer membrane while an influx of neutral lipid molecules must

occur to fill up the core. The building blocks for the membrane can either come from *de novo* synthesis or conversion of the by-products from the lipolysis process. The major phospholipid components are synthesized in the (ER), where loss of the corresponding enzyme resulted in enlarged lipid droplets, likely due to increased fusion events (Guo et al., 2008). Addition of neutral lipids to the lipid droplet core requires TG synthesis involving addition of fatty acid residues sequentially to a glycerol backbone. The final step of TG synthesis is catalyzed by the enzyme diacylglycerol acyltransferase (DGAT), which functions together with the acyl-CoA synthetase FATP1 to facilitate lipid droplet expansion by coupling TG synthesis with deposition (Yen et al., 2008; Xu et al., 2012).

The prevailing model for lipid droplet generation posts that TG molecules are synthesized in the ER and accumulate between the two layers of the ER membrane. When the synthesized TG molecules reach a certain threshold within the bilayer, a portion will protrude from the cytoplasmic side of the membrane and bud off into the cytoplasm (Wolins et al., 2006b; Brown, 2001). There are still a lot of puzzles that must be solved for this model, such as how the synthesized lipids enter the inter membrane space, what is the mechanical force that drives these droplets to bud off the membrane and what drives the direction of budding into the cytoplasm instead of the ER lumen. The vesicular budding model suggests that the newly formed neutral lipids are deposited into the pre-existing vesicles embedded in the ER membrane and either detach or remain associated with the membrane thereafter (Walther and Farese, 2009; Farese and Walther, 2009).

Multiple lines of evidence suggest that lipid droplets are derived from the ER. Enzymes that are responsible for lipid synthesis, like DGAT, are primarily ER residential proteins. In addition, lipid droplets have been demonstrated in several studies that they are in close proximity with ER membranes (Robenek et al., 2006; Goodman, 2008). Given that the major function of ER is to provide lipid-favourable avenues for the transport of newly synthesized proteins committed for secretion, the close proximity of the lipid droplets with the ER can facilitate the rapid exchange of lipid and protein cargos between the two compartments. Lipid droplets were found to be associated with the bacterial plasma membrane possibly due to the absence of ER in bacteria cells (Wältermann et al., 2005).

There is also evidence suggesting potential interactions between the lipid droplets and peroxisomes, mitochondria or replication vacuoles of intracellular parasites (Goodman, 2008; Walther and Farese, 2009). Although genome wide screens carried out in *Drosophila* and yeast have identified a number of genes that when disrupted resulted in less or smaller lipid droplets (Beller et al., 2008; Guo et al., 2008; Fei et al., 2008; Szymanski et al., 2007); detailed mechanistic insight as to how lipid droplet size and morphology are controlled is still lacking.

Another mechanism that may underlie the expansion of lipid droplets is fusion of smaller lipid droplets into larger ones. This is supported by the studies carried out in *Arabidopsis thaliana* where the loss of the major structural protein on the lipid droplets resulted in obvious fusion of the variant lipid droplets (Siloto et al., 2006). There is also evidence suggesting that at any given concentration, approximately 15% of the total lipid droplets undergo fusion events, which was mediated by SNARE proteins consistent with their role in vesicle fusion (Boström et al., 2007).

Lipid Droplet Catabolism

During energy-demanding periods, lipids stored in the lipid droplets are mobilized via the process of lipolysis to provide the cells with extra energy supply. Lipolysis consists of a series of sequential reactions, each of which is catalyzed by a highly specific lipase. At each step, a free fatty acid molecule is released from the triglyceride backbone for further cleavage through the process of β-oxidation. In mammals, catecholamine family molecules, such as adrenaline and noradrenaline, are the major stimulants of lipolysis during fasting and exercise periods (Zechner et al., 2009). When cellular energy is low, catecholamines are produced by the sympathetic nervous system and bind to the G-protein coupled receptors (GPCR) on the cell surface. The binding induces a conformational change, resulting in the dissociation of the α subunit from the receptor to activate adenylate cyclase, the enzyme that catalyzes the conversion of ATP to cAMP. The eventual increase in intracellular cAMP level leads to the activation of protein kinase A (PKA) that can phosphorylate Perilipin and hormone sensitive lipase (HSL)

(Brasaemle et al., 2009). PKA phosphorylation of the lipid droplet residential protein Perilipin causes it to release its common binding partner CGI-58, making the latter available to act as the co-activator of adipose triglyceride lipase (ATGL) to promote lipolysis. Phosphorylation of HSL leads to its activation and localization to the lipid droplets to cleave fatty acid from diglyceride molecules (Yang et al., 2010). In 3T3-L1 adipocytes, stimulation of lipolysis with a β-adrenergic receptor agonist resulted in translocation of HSL from the cytosol to the lipid droplets accompanied by the activation of lipolysis (Brasaemle et al., 2000).

During lipolysis, various lipases are recruited to the surface of lipid droplets where they interact with their respective substrates. How these enzymes penetrate the lipid droplet membrane and access their substrates remains unclear. There is speculation that the lipase complex could effectively bind to the lipid monolayer of the droplet and split the membrane to access the internal neutral lipids (Farese and Walther, 2009). Such deformation of the lipid droplet membrane is possibly facilitated by proteins involved in coating and vesicular transport (Guo et al., 2008). Autophagy could be another potential mechanism that opens up the lipid droplet. Inhibition of autophagy in cultured hepatocytes has been shown to block lipolysis and increase triglyceride storage (Singh et al., 2009). Under maximal stimulation, larger lipid droplets may break down into smaller ones to increase the surface area to enhance the efficacies of the reactions. Constant activation of PKA for several hours has been shown to result in lipid droplet fragmentation, which is dependent on Perilipin A phosphorylation at a specific serine residue (Marcinkiewicz et al., 2006). These evidences suggest that multiple regulatory mechanisms may converge to open up the lipid droplets to initiate the lipolysis process.

Chapter 1.6 Thesis Rationale

During periods of nutrient scarcity, organisms readjust their metabolic status to adapt to the environment. Upon encountering high population density, instead of completing the normal reproductive life cycle, *C. elegans* can enter an alternative state, called dauer where they initially build up lipid reserves for later usage as their sole energy source, given that they do not feed once entering the dauer state. In addition to the key trigger, conditions like high temperature and low nutrient resources can potentiate the dauer entry decision. Such a shift of energy dependency from external feeding to internal lipid utilisation perfectly reflects the organism's ability to adjust their metabolic profile to fit in the changing environment. This phenomenon provides us with an excellent model to investigate how signaling pathways regulate lipid metabolism in response to change in external nutrient intake. Understanding how lipid metabolism is regulated is of particular importance in developing novel therapeutic alternatives for metabolic disorders including diabetes, obesity and certain types of cancer.

Given that *C. elegans* with impaired AMPK function expire at early dauer stage due to rapid depletion of lipid storage as a result of over activated ATGL (Narbonne and Roy, 2009), I started off my thesis research by performing a non-biased genome-wide screen to identify genes, when compromised, that can extend the survival of those AMPK mutant dauers. The identified gene list will help us to build a framework to better understand how AMPK converges on a plethora of cellular processes required to promote the typical long-term survival of the dauer larva. Many of the gene candidates will function together or in parallel with ATGL to affect lipid utilisation and storage. Characterization of their mechanism of action will further unveil the regulatory pathways involved in lipid metabolism and eventually shed light on development of novel treatments to lipid associated diseases such as obesity, diabetes and certain types of cancer.

References

Ahmadian, M., Abbott, M. J., Tang, T., Hudak, C. S., Kim, Y., Bruss, M., Hellerstein, M. K., Lee, H. Y., Samuel, V. T., Shulman, G. I., Wang, Y., Dunca, R. E., Kang, C. and Sul, H. S. (2011). Desnutrin/ATGL is regulated by AMPK and is required for a brown adipose phenotype. *Cell Metab.* **13**, 739–48.

Ailion, M., Inoue, T., Weaver, C. I., Holdcraft, R. W. and Thomas, J. H. (1999). Neurosecretory control of aging in Caenorhabditis elegans. *Proc. Natl. Acad. Sci.* **96**, 7394–7.

Ailion, M. and Thomas, J. H. (2000). Dauer formation induced by high temperatures in *Caenorhabditis elegans*. *Genetics* **156**, 1047–67.

Albert, P. S. and Riddle, D. L. (1988). Mutants of *Caenorhabditis elegans* that form dauer-like larvae*. Dev. Biol.* **126**, 270–93.

Alcedo, J. and Kenyon, C. (2004). Regulation of C. elegans longevity by specific gustatory and olfactory neurons. *Neuron*. **41**, 45-55.

Antebi, A., Culotti, J. G. and Hedgecock, E. M. (1998). *daf-12* regulates developmental age and the dauer alternative in *Caenorhabditis elegans*. *Development* **125**, 1191–205.

Antebi, A., Yeh, W. H., Tait, D., Hedgecock, E. M. and Riddle, D. L. (2000) daf-12 encodes a nuclear receptor that regulates the dauer diapause and developmental age in C. elegans. *Genes & Dev.* **14**, 1512–27.

Anthonsen, M. W., Ronnstrand, L., Wernstedt, C., Degerman, E. and Holm, C. (1998). Identification of novel phosphorylation sites in hormone-sensitive lipase that are phosphorylated in response to isoproterenol and govern activation properties in vitro. *J Biol Chem* **273**, 215–21.

Anthony, N. M., Gaidhu, M. P. and Ceddia, R. B. (2009). Regulation of visceral and subcutaneous adipocyte lipolysis by acute AICAR-induced AMPK activation. *Obesity* **17**, 1312-7.

Apfeld, J. and Kenyon, C. (1998). Cell nonautonomy of *C. elegans daf-2* function in the regulation of diapause and life span. *Cell* ***95***, 199–210.

Apfeld, J., O'Connor, G., McDonagh, T., DiStefano, P. S. and Curtis, R. (2004). The AMP-activated protein kinase AAK-2 links energy levels and insulin-like signals to lifespan in C. elegans. *Genes & Dev.* **18**, 3004–9.

Ashrafi, K., Chang, F. Y., Watts, J. L., Fraser, A. G., Kamath, R. S., Ahringer, J. and Ruvkun, G. (2003). Genome-wide RNAi analysis of Caenorhabditis elegans fat regulatory genes. *Nature* **421**, 268-72.

Baas, A. F., Boudeau, J., Sapkota, G. P., Smit, L., Medema, R., Morrice, N. A., Alessi, D. R. and Clevers, H. C. (2003**).** Activation of the tumour suppressor kinase LKB1 by the STE20-like pseudokinase STRAD. *EMBO J* **22,** 3062-72.

Barnes, B. R., Long, Y. C., Steiler, T. L., Leng, Y., Galuska, D., Wojtaszewski, J. F., Andersson, L. and Zierath, J. R. (2005). Changes in exercise-induced gene expression in 5′-AMP-activated protein kinase γ3-null and γ3 R225Q transgenic mice. *Diabetes* **54**, 3484-9.

Bartz, R., Zehmer, J. K., Zhu, M., Chen, Y., Serrero, G., Zhao, Y. and Liu, P. (2007). Dynamic activity of lipid droplets: protein phosphorylation and GTP-mediated protein translocation. *J Proteome Res.* **6**, 3256-65.

Baugh, L. R. and Sternberg, P. W. (2006). DAF-16/FOXO regulates transcription of cki-1/Cip/Kip and repression of lin-4 during C. elegans L1 arrest. *Curr Biol.* **16**, 780-5.

Beg, Z. H., Allmann, D. W. and Gibson, D. M. (1973). Modulation of 3-hydroxy-3-methylglutaryl coenzyme A reductase activity with cAMP and wth protein fractions of rat liver cytosol. *Biochem Biophys Res Commun.* **54**, 1362-9.

Bell, M., Wang, H., Chen, H., McLenithan, J.C., Gong, D.W., Yang, R.Z., Yu, D., Fried, S. K., Quon, M. J., Londos, C. and Sztalryd, C. (2008). Consequences of lipid droplet coat protein downregulation in liver cells: abnormal lipid droplet metabolism and induction of insulin resistance. *Diabetes.* **57**, 2037-45.

Beller, M., Sztalryd, C., Southall, N., Bell, M., Jäckle, H., Auld, D. S. and Oliver, B. (2008). COPI complex is a regulator of lipid homeostasis. *PLoS Biol.* **6**, e292.

Berdichevsky, A., Viswanathan, M., Horvitz, H. R. and Guarente, L. (2006). *C. elegans* SIR-2.1 interacts with 14-3-3 proteins to activate DAF-16 and extend life span. *Cell* ***125***, 1165–77.

Berman, J. R. and Kenyon, C. (2006). Germ-cell loss extends C. elegans life span through regulation of DAF-16 by kri-1 and lipophilic-hormone signaling. *Cell* **124**, 1055-68.

Birnby, D. A., Link, E. M., Vowels, J. J., Tian, H., Colacurcio, P. L. and Thomas, J. H. (2000). A transmembrane guanylyl cyclase (DAF-11) and Hsp90 (DAF-21) regulate a common set of chemosensory behaviors in C. elegans. *Genetics* **155**, 85–104.

Bishop, N. A. and Guarente, L. (2007). Two neurons mediate diet-restriction-induced longevity in *C. elegans*. *Nature* **447**, 545–50.

Bjorntorp, P. and Furman, R. H. (1962). Lipolytic activity in rat epididymal fat pads. *Am JPhysiol* **203**, 316–22.

Boström, P., Andersson, L., Rutberg, M., Perman, J., Lidberg, U., Johansson, B. R., Fernandez-Rodriguez, J., Ericson, J., Nilsson, T., Borén, J. and Olofsson, S. O. (2007). SNARE proteins mediate fusion between cytosolic lipid droplets and are implicated in insulin sensitivity. *Nat Cell Biol*. **9**, 1286-93.

Boudeau, J., Baas, A. F., Deak, M., Morrice, N. A., Kieloch, A., Schutowski, M., Prescott, A. R., Clevers, H. C. and Alessi, D. R. (2003). MO25 isoforms interact with the STE20-related pseudokinase STRADα/β and enhance their ability to bind, activate and localise the LKB1 tumour suppressor in the cytoplasm. *EMBO J* **22,** 5102-14.

Boyle, J. G., Logan, P. J., Jones, G. C., Small, M., Sattar, N., Connell, J. M., Cleland, S. J. and Salt, I. P. (2011). AMP-activated protein kinase is activated in adipose tissue of individuals with type 2 diabetes treated with metformin: a randomised glycaemia-controlled crossover study. *Diabetologia* **54**, 1799-809.

Branicky, R., Shibata, Y., Feng, J. and Hekimi, S. (2001). Phenotypic and suppressor analysis of defecation in *clk-1* mutants reveals that reaction to changes in temperature is an active process in *Caenorhabditis elegans*. *Genetics* **159**, 997–1006.

Brasaemle, D. L., Levin, D. M., Adler-Wailes, D. C. and Londos, C. (2000). The lipolytic stimulation of 3T3-L1 adipocytes promotes the translocation of hormone-sensitive lipase to the surfaces of lipid storage droplets. *Biochim Biophys Acta.* **1483**, 251-62.

Brasaemle, D. L., Subramanian, V., Garcia, A., Marcinkiewicz, A. and Rothenberg, A. (2009). Perilipin A and the control of triacylglycerol metabolism. *Mol Cell Biochem.* **326**, 15-21.

Brown, D. A. (2001). Lipid droplets: proteins floating on a pool of fat. *Curr Biol.* **11**, 446-9.

Burdon, K. L., Stokes, J. C. and Kimbrough, C. E. (1942). Studies of the Common Aerobic Spore-Forming Bacilli: II. Fermentation Reactions in Agar Butt-Slants. *J Bacteriol*. **44**, 163-8.

Burnell, A. M., Houthoofd, K., O'Hanlon, K. and Vanfleteren, J. R. (2005). Alternate metabolism during the dauer stage of the nematode Caenorhabditis elegans. *Exp Gerontol.* **40**, 850-6.

Carling, D., Thornton, C., Woods, A. and Sanders, M. J. (2012). AMP-activated protein kinase: new regulation, new roles? *Biochem. J.* **445**, 11-27.

Carling, D., Zammit, V. A. and Hardie, D. G. (1987). A common bicyclic protein kinase cascade inactivates the regulatory enzymes of fatty acid and cholesterol biosynthesis. *FEBS Lett.* **223**, 217-22.

Carlson, C. A. and Kim, K. H. (1973). Regulation of hepatic acetyl coenzyme A carboxylase by phosphorylation and dephosphorylation. *J Biol Chem.* **248**, 378-80.

Cassada, R. C. and Russell, R. L. (1975). The dauerlarva, a post-embryonic developmental variant of the nematode *Caenorhabditis elegans*. *Dev. Biol.* **46**, 326–42.

Cermelli, S., Guo, Y., Gross, S. P. and Welte, M. A. (2006). The lipid-droplet proteome reveals that droplets are a protein-storage depot. *Curr Biol.* **16**, 1783-95.

Chalfie, M., Tu, Y., Euskirchen, G., Ward, W. W. and Prasher, D. C. (1994). Green fluorescent protein as a marker for gene expression. *Science* **263**, 802-5.

Chakrabarti, P., English, T., Karki, S., Qiang, L., Tao, R., Kim, J., Luo, Z., Farmer, S. R. and Kandror, K. V. (2011). SIRT1 controls lipolysis in adipocytes via FOXO1-mediated expression of ATGL. *J. Lipid Res.* **52**, 1693–701.

Chavez, J. A., Roach, W. G., Keller, S. R., Lane, W. S. and Lienhard, G. E. (2008). Inhibition of GLUT4 translocation by Tbc1d1, a Rab GTPase-activating protein abundant in skeletal muscle, is partially relieved by AMP-activated protein kinase activation. *J. Biol. Chem.* **283**, 9187-95.

Chen, S., Murphy, J., Toth, R., Campbell, D. G., Morrice, N. A. and Mackintosh, C. (2008). Complementary regulation of TBC1D1 and AS160 by growth factors, insulin and AMPK activators. *Biochem J.* **409**, 449-59.

Chen, S. and Mackintosh, C. (2009). Differential regulation of NHE1 phosphorylation and glucose uptake by inhibitors of the ERK pathway and p90RSK in 3T3-L1 adipocytes. *Cell. Signalling* **21**, 1984-93.

Cheung, P. C., Salt, I. P., Davies, S. P., Hardie, D. G. and Carling, D. (2000). Characterization of AMP-activated protein kinase γ subunit isoforms and their role in AMP binding. *Biochem. J.* **346**, 659-69.

Clancy, D. J., Gems, D., Harshman, L. G., Oldham, S., Stocker, H., Hafen, E., Leevers, S. J. and Partridge, L. (2001). Extension of life-span by loss of CHICO, a Drosophila insulin receptor substrate protein. *Science* **292**, 104–6.

Coburn, C. M. and Bargmann, C. I. (1996). A putative cyclic nucleotide-gated channel is required for sensory development and function in *C. elegans*. *Neuron* **17**, 695–706.

Coburn, C. M., Mori, I., Ohshima, Y. and Bargmann, C. I. (1998). A cyclic nucleotide-gated channel inhibits sensory axon outgrowth in larval and adult *Caenorhabditis elegans*: a distinct pathway for maintenance of sensory axon structure. *Development* **125**, 249–58.

Da Graca, L. S., Zimmerman, K. K., Mitchell, M. C., Kozhan-Gorodetska, M., Sekiewicz, K., Morales, Y. and Patterson, G. I. (2004). DAF-5 is a Ski oncoprotein homolog that functions in a neuronal TGF-beta pathway to regulate *C. elegans* dauer development. *Development* **131**, 435–46.

Dalen, K. T., Dahl, T., Holter, E., Arntsen, B., Londos, C., Sztalryd, C. and Nebb, H. I. (2007). LSDP5 is a PAT protein specifically expressed in fatty acid oxidizing tissues. *Biochim Biophys Acta.* **1771**, 210-27.

Daval, M., Diot-Dupuy, F., Bazin, R., Hainault, I., Viollet, B., Vaulont, S., Hajduch, E., Ferré, P. and Foufelle, F. (2005). Anti-lipolytic action of AMP-activated protein kinase in rodent adipocytes. *J. Biol. Chem.* **280**, 25250-7.

Dillin, A., Crawford, D. K. and Kenyon, C. (2002). Timing requirements for insulin/IGF-1 signaling in *C. elegans*. *Science* **298**, 830–34.

Donsmark, M., Langfort, J., Holm, C., Ploug, T. and Galbo, H. (2004). Contractions induce phosphorylation of the AMPK site Ser565 in hormone-sensitive lipase in muscle. *Biochem Biophys Res Commun.* **316**, 867-71.

Ducharme, N. A. and Bickel, P. E. (2008). Lipid droplets in lipogenesis and lipolysis. *Endocrinology*. **149**, 942-9.

Duncan, R. E., Wang, Y., Ahmadian, M., Lu, J., Sarkadi-Nagy, E. and Sul, H. S. (2010). Characterization of desnutrin functional domains: critical residues for triacylglycerol hydrolysis in cultured cells. *J Lipid Res* **51**, 309–17.

Dzamko, N., van Denderen, B. J., Hevener, A. L., Jørgensen, S. B., Honeyman, J., Galic, S., Chen, Z. P., Watt, M. J., Campbell, D. J., Steinberg, G. R. and Kemp, B. E. (2010). AMPK beta1 deletion reduces appetite, preventing obesity and hepatic insulin resistance. *J. Biol. Chem.* **285**, 115-22.

Essers, M. A., de Vries-Smits, L. M., Barker, N., Polderman, P. E., Burgering, B. M. and Korswagen, H. C. (2005). Functional interaction between β-catenin and FOXO in oxidative stress signaling. *Science* **308**, 1181–4.

Estevez, M., Attisano, L., Wrana, J. L., Albert, P. S., Massague, J. and Riddle, D. L. (1993). The *daf-4* gene encodes a bone morphogenetic protein receptor controlling *C. elegans* dauer larva development. *Nature* **365**, 644–9.

Farese, R. V. Jr. and Walther, T. C. (2009). Lipid droplets finally get a little R-E-S-P-E-C-T. *Cell* **139**, 855-60.

Fei, W., Shui, G., Gaeta, B., Du, X., Kuerschner, L., Li, P., Brown, A. J., Wenk, M. R., Parton, R. G. and Yang, H. (2008). Fld1p, a functional homologue of human seipin, regulates the size of lipid droplets in yeast. *J Cell Biol.* **180**, 473-82.

Ferrer, A., Caelles, C., Massot, N. and Hegardt, F. G. (1985). Activation of rat liver cytosolic 3-hydroxy-3-methylglutaryl coenzyme A reductase kinase by adenosine 5'-monophosphate. *Biochem Biophys Res Commun.* **132**, 497-504.

Fielenbach, N. and Antebi, A. (2008). C. elegans dauer formation and the molecular basis of plasticity. *Genes&Development* **22**, 2149-65.

Fire, A., Xu, S., Montgomery, M.K., Kostas, S. A., Driver, S. E. and Mello, C. C. (1998). Potent and specific genetic interference by double-stranded RNA in Caenorhabditis elegans. *Nature* **125**, 421-9.

Fogarty, S., Hawley, S. A., Green, K. A., Saner, N., Mustard, K. J. and Hardie, D. G. (2010). Calmodulin-dependent protein kinase kinase-beta activates AMPK without forming a stable complex: synergistic effects of Ca2+ and AMP. *Biochem J.* **426**, 109-18.

Föll, R. L., Pleyers, A., Lewandovski, G. J., Wermter, C., Hegemann, V. and Paul, R. J. (1999). Anaerobiosis in the nematode *Caenorhabditis elegans*. *Comp. Biochem. Physiol.* **124B**, 269–80.

Fredrikson, G., Tornqvist, H. and Belfrage, P. (1986). Hormone-sensitive lipase and monoacylglycerol lipase are both required for complete degradation of adipocyte triacylglycerol. *Biochim Biophys Acta.* **876**, 288-93.

Fryer, L. G., Parbu-Patel, A. and Carling, D. (2002). The Anti-diabetic drugs rosiglitazone and metformin stimulate AMP-activated protein kinase through distinct signaling pathways. *J. Biol. Chem.* **277**, 25226-32.

Freudiger, C. W., Min, W., Saar, B. G., Lu, S., Holtom, G. R., He, C., Tsai, J. C., Kang, J. X. and Xie, X. S. (2008). Label-free biomedical imaging with high sensitivity by stimulated Raman scattering microscopy. *Science* **322**, 1857–61

Gaidhu, M. P., Fediuc, S., Anthony, N. M., So, M., Mirpourian, M., Perry, R. L. and Ceddia, R. B. (2009). Prolonged AICAR-induced AMP-kinase activation promotes energy dissipation in white adipocytes: novel mechanisms integrating HSL and ATGL. *J. Lipid Res.* **50**, 704-15.

Garsin, D. A., Villanueva, J. M., Begun, J., Kim, D. H., Sifri, C. D., Calderwood, S. B., Ruvkun, G. and Ausubel, F. M. (2003). Long-lived C. elegans daf-2 mutants are resistant to bacterial pathogens. *Science* **300**, 1921.

Garton, A. J. and Yeaman, S. J. (1990). Identification and role of the basal phosphorylation site on hormone-sensitive lipase. *Eur. J. Biochem.* **191**, 245–50.

Gauthier, M. S., Miyoshi, H., Souza, S. C., Cacicedo, J. M., Saha, A. K., Greenberg, A. S. and Ruderman, N. B. (2008). AMP-activated protein kinase is activated as a

consequence of lipolysis in the adipocyte: potential mechanism and physiological relevance. *J. Biol. Chem.* **283**, 16514-24.

Geiser, F. (2013). Hibernation. *Curr Biol.* **23**, R188-93.

Gems, D., Sutton, A. J., Sundermeyer, M. L., Albert, P. S., King, K. V., Edgley, M. L., Larsen, P. L. and Riddle, D. L. (1998). Two pleiotropic classes of *daf-2* mutation affect larval arrest, adult behavior, reproduction and longevity in *Caenorhabditis elegans*. *Genetics* **150**, 129–55.

Georgi, L. L., Albert, P. S. and Riddle, D. L. (1990). *daf-1*, a *C. elegans* gene controlling dauer larva development, encodes a novel receptor protein kinase. *Cell* **61**, 635–45.

Gerisch, B., Weitzel, C., Kober-Eisermann, C., Rottiers, V. and Antebi, A. (2001). A hormonal signaling pathway influencing *C. elegans* metabolism, reproductive development, and life span. *Dev. Cell **1***, 841–51.

Ghosh, A. K., Ramakrishnan, G., Chandramohan, C. and Rajasekharan, R. (2008). CGI-58, the causative gene for Chanarin-Dorfman syndrome, mediates acylation of lysophosphatidic acid. *J Biol Chem.* **283**, 24525-33.

Gil, E. B., Malone Link, E., Liu, L. X., Johnson, C. D. and Lees, J. A. (1999). Regulation of the insulin-like developmental pathway of *Caenorhabditis elegans* by a homolog of the PTEN tumor suppressor gene. *Proc. Natl. Acad. Sci. U.S.A.* **96**, 2925–30.

Gilham, D., Alam, M., Gao, W., Vance, D. E. and Lehner, R. (2005). Triacylglycerol hydrolase is localized to the endoplasmic reticulum by an unusual retrieval sequence where it participates in VLDL assembly without utilizing VLDL lipids as substrates. *Mol Biol Cell* **16**, 984–96.

Golden, J. W. and Riddle, D. L. (1984a). The *Caenorhabditis elegans* dauer larva: developmental effects of pheromone, food, and temperature. *Dev. Biol.* **102**, 368–78.

Golden, J. W. and Riddle, D. L. (1984b). A pheromone-induced developmental switch in *Caenorhabditis elegans*: Temperature-sensitive mutants reveal a wild-type temperature-dependent process. *Proc. Natl. Acad. Sci. USA* **8**1, 819–23.

Goodman, J. M. (2008). The gregarious lipid droplet. *J Biol Chem*. **283**, 28005-9.

Gottlieb, S. and Ruvkun, G. (1994). *daf-2, daf-16* and *daf-23*: genetically interacting genes controlling Dauer formation in *Caenorhabditis elegans*. *Genetics* **137**, 107–20.

Grant, B. and Hirsh, D. (1999). Receptor-mediated endocytosis in the Caenorhabditis elegans oocyte. *Mol Biol Cell* **10**, 4311–26.

Granneman, J. G., Moore, H. P., Granneman, R. L., Greenberg, A. S., Obin, M. S. and Zhu, Z. (2007). Analysis of lipolytic protein trafficking and interactions in adipocytes. *J Biol Chem.* **282**, 5726-35.

Granneman, J. G., Moore, H. P., Krishnamoorthy, R. and Rathod, M. (2009a). Perilipin controls lipolysis by regulating the interactions of AB-hydrolase containing 5 (Abhd5) and adipose triglyceride lipase (Atgl). *J Biol Chem.* **284**, 34538-44.

Granneman, J. G., Moore, H. P., Mottillo, E. P. and Zhu, Z. (2009b). Functional interactions between Mldp (LSDP5) and Abhd5 in the control of intracellular lipid accumulation. *J Biol Chem.* **284**, 3049-57.

Greenberg, A. S., Egan, J. J., Wek, S. A., Garty, N. B., Blanchette-Mackie, E. J. and Londos, C. (1991). Perilipin, a major hormonally regulated adipocyte-specific phosphoprotein associated with the periphery of lipid storage droplets. *J Biol Chem.* **266**, 11341-6.

Greenspan, P., Mayer, E. P. and Fowler, S. D. (1985). Nile red: a selective fluorescent stain for intracellular lipid droplets. *J. Cell Biol.* **100**, 965–973.

Greenwald, I. (1998). LIN-12/Notch signaling: lessons from worms and flies. *Genes Dev.* **12**, 1751-62.

Greer, E. R., Perez, C. L., Van Gilst, M. R., Lee, B. H. and Ashrafi K. (2008). Neural and molecular dissection of a C. elegans sensory circuit that regulates fat and feeding. *Cell Metab.* **8**, 118–131.

Greer, E. L., Dowlatshahi, D., Banko, M. R., Villen, J., Hoang, K., Blanchard, D., Gygi, S. P. and Brunet, A. (2007). An AMPK-FOXO pathway mediates longevity induced by a novel method of dietary restriction in C. elegans. *Curr. Biol.* **17**, 1646–56.

Grönke, S., Mildner, A., Fellert, S., Tennagels, N., Petry, S., Müller, G., Jäckle, H. and Kühnlein, R. P. (2005). Brummer lipase is an evolutionary conserved fat storage regulator in Drosophila. *Cell Metab* **1**, 323-30.

Gruber, A., Cornaciu, I., Lass, A., Schweiger, M., Poeschl, M., Eder, C., Kumari, M., Schoiswohl, G., Wolinski, H., Kohlwein, S. D., Zechner, R., Zimmermann, R. and Oberer, M. (2010). The N-terminal region of comparative gene identification-58 (CGI-58) is important for lipid droplet binding and activation of adipose triglyceride lipase. *J Biol Chem.* **285**, 12289-98.

Gunther, C. V., Georgi, L. L. and Riddle, D. L. (2000) A Caenorhabditis elegans type I TGF β receptor can function in the absence of type II kinase to promote larval development. *Development* **127**, 3337–47.

Guo, Y., Walther, T. C., Rao, M., Stuurman, N., Goshima, G., Terayama, K., Wong, J. S., Vale, R. D., Walter, P. and Farese, R. V. (2008). Functional genomic screen reveals genes involved in lipid-droplet formation and utilization. *Nature.* **453**, 657-61.

Haemmerle, G., Lass, A., Zimmermann, R., Gorkiewicz, G., Meyer, C., Rozman, J., Heldmaier, G., Maier, R., Theussl, C., Eder, S., Kratky, D., Wagner, E. F., Klingenspor, M., Hoefler, G. and Zechner, R. (2006). Defective lipolysis and altered energy metabolism in mice lacking adipose triglyceride lipase. *Science* **312**, 734-7.

Hansen M., Chandra, A., Mitic, L. L., Onken, B., Driscoll, M. and Kenyon, C. (2008). A role for autophagy in the extension of lifespan by dietary restriction in *C. elegans*. *PLoS Genetics* **4**, e24.

Hardie, D. G., Ross, F. A. and Hawley, S. A. (2012). AMPK: a nutrient and energy sensor that maintains energy homeostasis. *Nature Reviews Molecular Cell Biology* **13**, 251-62.

Hawley, S. A., Davison, M., Woods, A., Davies, S. P., Beri, R. K., Carling, D. and Hardie, D. G. (1996). Characterization of the AMP-activated protein kinase kinase from rat liver and identification of threonine 172 as the major site at which it phosphorylates AMP-activated protein kinase*. J Biol Chem.* **271**, 27879-87.

Hawley, S. A., Boudeau, J., Reid, J. L., Mustard, K. J., Udd, L., Mäkelä, T. P., Alessi, D. R. and Hardie, D. G. (2003). Complexes between the LKB1 tumor suppressor, STRAD alpha/beta and MO25 alpha/beta are upstream kinases in the AMP-activated protein kinase cascade. *J Biol.* **2**, 28.

Hawley, S. A., Ross, F. A., Chevtzoff, C., Green, K. A., Evans, A., Fogarty, S., Towler, M. C., Brown, L. J., Ogunbayo, O. A., Evans, A. M. and Hardie, D. G. (2010). Use of cells expressing gamma subunit variants to identify diverse mechanisms of AMPK activation. *Cell Metab.* **11**, 554-65.

Hellerer, T., Axäng, C., Brackmann, C., Hillertz, P., Pilon, M. and Enejder, A. (2007). Monitoring of lipid storage in Caenorhabditis elegans using coherent anti-Stokes Raman scattering (CARS) microscopy. *Proc. Natl. Acad. Sci. USA.* **104**, 14658–63.

Henderson, S. T. and Johnson, T. E. (2001) daf-16 integrates developmental and environmental inputs to mediate aging in the nematode C. elegans. *Curr. Biol.* **11**, 1975–80.

Hertweck, M., Gobel, C. and Baumeister, R. (2004). *C. elegans* SGK-1 is the critical component in the Akt/PKB kinase complex to control stress response and life span. *Dev. Cell* **6**, 577–88.

Hollenberg, C. H., Raben, M. S. and Astwood, E. B. (1961). The lipolytic response to corticotropin. *Endocrinology* **68**, 589–98.

Holmes, B. F., Kurth-Kraczek, E. J. and Winder, W. W. (1999). Chronic activation of 5′-AMP-activated protein kinase increases GLUT-4, hexokinase, and glycogen in muscle. *J. Appl. Physiol.* **87**, 1990-5.

Holt, S. J. and Riddle, D. L. (2003). SAGE surveys *C. elegans* carbohydrate metabolism: evidence for an anaerobic shift in the long-lived dauer larva. *Mech. Ageing Dev.* **124**, 779–800.

Holzenberger, M., Dupont, J., Ducos, B., Leneuve, P., Geloen, A., Even, P. C., Cervera, P. and Le Bouc, Y. (2003). IGF-1 receptor regulates lifespan and resistance to oxidative stress in mice. *Nature* **421**, 182–7.

Hong, Y., Roy, R. and Ambros, V. (1998). Developmental regulation of a cyclin-dependent kinase inhibitor controls postembryonic cell cycle progression in Caenorhabditis elegans. *Development*. **125**, 3585-97.

Horvitz, H. R. and Sulston, J. E. (1980). Isolation and genetic characterization of cell-lineage mutants of the nematode Caenorhabditis elegans. *Genetics* **96**, 435-54.

Houthoofd, K., Braeckman, B. P., Lenaerts, I., Brys, K., De Vreese, A., Van Eygen, S. and Vanfleteren, J. R. (2002). Ageing is reversed, and metabolism is reset to young levels in recovering dauer larvae of *C. elegans*. *Exp. Gerontol.* **37**, 1015–21.

Hruz, P. W. and Mueckler, M. M. (2001). Structural analysis of the GLUT1 facilitative glucose transporter. *Mol. Membr. Biol.* **18**, 183-93.

Hsu, A. L., Murphy, C. T. and Kenyon, C. (2003). Regulation of aging and age-related disease by DAF-16 and heat-shock factor. *Science* **300**, 1142–5.

Huang, S. and Czech, M. P. (2007). The GLUT4 glucose transporter. *Cell Metab* **5**, 237–52.

Hu, P. J., Xu, J. and Ruvkun, G. (2006). Two membrane-associated tyrosine phosphatase homologs potentiate *C. elegans* AKT-1/PKB signaling. *PLoS Genet.* **2**, e99.

Inoue, T. and Thomas, J. H. (2000a). Suppressors of transforming growth factor-beta pathway mutants in the *Caenorhabditis elegans* dauer formation pathway. *Genetics* **156**, 1035–46.

Inoue, T. and Thomas, J. H. (2000b). Targets of TGF-beta signaling in *Caenorhabditis elegans* dauer formation. *Dev. Biol.* **217**, 192–204.

Jenkins, C. M., Mancuso, D. J., Yan, W., Sims, H. F., Gibson, B. and Gross, R. W. (2004). Identification, cloning, expression, and purification of three novel human calciumindependent phospholipase A2 family members possessing triacylglycerol lipase and acylglycerol transacylase activities. *J Biol Chem* **279**, 48968–75.

Jia, K., Chen, D. and Riddle, D. L. (2004). The TOR pathway interacts with the insulin signaling pathway to regulate C. elegans larval development, metabolism and life span. *Development* **131**, 3897–906.

Jia, K., Albert, P. S. and Riddle, D. L. (2002). DAF-9, a cytochrome P450 regulating *C. elegans* larval development and adult longevity. *Development* **129**, 221–31.

Jia, K. and Levine, B. (2007). Autophagy is required for dietary restriction-mediated life span extension in *C. elegans*. *Autophagy* ***3***, 597–9.

Jones, S. J., Riddle, D. L., Pouzyrev, A. T., Velculescu, V. E., Hillier, L., Eddy, S. R., Stricklin, S. L., Baillie, D. L., Waterston, R. and Marra, M. A. (2001). Changes in gene expression associated with developmental arrest and longevity in *Caenorhabditis elegans*. *Genome Res.* **11**, 1346–52.

Joost, H. G. and Thorens, B. (2001). The extended GLUT-family of sugar/polyol transport facilitators: nomenclature, sequence characteristics, and potential function of its novel members. *Mol. Membr. Biol.* **18**, 247–56.

Jørgensen, S. B., Viollet, B., Andreelli, F., Frøsig, C., Birk, J. B., Schjerling, P., Vaulont, S., Richter, E. A. and Wojtaszewski, J. F. (2004). Knockout of the α2 but not α1 5′-AMP-activated protein kinase isoform abolishes 5-aminoimidazole-4-carboxamide-

1-β-4-ribofuranoside but not contraction-induced glucose uptake in skeletal muscle. *J. Biol. Chem.* **279**, 1070–9.

Kao, G., Nordenson, C., Still, M., Ronnlund, A., Tuck, S. and Naredi, P. (2007) ASNA-1 positively regulates insulin secretion in C. elegans and mammalian cells. *Cell* **128**, 577–87.

Karlsson, M., Contreras, J. A., Hellman, U., Tornqvist, H. and Holm, C. (1997). cDNA cloning, tissue distribution, and identification of the catalytic triad of monoglyceride lipase. Evolutionary relationship to esterases, lysophospholipases, and haloperoxidases. *J Biol Chem* **272**, 27218–23.

Keller, P., Petrie, J. T., De Rose, P., Gerin, I., Wright, W. S., Chiang, S. H., Nielsen, A. R., Fischer, C. P., Pedersen, B. K. and MacDougald, O. A. (2008). Fat-specific protein 27 regulates storage of triacylglycerol. *J Biol Chem*. **283**, 14355-65.

Kenyon, C., Chang, J., Gensch, E., Rudner, A. and Tabtiang, R. (1993). A C. elegans mutant that lives twice as long as wild type. *Nature*. **366**, 461-4.

Kienesberger, P. C., Oberer, M., Lass, A. and Zechner, R. (2009). Mammalian patatin domain containing proteins: a family with diverse lipolytic activities involved in multiple biological functions. *J Lipid Res* **50**, 63–8.

Kimura, K. D., Tissenbaum, H. A., Liu, Y. and Ruvkun, G. (*1997*). daf-2, an insulin receptor-like gene that regulates longevity and diapause in Caenorhabditis elegans. *Science* **277***,*942-46.

Khavari, T. A. and Rinn, J. (2007). Ras/Erk MAPK signaling in epidermal homeostasis and neoplasia. *Cell Cycle.* **6**, 2928-31.

Khoo, J. C., Reue, K., Steinberg, D. and Schotz, M. C. (1993). Expression of hormone-sensitive lipase mRNA in macrophages. *J Lipid Res* **34**, 1969–74.

Klass, M. R. (1977). Aging in the nematode *Caenorhabditis elegans*: major biological and environmental factors influencing life span. *Mech. Ageing Dev.* **6**, 413–29.

Kobayashi, K., Inoguchi, T., Maeda, Y., Nakashima, N., Kuwano, A., Eto, E., Ueno, N., Sasaki, S., Sawada, F., Fujii, M., Matoba, Y., Sumiyoshi, S., Kawate, H. and Takayanagi, R. (2008). The lack of the C-terminal domain of adipose triglyceride lipase causes neutral lipid storage disease through impaired interactions with lipid droplets. *J Clin Endocrinol Metab.* **93**, 2877-84.

Koh, H. J., Hirshman, M. F., He, H., Li, Y., Manabe, Y., Balschi, J. A. and Goodyear, L. J. (2007). Adrenaline is a critical mediator of acute exercise-induced AMP-activated protein kinase activation in adipocytes. *Biochem. J.* **403**, 473-81.

Komatsu, H., Mori, I., Rhee, J. S., Akaike, N. and Ohshima, Y. (1996). Mutations in a cyclic nucleotide-gated channel lead to abnormal thermosensation and chemosensation in *C. elegans*. *Neuron* **17**, 707–18.

Kondo, M., Senoo-Matsuda, N., Yanase, S., Ishii, T., Hartman, P. S. and Ishii, N. (2005). Effect of oxidative stress on translocation of DAF-16 in oxygen-sensitive mutants, *mev-1* and *gas-1* of *Caenorhabditis elegans*. *Mech. Ageing Dev.* **126**, 637–41.

Kondrashov, F. A., Koonin, E. V., Morgunov, I. G., Finogenova, T. V. and Kondrashova, M. N. (2006). Evolution of glyoxylate cycle enzymes in Metazoa: evidence of multiple horizontal transfer events and pseudogene formatio. *Biology Direct* **1**, 31.

Kraemer, F. B., Patel, S., Saedi, M. S. and Sztalryd, C. (1993). Detection of hormone-sensitive lipase in various tissues. I. Expression of an HSL/bacterial fusion protein and generation of anti-HSL antibodies. *J Lipid Res* **34**, 663–71.

Kraemer, F. B. and Shen, W. J. (2002). Hormone-sensitive lipase: control of intracellular tri-(di-)acylglycerol and cholesteryl ester hydrolysis. *J Lipid Res.* **43**, 1585-94.

Krintel, C., Osmark, P., Larsen, M. R., Resjö, S., Logan, D. T. and Holm, C. (2008). Ser649 and Ser650 are the major determinants of protein kinase A-mediated activation of human hormone-sensitive lipase against lipid substrates. *PLoS One.* **3**, e3756.

Kurat, C. F., Wolinski, H., Petschnigg, J., Kaluarachchi, S., Andrews, B., Natter, K. and Kohlwein, S. D. (2009). Cdk1/Cdc28-dependent activation of the major triacylglycerol lipase Tgl4 in yeast links lipolysis to cell-cycle progression. *Mol Cell.* **33**, 53-63.

Lass, A., Zimmermann, R., Haemmerle, G., Riederer, M., Schoiswohl, G., Schweiger, M., Kienesberger, P., Strauss, J. G., Gorkiewicz, G. and Zechner, R. (2006). Adipose triglyceride lipase-mediated lipolysis of cellular fat stores is activated by CGI-58 and defective in Chanarin-Dorfman syndrome. *Cell Metab.* **3**, 309–19.

Lass, A., Zimmermann, R., Oberer, M. and Zechner, R. (2011). Lipolysis - a highly regulated multi-enzyme complex mediates the catabolism of cellular fat stores. *Prog Lipid Res.* **50**, 14-27.

Lamitina, S. T. and Strange, K. (2005). Transcriptional targets of DAF-16 insulin signaling pathway protect *C. elegans* from extreme hypertonic stress. *Am. J. Physiol. Cell Physiol.* **288**, C467-74.

Lamitina, S. T., Morrison, R., Moeckel, G. M. and Strange, K. (2004). Adaptation of the nematode *Caenorhabditis elegans* to extreme osmotic stress. *Am. J. Physiol. Cell Physiol.* **286**, C785-91.

Lamitina, S. T., Huang, C. G. and Strange, K. (2006). Genome-wide RNAi screening identifies protein damage as a regulator of osmoprotective gene expression. *Proc. Natl. Acad. Sci. USA* **103**, 12173–8.

Le, T. T., Duren, H. M., Slipchenko, M. N., Hu, C. D. and Cheng, J. X. (2010). Label-free quantitative analysis of lipid metabolism in living Caenorhabditis elegans. *J. Lipid Res.* **51**, 672-7.

Lee, R. Y., Hench, J. and Ruvkun, G. (2001). Regulation of *C. elegans* DAF-16 and its human ortholog FKHRL1 by the *daf-2* insulin-like signaling pathway. *Curr. Biol.* **11**, 1950–7.

Lee, I., Hendrix, A., Kim, J., Yoshimoto, J. and You, Y. J. (2012). Metabolic rate regulates L1 longevity in C. elegans. *PLoS One.* **7**, e44720.

Li, J., Tewari, M., Vidal, M. and Lee, S. S. (2007a). The 14-3-3 protein FTT-2 regulates DAF-16 in *Caenorhabditis elegans*. *Dev. Biol.* **301**, 82–91.

Li, W., Gao, B., Lee, S. M., Bennett, K. and Fang, D. (2007b). RLE-1, an E3 Ubiquitin Ligase, Regulates *C. elegans* Aging by Catalyzing DAF-16 Polyubiquitination. *Dev. Cell* **12**, 235–46.

Li, W., Kennedy, S. G. and Ruvkun, G. (2003). daf-28 encodes a C. elegans insulin superfamily member that is regulated by environmental cues and acts in the DAF-2 signaling pathway. *Genes & Dev.* **17**, 844–58.

Li, Y., Xu, S., Mihaylova, M. M., Zheng, B., Hou, X., Jiang, B., Park, O., Luo, Z., Lefai, E. and Shyy, J. Y. (2011). AMPK phosphorylates and inhibits SREBP activity to attenuate hepatic steatosis and atherosclerosis in diet-induced insulin-resistant mice. *Cell Metab.* **13**, 376-88.

Libina, N., Berman, J. R. and Kenyon, C. (2003). Tissue-specific activities of *C. elegans* DAF-16 in the regulation of lifespan. *Cell* **115**, 489–502.

Lin, Y. Y., Kiihl, S., Suhail, Y., Liu, S. Y., Chou, Y. H., Kuang, Z., Lu, J. Y., Khor, C. N., Lin, C. L. and Bader, J. S. (2012). Functional dissection of lysine deacetylases reveals that HDAC1 and p300 regulate AMPK. *Nature* **482**, 251-55.

Lin, K., Dorman, J. B., Rodan, A. and Kenyon, C. (1997). *daf-16*: An HNF-3/forkhead family member that can function to double the life-span of *Caenorhabditis elegans*. *Science* **278**, 1319–22.

Lin, K., Hsin, H., Libina, N. and Kenyon, C. (2001). Regulation of the *Caenorhabditis elegans* longevity protein DAF-16 by insulin/IGF-1 and germline signaling. *Nat. Genet.* **28**, 139–45.

Listenberger, L. L., Ostermeyer-Fay, A. G., Goldberg, E. B., Brown, W. J. and Brown, D. A. (2007). Adipocyte differentiation-related protein reduces the lipid droplet

association of adipose triglyceride lipase and slows triacylglycerol turnover. *J Lipid Res.* **48**, 2751-61.

Lithgow, G. J. and Walker, G. A. (2002). Stress resistance as a determinate of C. elegans lifespan. *Mech. Ageing Dev.* **123**, 765–71.

Liu, T., Zimmerman, K. K. and Patterson, G. I. (2004) Regulation of signaling genes by TGFβ during entry into dauer diapause in C. elegans. *BMC Dev. Biol.* **4**, 11, doi:10.1186/1471-213X-4-11.

Long, X., Spycher, C., Han, Z. S., Rose, A. M., Muller, F. and Avruch, J. (2002). TOR deficiency in C. elegans causes developmental arrest and intestinal atrophy by inhibition of mRNA translation. *Curr Biol.* **12**, 1448–61.

Mak, H. Y. and Ruvkun, G. (2004). Intercellular signaling of reproductive development by the *C. elegans* DAF-9 cytochrome P450. *Development* **131**, 1777–86.

Marcinkiewicz, A., Gauthier, D., Garcia, A. and Brasaemle, D. L. (2006). The phosphorylation of serine 492 of Perilipin a directs lipid droplet fragmentation and dispersion. *J Biol Chem.* **281**, 11901-9.

Maxfield, F. R. and Tabas, I. (2005). Role of cholesterol and lipid organization in disease. *Nature.* **438**, 612-21.

McBride, A., Ghilagaber, S., Nikolaev, A. and Hardie, D. G. (2009). The glycogen-binding domain on the AMPKβ subunit allows the kinase to act as a glycogen sensor. *Cell Metab.* **9**, 23-34.

McElwee, J., Bubb, K. and Thomas, J. H. (2003). Transcriptional outputs of the Caenorhabditis elegans forkhead protein DAF-16. *Aging Cell* **2**, 111–21.

McElwee, J. J., Schuster, E., Blanc, E., Thomas, J. H. and Gems, D. (2004). Shared transcriptional signature in *Caenorhabditis elegans* dauer larvae and long-lived *daf-2* mutants implicates detoxification system in longevity assurance. *J. Biol. Chem.* **279**, 44533–43.

McElwee, J. J., Schuster, E., Blanc, E., Thornton, J. and Gems, D. (2006). Diapause-associated metabolic traits reiterated in long-lived *daf-2* mutants in the nematode *Caenorhabditis elegans*. *Mech. Ageing Dev.* **127***,* 458–72.

McGee, S. L., van Denderen, B. J., Howlett, K. F., Mollica, J., Schertzer, J. D., Kemp, B. E. and Hargreaves, M. (2008). AMP-activated protein kinase regulates GLUT4 transcription by phosphorylating histone deacetylase 5. *Diabetes* **57**, 860-7.

McKay, R. M., McKay, J. P., Avery, L. and Graff, J. M. (2003). C elegans: a model for exploring the genetics of fat storage. *Dev Cell* **4**, 131–42.

Mihaylova, V. T., Borland, C. Z., Manjarrez, L., Stern, M. J. and Sun, H. (1999). The PTEN tumor suppressor homolog in *Caenorhabditis elegans* regulates longevity and dauer formation in an insulin receptor-like signaling pathway. *Proc. Natl. Acad. Sci. U.S.A.* **96**, 7427–32.

Mishra, R. and Simonson, M. S. (2005). Saturated free fatty acids and apoptosis in microvascular mesangial cells: palmitate activates pro-apoptotic signaling involving caspase 9 and mitochondrial release of endonuclease G. *Cardiovasc Diabetol.* **4**, 2.

Miyanari, Y., Atsuzawa, K., Usuda, N., Watashi, K., Hishiki, T., Zayas, M., Bartenschlager, R., Wakita, T., Hijikata, M. and Shimotohno, K. (2007). The lipid droplet is an important organelle for hepatitis C virus production. *Nat Cell Biol.* **9**, 1089-97.

Miyoshi, H., Perfield, J. W. 2nd., Souza, S. C., Shen, W. J., Zhang, H. H., Stancheva, Z. S., Kraemer, F. B., Obin, M. S. and Greenberg, A. S. (2007). Control of adipose triglyceride lipase action by serine 517 of Perilipin A globally regulates protein kinase A-stimulated lipolysis in adipocytes. *J Biol Chem.* **282**, 996-1002.

Montero-Moran, G., Caviglia, J. M., McMahon, D., Rothenberg, A., Subramanian, V., Xu, Z., Lara-Gonzalez, S., Storch, J., Carman, G. M. and Brasaemle, D. L. (2010). CGI-58/ABHD5 is a coenzyme A-dependent lysophosphatidic acid acyltransferase. *J Lipid Res.* **51**, 709-19.

Morris, J. Z., Tissenbaum, H. A. and Ruvkun, G. (1996). A phosphatidylinositol-3-OH kinase family member regulating longevity and diapause in *Caenorhabditis elegans*. *Nature* **382**, 536–9.

Motola, D. L., Cummins, C. L., Rottiers, V., Sharma, K., Sunino, K., Xu, E., Auchus, R., Antebi, A. and Mangelsdorf, M. (2006). Identification of DAF-12 ligands that govern dauer formation and reproduction in C. elegans. *Cell* **124**, 1209–23.

Munoz, M. J. and Riddle, D. L. (2003). Positive selection of C. elegans mutants with increased stress resistance and longevity. *Genetics* **163**, 171–180.

Murakami, M., Koga, M. and Ohshima, Y. (2001). DAF-7/TGF-β expression required for the normal larval development in C. elegans is controlled by a presumed guanylyl cyclase DAF-11. *Mech. Dev.* **109**, 27–35.

Murphy, C. T., McCarroll, S. A., Bargmann, C. I., Fraser, A., Kamath, R. S., Ahringer, J., Li, H. and Kenyon, C. (2003). Genes that act downstream of DAF-16 to influence the lifespan of Caenorhabditis elegans. *Nature.* **424**, 277-83.

Nan, X., Cheng, J. X.and Xie, X. S. (2003). Vibrational imaging of lipid droplets in live fibroblast cells with coherent anti-Stokes Raman scattering microscopy. *J. Lipid Res.* **44**, 2202–8.

Nanji, M., Hopper, N. A. and Gems, D. (2005). LET-60 RAS modulates effects of insulin/IGF-1 signaling on development and aging in Caenorhabditis elegans. *Aging Cell* **4**, 235–45.

Narbonne, P. and Roy, R. (2006). Inhibition of germline proliferation during C. elegans dauer development requires PTEN, LKB1 and AMPK signalling. *Development* **133**, 611-9.

Narbonne, P. and Roy, R. (2009). Caenorhabditis elegans dauers need LKB1/AMPK to ration lipid reserves and ensure long-term survival. *Nature* **457**, 210–4.

Nelson, F. K. and Riddle, D. L. (1984). Functional study of the Caenorhabditis elegans secretory-excretory system using laser microsurgery. *J Exp Zool.* **231**, 45-56.

Oakhill, J. S., Chen, Z. P., Scott, J. W., Steel, R., Castelli, L. A., Ling, N., Macaulay, S. L. and Kemp, B. E. (2010). β-Subunit myristoylation is the gatekeeper for initiating metabolic stress sensing by AMP-activated protein kinase (AMPK). *Proc Natl Acad Sci U S A.* **107**, 19237-41.

Ogg, S., Paradis, S., Gottlieb, S., Patterson, G. I., Lee, L., Tissenbaum, H. A. and Ruvkun, G. (1997). The Fork head transcription factor DAF-16 transduces insulin-like metabolic and longevity signals in C. elegans*. Nature* **389**, 994–9.

Ogg, S. and Ruvkun, G. (1998). The *C. elegans* PTEN homolog, DAF-18, acts in the insulin receptor-like metabolic signaling pathway. *Mol. Cell* **2**, 887–93.

Oh, S. W., Mukhopadhyay, A., Svrzikapa, N., Jiang, F., Davis, R. J. and Tissenbaum, H. A. (2005). JNK regulates lifespan in Caenorhabditis elegans by modulating nuclear translocation of forkhead transcription factor/DAF-16. *Proc. Natl. Acad. Sci.* **102**, 4494-9.

Ohkura, K., Suzuki, N., Ishihara, T. and Katsura, I. (2003). SDF-9, a protein tyrosine phosphatase-like molecule, regulates the L3/dauer developmental decision through hormonal signaling in *C. elegans*. *Development* **130**, 3237–48.

Ohsaki, Y., Cheng, J., Fujita, A., Tokumoto, T. and Fujimoto, T. (2006). Cytoplasmic lipid droplets are sites of convergence of proteasomal and autophagic degradation of apolipoprotein B. *Mol Biol Cell.* **17**, 2674-83.

Ojuka, E. O., Nolte, L. A. and Holloszy, J. O. (2000). Increased expression of GLUT-4 and hexokinase in rat epitrochlearis muscles exposed to AICAR *in vitro*. *J. Appl. Physiol.* **88**, 1072-5.

Okazaki, H., Igarashi, M., Nishi, M., Tajima, M., Sekiya, M., Okazaki, S., Yahagi, N., Ohashi, K., Tsukamoto, K., Amemiya-Kudo, M., Matsuzaka, T., Shimano, H., Yamada, N., Aoki, J., Morikawa, R., Takanezawa, Y., Arai, H., Nagai, R., Kadowaki, T., Osuga, J. and Ishibashi, S. (2006). Identification of a novel member of the carboxylesterase family that hydrolyzes triacylglycerol: a potential role in adipocyte lipolysis. *Diabetes* **55**, 2091–7.

O'Neill, H. M., Maarbjerg, S. J., Crane, J. D., Jeppesen, J., Jørgensen, S. B., Schertzer, J. D., Shyroka, O., Kiens, B., van Denderen, B. J., Tarnopolsky, M. A., Kemp, B. E., Richter, E. A. and Steinberg, G. R. (2011). AMP-activated protein kinase (AMPK) beta1beta2 muscle null mice reveal an essential role for AMPK in maintaining mitochondrial content and glucose uptake during exercise. *Proc Natl Acad Sci U S A.* **108**, 16092-7.

Orci, L., Cook, W. S., Ravazzola, M., Wang, M. Y., Park, B. H., Montesano, R. and Unger, R. H. (2004). Rapid transformation of white adipocytes into fat-oxidizing machines. *Proc. Natl. Acad. Sci. U.S.A.* **101**, 2058-63.

Osterlund, T., Danielsson, B., Degerman, E., Contreras, J. A., Edgren, G., Davis, R. C., Schotz, M. C. and Holm, C. (1996). Domain-structure analysis of recombinant rat hormone-sensitive lipase*. Biochem J* **319**, 411–20.

O'Riordan, V. B. and Burnell, A. M. (1989). Intermediary metabolism in the dauer larva of the nematode *Caenorhabditis elegans* - 1. Glycolysis, gluconeogenesis, oxidative phosphorylation and the tricarboxylic acid cycle. *Comp. Biochem. Physiol*. **92B**, 233–38

O'Rourke, E. J., Soukas, A. A., Carr, C. E. and Ruvkun, G. (2009). C. elegans major fats are stored in vesicles distinct from lysosome-related organelles. *Cell Metab*. **10**, 430-5.

Pagnon, J., Matzaris, M., Stark, R., Meex, R. C., Macaulay, S. L., Brown, W., O'Brien, P. E., Tiganis, T. and Watt, M. J. (2012). Identification and functional characterization of protein kinase a phosphorylation sites in the major lipolytic protein, adipose triglyceride lipase. *Endocrinology* **153**, 4278–89.

Panowski, S. H., Wolff, S., Aguilaniu, H., Durieux, J. and Dillin, A. (2007). PHA-4/Foxa mediates diet-restriction-induced longevity of *C. elegans. Nature* **447**, 536–7.

Paradis, S., Ailion, M., Toker, A., Thomas, J. H. and Ruvkun, G. (1999). A PDK1 homolog is necessary and sufficient to transduce AGE-1 PI3 kinase signals that regulate diapause in *Caenorhabditis elegans*. *Genes Dev.* **13**, 1438–52.

Paradis, S. and Ruvkun, G. (1998). *Caenorhabditis elegans* Akt/PKB transduces insulin receptor-like signals from AGE-1 PI3 kinase to the DAF-16 transcription factor. *Genes Dev.* **12**, 2488–98.

Patterson, G. I., Koweek, A., Wong, A., Liu, Y. and Ruvkun, G. (1997). The DAF-3 Smad protein antagonizes TGF-beta-related receptor signaling in the *Caenorhabditis elegans* dauer pathway. *Genes Dev.* **11**, 2679–90.

Patterson, G. I. and Padgett, R. W. (2000). TGF beta-related pathways. Roles in *Caenorhabditis elegans* development. *Trends Genet.* **16**, 27–33.

Paul, R. J., Gohla, J., Föll, R. and Schneckenburger, H. (2000). Metabolic adaptations to environmental changes in *Caenorhabditis elegans*. *Comp. Biochem. Physiol.* **127B**, 469–79.

Pazdernik, N. and Schedl, T. (2013). Introduction to germ cell development in Caenorhabditis elegans. *Adv Exp Med Biol.* **757**, 1-16.

Pehmøller, C., Treebak, J. T., Birk, J. B., Chen, S., Mackintosh, C., Hardie, D. G., Richter, E. A. and Wojtaszewski, J. F. (2009). Genetic disruption of AMPK signaling abolishes both contraction- and insulin-stimulated TBC1D1 phosphorylation and 14-3-3 binding in mouse skeletal muscle. *Am J Physiol Endocrinol Metab.* **297**, 665-75.

Peng, I. C., Chen, Z., Sun, W., Li, Y. S., Marin, T. L., Hsu, P. H., Su, M. I., Cui, X., Pan, S. and Lytle, C. Y. (2012). Glucagon regulates ACC activity in adipocytes through the CAMKKβ/AMPK pathway. *Am. J. Physiol. Endocrinol. Metab.* **302**, 1560-8.

Petriv, O. I. and Rachubinski, R. A. (2004). Lack of peroxisomal catalase causes a progeric phenotype in Caenorhabditis elegans. *J Biol Chem.* **279**, 19996-20001.

Pierce, S. B., Costa, M., Wisotzkey, R., Devadhar, S., Homburger, S. A., Buchman, A. R., Ferguson, K. C., Heller, J., Platt, D. M., Pasquinelli, A. A., Liu, L. X., Dorberstain, S. K. and Ruvkun, G. (2001). Regulation of DAF-2 receptor signaling by human insulin and *ins-1*, a member of the unusually large and diverse *C. elegans* insulin gene family. *Genes Dev.* **15**, 672–86.

Polakof, S., Moon, T. W., Aguirre, P., Skiba-Cassy, S. and Panserat, S. (2011). Glucose homeostasis in rainbow trout fed a high-carbohydrate diet: metformin and insulin interact in a tissue-dependent manner. *Am. J. Physiol. Regul. Integr. Comp. Physiol.* **300**, 166-74.

Puri, V., Konda, S., Ranjit, S., Aouadi, M., Chawla, A., Chouinard, M., Chakladar, A. and Czech, M. P. (2007). Fat-specific protein 27, a novel lipid droplet protein that enhances triglyceride storage. *J Biol Chem.* **282**, 34213-8.

Ren, P., Lim, C. S., Johnsen, R., Albert, P. S., Pilgrim, D. and Riddle, D. L. (1996). Control of *C. elegans* larval development by neuronal expression of a TGF-beta homolog. *Science* **274**, 1389–91.

Riddle, D. L. and Albert, P. (1997). Genetic and environmental regulation of dauer larva development. *C. elegans II*, 739-68.

Riddle, D. L., Swanson, M. M. and Albert, P. S. (1981). Interacting genes in nematode dauer larva formation. *Nature* **290**, 668–71.

Rinia, H. A., Burger, K. N., Bonn, M. and Muller, M. (2008). Quantitative label-free imaging of lipid composition and packing of individual cellular lipid droplets using multiplex CARS microscopy. *Biophys. J.* **95**, 4908–14.

Robinson-Rechavi, M., Maina, C. V., Gissendanner, C. R., Laudet, V. and Sluder, A. (2005). Explosive lineage-specific expansion of the orphan nuclear receptor HNF4 in nematodes. *J. Mol. Evol.* **60**, 577–86.

Robenek, H., Hofnagel, O., Buers, I., Robenek, M. J., Troyer, D. and Severs, N. J. (2006). Adipophilin-enriched domains in the ER membrane are sites of lipid droplet biogenesis. *J Cell Sci.* **119**, 4215-24.

Romeo, S., Huang-Doran, I., Baroni, M. G. and Kotronen, A. (2010). Unravelling the pathogenesis of fatty liver disease: patatin-like phospholipase domaincontaining 3 protein. *Curr Opin Lipidol.* **21**, 247–52.

Rouault, J. P., Kuwabara, P. E., Sinilnikova, O. M., Duret, L., Thierry-Mieg, D. and Billaud, M. (1999). Regulation of dauer larva development in *Caenorhabditis elegans* by *daf-18*, a homologue of the tumour suppressor PTEN. *Curr. Biol.* **9**, 329–32.

Russell, L. and Forsdyke, D. R. (1991). A human putative lymphocyte G0/G1 switch gene containing a CpG-rich island encodes a small basic protein with the potential to be phosphorylated. *DNA Cell Biol.* **10**, 581-91.

Sakamoto, K. and Holman, G. D. (2008). Emerging role for AS160/TBC1D4 and TBC1D1 in the regulation of GLUT4 traffic. *Am. J. Physiol. Endocrinol. Metab.* **295**, 29–37.

Sakamoto, K., Zarrinpashneh, E., Budas, G. R., Pouleur, A. C., Dutta, A., Prescott, A. R., Vanoverschelde, J. L., Ashworth, A., Jovanović, A., Alessi, D. R. and Bertrand, L. (2005). Deficiency of LKB1 in skeletal muscle prevents AMPK activation and glucose uptake during contraction. *EMBO J.* **24**, 1810–20.

Salt, I. P., Celler, J. W., Hawley, S. A., Prescott, A., Woods, A., Carling, D. and Hardie, D. G. (1998). AMP-activated protein kinase: greater AMP dependence, and preferential nuclear localization, of complexes containing the α2 isoform. *Biochem. J.* **334**, 177-87.

Sanli, T., Rashid, A., Liu, C., Harding, S., Bristow, R. G., Cutz, J. C., Singh, G., Wright, J. and Tsakiridis, T. (2010). Ionizing radiation activates AMP-activated kinase (AMPK): a target for radiosensitization of human cancer cells. *Int J Radiat Oncol Biol Phys.* **78**, 221-9.

Sawin, E. R., Ranganathan, R. and Horvitz, H. R. (2000). C. elegans locomotory rate is modulated by the environment through a dopaminergic pathway and by experience through a serotonergic pathway. *Neuron* **26**, 619–31.

Schaffer, J. E. and Lodish, H. F. (1994). Expression cloning and characterization of a novel adipocyte long chain fatty acid transport protein. *Cell* **79**, 427–436.

Schackwitz, W. S., Inoue, T. and Thomas, J. H. (1996). Chemosensory neurons function in parallel to mediate a pheromone response in C. elegans. *Neuron* **17**, 719–28.

Schweiger, M., Schreiber, R., Haemmerle, G., Lass, A., Fledelius, C., Jacobsen, P. Tornqvist, H., Zechner, R. and Zimmermann, R. (2006). Adipose triglyceride lipase and hormone-sensitive lipase are the major enzymes in adipose tissue triacylglycerol catabolism. *J Biol Chem* **281**, 40236–41.

Schweiger, M., Schoiswohl, G., Lass, A., Radner, F. P., Haemmerle, G., Malli, R., Graier, W., Cornaciu, I., Oberer, M., Salvayre, R., Fischer, J., Zechner, R. and Zimmermann, R. (2008). The C-terminal region of human adipose triglyceride lipase affects enzyme activity and lipid droplet binding. *J Biol Chem* **283**, 17211–20.

Senoo-Matsuda, N., Yasuda, K., Tsuda, M., Ohkubo, T., Yoshimura, S., Nakazawa, H., Hartman, P. S. and Ishii, N. (2001). A defect in the cytochrome b large subunit in complex II causes both superoxide anion overproduction and abnormal energy metabolism in *Caenorhabditis elegans*. *J. Biol. Chem.* **276**, 41553–8.

Shaw, R. J., Kosmatka, M., Bardeesy, N., Hurley, R. L., Witters, L. A., DePinho, R. A. and Cantley, L. C. (2004). The tumor suppressor LKB1 kinase directly activates AMP-activated kinase and regulates apoptosis in response to energy stress. *Proc Natl Acad Sci U S A.* **101**, 3329-35.

Shaw, W. M., Luo, S., Landis, J., Ashraf, J. and Murphy, C. T. (2007). The C. elegans TGF-β dauer pathway regulates longevity via insulin signaling. *Curr. Biol.* **17**, 1635–45.

Shen, W. J., Patel, S., Natu, V. and Kraemer, F. B. (1998). Mutational analysis of structural features of rat hormone-sensitive lipase. *Biochemistry* **37**, 8973–9.

Shen, C. and Powell-Coffman, J. A. (2003). Genetic analysis of hypoxia signaling and response in *C. elegans*. *Ann. N. Y. Acad. Sci.* **995**, 191–9.

Shen, W. J., Sridhar, K., Bernlohr, D. A. and Kraemer, F. B. (1999). Interaction of rat hormonesensitive lipase with adipocyte lipid-binding protein. *Proc Natl Acad Sci USA* **96**, 5528–32.

Siloto, R. M., Findlay, K., Lopez-Villalobos, A., Yeung, E. C., Nykiforuk, C. L. and Moloney, M. M. (2006). The accumulation of oleosins determines the size of seed oilbodies in Arabidopsis. *Plant Cell.* **18**, 1961-74.

Singh, R., Kaushik, S., Wang, Y., Xiang, Y., Novak, I., Komatsu, M., Tanaka, K., Cuervo, A. M. and Czaja, M. J. (2009). Autophagy regulates lipid metabolism. *Nature* **458**, 1131-5.

Snow, M. I. and Larsen, P. L. (2000). Structure and expression of daf-12: A nuclear hormone receptor with three isoforms that are involved in development and aging in Caenorhabditis elegans. *Biochim. Biophys. Acta* **1494**, 104–16.

Sohal, R.S. and Weindruch, R. (1996). Oxidative stress, caloric restriction, and aging. *Science* **273**, 59–63.

Srinivasan, S., Sadegh, L., Elle, I. C., Christensen, A. G., Faergeman, N. J. and Ashrafi, K. (2008). Serotonin regulates C. elegans fat and feeding through independent molecular mechanisms. *Cell Metab.* **7**, 533–44.

Su, C. L., Sztalryd, C., Contreras, J. A., Holm, C., Kimmel, A. R. and Londos, C. (2003). Mutational analysis of thehormone-sensitive lipase translocation reaction in adipocytes.*J. Biol. Chem.* **278**, 43615–9.

Subramanian, V., Rothenberg, A., Gomez, C., Cohen, A. W., Garcia, A., Bhattacharyya, S., Shapiro, L., Dolios, G., Wang, R., Lisanti, M. P. and Brasaemle, D. L. (2004). Perilipin A mediates the reversible binding of CGI-58 to lipid droplets in 3T3-L1 adipocytes. *J Biol Chem.* **279**, 42062-71.

Sullivan, J. E., Brocklehurst, K. J., Marley, A. E., Carey, F., Carling, D. and Beri, R. K. (1994). Inhibition of lipolysis and lipogenesis in isolated rat adipocytes with AICAR, a cell-permeable activator of AMP-activated protein kinase. *FEBS Lett.* **353**, 33-6.

Sulston, J. E., Schierenberg, E., White, J. G. and Thomson, J. N. (1983).The embryonic cell lineage of the nematode Caenorhabditis elegans. *Dev Biol.* **100**, 64-119.

Suter, M., Riek, U., Tuerk, R., Schlattner, U., Wallimann, T. and Neumann, D. (2006). Dissecting the role of 5'-AMP for allosteric stimulation, activation, and deactivation of AMP-activated protein kinase. *J Biol Chem.* **281**, 32207-16.

Szymanski, K. M., Binns, D., Bartz, R., Grishin, N. V., Li, W. P., Agarwal, A. K., Garg, A., Anderson, R. G. and Goodman, J. M. (2007). The lipodystrophy protein seipin is found at endoplasmic reticulum lipid droplet junctions and is important for droplet morphology. *Proc Natl Acad Sci U S A.* **104**, 20890-5.

Takekoshi, K., Fukuhara, M., Quin, Z., Nissato, S., Isobe, K., Kawakami, Y. and Ohmori, H. (2006). Long-term exercise stimulates adenosine monophosphate-activated protein kinase activity and subunit expression in rat visceral adipose tissue and liver. *Metab. Clin. Exp.* **55**, 1122-8.

Tansey, J. T., Sztalryd, C., Gruia-Gray, J., Roush, D. L., Zee, J. V., Gavrilova, O., Reitman, M. L., Deng, C. X., Li, C., Kimmel, A. R. and Londos, C. (2001). Perilipin ablation results in a lean mouse with aberrant adipocyte lipolysis, enhanced leptin production, and resistance to diet-induced obesity. *Proc Natl Acad Sci U S A.* **98**, 6494-9.

Tatar, M., Kopelman, A., Epstein, D., Tu, M. P., Yin, C. M. and Garofalo, R. S. (2001). A mutant Drosophila insulin receptor homolog that extends life-span and impairs neuroendocrine function. *Science* **292**, 107–10.

Tecott, L. H., Sun, L. M., Akana, S. F., Strack, A. M., Lowenstein, D. H., Dallman, M. F. and Julius, D. (1995). Eating disorder and epilepsy in mice lacking 5-HT2c serotonin receptors. *Nature* **374**, 542–6.

Tewari, M., Hu, P. J., Ahn, J. S., Ayivi-Guedehoussou, N., Vidalain, P. O., Li, S., Milstein, S., Armstrong, C. M., Boxem, M., Butler, M. D., Busiguina, S., Rual, J. F., Ibarrola, N., Chaklos, S. T., Bertin, N., Vaglio, P., Edgley, M. L., King, K. V., Albert, P. S., Vandenhaute, J., Pandey, A., Riddle, D. L., Ruvkun, G. and Vidal, M. (2004).

Systematic interactome mapping and genetic perturbation analysis of a *C. elegans* TGF-beta signaling network. *Mol. Cell* ***13***, 469–82.

Thomas, J. H., Birnby, D. A. and Vowels, J. J. (1993). Evidence for parallel processing of sensory information controlling dauer formation in *Caenorhabditis elegans*. *Genetics* **134**, 1105–17.

Tornqvist, H. and Belfrage, P. (1976). Purification and some properties of a monoacylglycerol-hydrolyzing enzyme of rat adipose tissue. *J Biol Chem* **251**, 813–9.

Troemel, E. R., Chu, S. W., Reinke, V., Lee, S. S., Ausubel, F. M. and Kim, D. H. (2006). p38 MAPK regulates expression of immune response genes and contributes to longevity in C. elegans. *PLoS Genet.* **2**, e183, doi:10.131/journal.pgen.0020183.

Vanfleteren, J. R. and De Vreese, A. (1996). Rate of aerobic metabolism and superoxide production rate potential in the nematode *Caenorhabditis elegans. J. Exp. Zool.* **274**, 93–100.

Van Voorhies, W. A. and Ward, S. (1999). Genetic and environmental conditions that increase longevity in *Caenorhabditis elegans* decrease metabolic rate. *Proc. Natl. Acad. Sci. USA* **96**, 11399–403.

Van Voorhies, W. A. and Ward, S. (2000). Broad oxygen tolerance in the nematode *Caenorhabditis elegans*. *J. Exp. Biol.* **203,** 2467–78.

Vaughan, M., Berger, J. E. and Steinberg, D. (1964). Hormone-sensitive lipase and monoglyceride lipase activities in adipose tissue. *J Biol Chem* **239**, 401–9.

Vellai, T., Takacs-Vellai, K., Zhang, Y., Kovacs, A. L., Orosz, L. and Müller, F. (2003). Genetics: influence of TOR kinase on lifespan in *C. elegans*. *Nature*, **426**, 620.

Villena, J. A., Roy, S., Sarkadi-Nagy, E., Kim, K. H. and Sul, H. S. (2004). Desnutrin, an adipocyte gene encoding a novel patatin domain-containing protein, is induced by fasting and glucocorticoids: ectopic expression of desnutrin increases triglyceride hydrolysis. *J Biol Chem* **279**, 47066–75.

Vowels, J. J. and Thomas, J. H. (1992). Genetic analysis of chemosensory control of dauer formation in *Caenorhabditis elegans*. *Genetics* **130**, 105–23.

Wältermann, M., Hinz, A., Robenek, H., Troyer, D., Reichelt, R., Malkus, U., Galla, H. J., Kalscheuer, R., Stöveken, T., von Landenberg, P. and Steinbüchel, A. (2005). Mechanism of lipid-body formation in prokaryotes: how bacteria fatten up. *Mol Microbiol.* **55**, 750-63.

Walther, T. C. and Farese, R. V. Jr. (2009). The life of lipid droplets. *Biochim Biophys Acta.* **1791**, 459-66.

Wang, J. and Kim, S. K. (2003). Global analysis of dauer gene expression in *Caenorhabditis elegans*. *Development* **130,** 1621–34.

Wang, M. C., Min, W., Freudiger, C. W., Ruvkun, G. and Xie, X. S. (2011). RNAi screening for fat regulatory genes with SRS microscopy. *Nat. Methods* **8**, 135–8.

Wang, M. C., O'Rourke, E. J. and Ruvkun, G. (2008). Fat metabolism links germline stem cells and longevity in C. elegans. *Science* **322**, 957–60.

Wang, H., Hu, L., Dalen, K., Dorward, H., Marcinkiewicz, A., Russell, D., Gong, D., Londos, C., Yamaguchi, T., Holm, C., Rizzo, M. A., Brasaemle, D. and Sztalryd, C. (2009). Activation of hormone-sensitive lipase requires two steps, protein phosphorylation and binding to the PAT-1 domain of lipid droplet coat proteins. *J Biol Chem.* **284**, 32116-25.

Wilson, E. (1896). The cell in development and Inheritance. *New York: Macmillan.*

Wolins, N. E., Skinner, J. R., Schoenfish, M. J., Tzekov, A., Bensch, K. G. and Bickel, P. E. (2003). Adipocyte protein S3-12 coats nascent lipid droplets. *J Biol Chem.* **278**, 37713-21.

Wolins, N. E., Quaynor, B. K., Skinner, J. R., Schoenfish, M. J., Tzekov, A. and Bickel, P. E. (2005). S3-12, Adipophilin, and TIP47 package lipid in adipocytes. *J Biol Chem.* **280**, 19146-55.

Wolins, N. E., Quaynor, B. K., Skinner, J. R., Tzekov, A., Croce, M. A., Gropler, M. C., Varma, V., Yao-Borengasser, A., Rasouli, N., Kern, P. A., Finck, B. N. and Bickel, P. E. (2006a). OXPAT/PAT-1 is a PPAR-induced lipid droplet protein that promotes fatty acid utilization. *Diabetes.* **55**, 3418-28.

Wolins, N. E., Brasaemle, D. L. and Bickel, P. E. (2006b). A proposed model of fat packaging by exchangeable lipid droplet proteins. *FEBS Lett.* **580**, 5484-91

Wolkow, C. A., Kimura, K. D., Lee, M. S. and Ruvkun, G. (2000). Regulation of *C. elegans* life-span by insulinlike signaling in the nervous system. *Science* **290**, 147–150.

Wolff, S., Ma, H., Burch, D., Maciel, G. A., Hunter, T. and Dillin, A. (2006) SMK-1, an essential regulator of DAF-16-mediated longevity. *Cell* **124**, 1039–53.

Wong, A., Boutis, P. and Hekimi, S. (1995). Mutations in the *clk-1* gene of *Caenorhabditis elegans* affect developmental and behavioral timing. *Genetics* **139**, 1247–59.

Wood, I. S. and Trayhurn, P. (2003). Glucose transporters (GLUT and SGLT): expanded families of sugar transport proteins. *Br J Nutr.* **89**, 3-9.

Xiao, B., Heath, R., Saiu, P., Leiper, F. C., Leone, P., Jing, C., Walker, P. A., Haire, L., Eccleston, J. F. and Davis, C. T. (2007). Structural basis for AMP binding to mammalian AMP-activated protein kinase. *Nature* **449**, 496-500.

Xiao, B., Sanders, M.J., Underwood, E., Heath, R., Mayer, F. V., Carmena, D., Jing, C., Walker, P. A., Eccleston, J. F., Haire, L. F., Saiu, P., Howell, S. A., Aasland, R., Martin, S. R., Carling, D. and Gamblin, S. J. (2011). Structure of mammalian AMPK and its regulation by ADP. *Nature.* **472**, 230-3.

Xu, N., Zhang, S. O., Cole, R. A., McKinney, S. A., Guo, F., Haas, J. T., Bobba, S., Farese, R. V. Jr. and Mak, H. Y. (2012). The FATP1-DGAT2 complex facilitates lipid droplet expansion at the ER-lipid droplet interface. *J Cell Biol.* **198**, 895-911.

Yang, X., Lu, X., Lombès, M., Rha, G. B., Chi, Y. I., Guerin, T. M., Smart, E. J. and Liu, J. (2010). The G(0)/G(1) switch gene 2 regulates adipose lipolysis through association with adipose triglyceride lipase. *Cell Metab.* **11**, 194-205.

Yang, F., Vought, B. W., Satterlee, J. S., Walker, A. K., Jim, Sun Z. Y., Watts, J. L., DeBeaumont, R., Saito, R. M. and Hyberts, S. G. (2006). An ARC/Mediator subunit required for SREBP control of cholesterol and lipid homeostasis. *Nature* **442**, 700–4.

Yeaman, S. J. (1990). Hormone-sensitive lipase – a multipurpose enzyme in lipid metabolism. *Biochim Biophys Acta* **1052**, 128–32.

Yeaman, S. J., Smith, G. M., Jepson, C. A., Wood, S. L. and Emmison, N. (1994). The multifunctional role of hormone-sensitive lipase in lipid metabolism. *Adv Enzyme Regul* **34**, 355–70.

Yen, K., Le, T. T., Bansal, A., Narasimhan, S. D., Cheng, J. X. and Tissenbaum, H. A. (2010). A comparative study of fat storage quantitation in nematode Caenorhabditis elegans using label and label-free methods. *PLoS ONE* **5**. pii:e12810.

Yen, C. L., Stone, S. J., Koliwad, S., Harris, C. and Farese, R. V. Jr. (2008). Thematic review series: glycerolipids. DGAT enzymes and triacylglycerol biosynthesis. *J Lipid Res.* **49**, 2283-301.

Yin, W., Mu, J. and Birnbaum, M. J. (2003). Role of AMP-activated protein kinase in cyclic AMP-dependent lipolysis in 3T3-L1 adipocytes. *J. Biol. Chem.* **278**, 43074-80.

Ylikorkala, A., Avizienyte, E., Tomlinson, I. P., Tiainen, M., Roth, S., Loukola, A., Hemminki, A., Johansson, M., Sistonen, P., Markie, D., Neale, K., Phillips, R., Zauber, P., Twama, T., Sampson, J., Järvinen, H., Mäkelä, T. P. and Aaltonen, L. A. (1999). Mutations and impaired function of LKB1 in familial and non-familial Peutz-Jeghers syndrome and a sporadic testicular cancer. *Hum Mol Genet.* **8**, 45-51.

Zechner, R., Kienesberger, P. C., Haemmerle, G., Zimmermann, R. and Lass, A. (2009). Adipose triglyceride lipase and the lipolytic catabolism of cellular fat stores. *J Lipid Res.* **50**, 3-21.

Zhang, B. B., Zhou, G. and Li, C. (2009). AMPK: an emerging drug target for diabetes and the metabolic syndrome. *Cell Metab.* **9**, 407-16.

Zhang, S. O., Trimble, R., Guo, F. and Mak, H. Y. (2010). Lipid droplets as ubiquitous fat storage organelles in C. elegans. *BMC Cell Biol.* **11**, 96.

Zimmermann, R., Strauss, J. G., Haemmerle, G., Schoiswohl, G., Birner-Gruenberger, R., Riederer, M., Lass, A., Neuberger, G., Eisenhaber, F., Hermetter, A. and Zechner, R. (2004). Fat mobilization in adipose tissue is promoted by adipose triglyceride lipase. *Science* **306**, 1383-6.

Zmijewski, J. W., Banerjee, S., Bae, H., Friggeri, A., Lazarowski, E. R. and Abraham, E. (2010). Exposure to hydrogen peroxide induces oxidation and activation of AMP-activated protein kinase. *J. Biol. Chem.* **285**, 33154-64.

Chapter 2: Increased Levels of Hydrogen Peroxide Induce a HIF-1-Dependent Modification of Lipid Metabolism in AMPK Compromised *C. elegans* Dauer Larvae

Meng Xie and Richard Roy

Reproduced (with permission) from: *Cell metabolism* 2012, 16:322-35

Summary

Cells have evolved numerous mechanisms to circumvent stresses caused by the environment and many of them are regulated by the AMP-activated kinase (AMPK). Unlike most organisms, *C. elegans* AMPK null mutants are viable, but die prematurely in the “long-lived” dauer stage due to exhaustion of triglyceride stores. Using a genome-wide RNAi approach we demonstrate that the disruption of genes that increase hydrogen peroxide levels enhance the survival of AMPK mutant dauers by altering both the abundance and the nature of the fatty acid content in the animal by increasing the HIF-1-dependent expression of several key enzymes involved in fatty acid biosynthesis. Our data provide a mechanistic foundation to explain how an optimal level of an often vilified ROS-generating compound such as hydrogen peroxide can provide cellular benefit; a phenomenon described as hormesis, by instructing cells to re-adjust their lipid biosynthetic capacity through downstream HIF-1 activation to correct cellular energy deficiencies.

Introduction

Throughout the course of evolutionary history environmental fluctuations have played a major role in determining both the number and the morphological diversity of our current biota. Factors such as limiting resource availability and/or accessibility were most likely instrumental in driving adaptations that, among other effects, were capable of enhancing survival during periods of environmental duress by impinging upon behaviour and metabolic changes that improved survivability. This is well demonstrated in animals that have adapted to prolonged periods of nutrient deprivation. In the case of bears for example, hibernation is preceded by a highly active preparatory phase during which the animal increases its body weight by 40%, mostly in form of both brown and white adipose tissue (Jonkel et al., 1977). In rodents and humans, extensive physical stress/activity or nutrient stress is often accompanied by hormonal imbalance and reproductive arrest, presumably to ensure that development is paused when macromolecular components are limiting. In doing so, animals link physiology to both development and behaviour (Holliday, 1989; Kirkwood, 1977; Selesniemi et al., 2008).

This is not unique to mammals, as many invertebrates have adapted diapause-like states to enhance survival during severe environmental stresses. Many parasitic nematodes develop through a highly resistant “dauer” stage that is important to escape host defenses during infection (Riddle and Georgi, 1990), while in the free living nematode *C. elegans*, the dauer stage is not obligatory, but instead provides the animal with an effective means of dispersal and increased stress resistance.

In *C. elegans* three parallel genetic pathways converge to ensure cell division arrest, behavioural and morphological alterations, and finally, a phase of global metabolic change that are all characteristic of dauer formation. One common downstream effector of these three pathways is the AMP-activated protein kinase (AMPK) (Narbonne and Roy, 2006). Following activating phosphorylation by LKB1/PAR-4, it will phosphorylate targets that block anabolic processes and activate gene products involved in energy generation (Hawley et al., 2003; Woods et al., 2003; Hardie, 2007).

In AMPK mutant dauer larvae the germ line contains greater than 4-fold the normal complement of germ cells (Narbonne and Roy, 2006). Independent of any effects on the germ line, the larvae die after 10 days because, despite their transient accumulation of fat upon dauer entry, they hydrolyse it rapidly and deplete their fat reservoirs in less than 48h following dauer formation (Narbonne and Roy, 2009).

In most animals fat is stored in the form of triglycerides, and the hydrolysis of these triglycerides into free fatty acids is catalysed by adipose triglyceride lipase (ATGL) (Zimmermann et al., 2004). In *C. elegans* ATGL-1 is phosphorylated and inhibited by AMPK to preserve the triglyceride stores for use during the course of the diapause (Narbonne and Roy, 2009). Loss of AMPK in *C. elegans* dauer larvae leads to the misregulation of ATGL-1, resulting in rapid mobilization of the triglyceride stores, and the consequent premature expiration of the larvae (Narbonne and Roy, 2009).

Removal of ATGL-1 partially rescues the premature lethality of AMPK mutant dauer larvae, therefore we reasoned that we could identify novel factors that act downstream of AMPK to enhance ATGL-1 function, to preserve the lipid stores and prolong survival of the AMPK mutant dauer larvae. Using an RNA interference (RNAi) feeding strategy we identified 551 genes that, when compromised, enhanced the survival of AMPK mutant dauer larvae. Surprisingly, the loss of any one of the three *C. elegans* catalase (*ctl)* genes could suppress all the previously described metabolic defects associated with compromised AMPK function.

Our characterisation of the effects of catalase mutations on AMPK mutant dauer survival reveal a hitherto unforeseen role of H_2O_2 in activating HIF-1 *in vivo*, which alters cell physiology to favour growth and survival under stress. Moreover, we provide molecular evidence to explain H_2O_2/ROS-mediated hormesis, while underscoring the need to establish a fine equilibrium between the beneficial and harmful effects of these oxygen species.

Results

A Global Genome Survey to Identify Genes that Enhance the Survival of AMPK Mutant Dauer Larvae

Loss of AMPK in *C. elegans* dauer larvae results in premature arrest due to exhaustion of fat reserves that would normally sustain the animal throughout the dauer stage (Narbonne and Roy, 2006). Compromise of ATGL-1 partially rescued the dauer-dependent lethality and the abnormal loss of lipid in AMPK compromised dauer larvae. To identify genes that cooperate with ATGL-1 and/or that may act downstream of AMPK in energy regulation, we conducted a global genome survey using an RNA interference (RNAi) feeding strategy (Kamath et al., 2001). We screened over 18,000 genes for candidates that, when compromised, enhanced the survival of AMPK mutant dauer larvae. The *atgl-1* RNAi clone was identified randomly as a positive candidate from our primary screen, assuring us that our strategy was specific and effective. 551 additional RNAi clones were identified, for which about 60% have been assigned a functional signature based on gene ontology and/or available experimental data (Figure 2.1A).

We noted that the compromise of any one of two catalase genes in the library (*ctl-1* and *ctl-2*) increased the survival of AMPK mutant dauers (Figure 2.1B). Catalases play an important role in the neutralisation of hydrogen peroxide (H_2O_2) and thus may regulate the cellular load of reactive oxygen species (ROS). Because ROS impinges on so many cellular processes including lifespan and lipid metabolism, we chose to further study how the loss of catalase function might affect these processes and hence enhance dauer survival in AMPK mutants.

We obtained three mutant strains, each of which has a single deletion in each of the catalase family members; *ctl-1* (*ok1242*), *ctl-2* (*ok1137*) and *ctl-3* (*ok2042*). The *ctl-1* mutation is a severe loss of function allele (Coolon et al., 2009), while *ctl-2* (*ok1137*) and *ctl-3* (*ok2042*) are unlikely to encode functional proteins (Boon et al., 2007).

AMPK mutant dauer larvae expire prematurely due to rapid mobilization of their triglyceride stores and failure of the excretory system to maintain osmotic balance (Narbonne and Roy, 2009). Surprisingly, mutation of any one of the *ctl* genes

significantly increased the survival of AMPK mutant dauers, most notably when *ctl-3* function was compromised (Figure 2.1C). In addition, each of the three alleles restored total lipid and triglyceride levels to near wild type levels (Figure 2.1D and E), and corrected the osmoresistance defect, especially at high salt concentrations (Figure 2.1F). Conversely, the germline hyperplasia typical of AMPK mutant dauers was unaffected by any of the catalase mutations.

Curiously, the catalase mutations do not provide the same survival benefit in AMPK mutant dauers that are induced with pheromone (data not shown). The reason for this distinction is not yet clear but is reminiscent of the differential effects of the dauer-inducing mutations on lifespan extension, wherein only *daf-2* mutations exhibit any appreciable effect (Kimura et al.,1997). This unique aspect of the *daf-2* mutants likely reflects the metabolic readjustment that these larvae undergo in response to the nutrient stress that accompanies a block in insulin signaling, which does not occur in dauer larvae where the insulin-like signaling pathway remains active.

Taken together, we conclude that compromise of any individual catalase gene function is sufficient to restore the regulated breakdown of stored triglycerides over a prolonged duration, while consequently re-establishing excretory/osmoregulatory function in the AMPK mutant dauer larvae.

Disruption of Catalase Function Increases Lipid Droplet Size and Attenuates ATGL-1 Activity in AMPK Mutant Dauers

Since we observed a significant improvement in lipid retention in AMPK mutant dauers that lacked catalase, we questioned whether the compromise of *ctl* function could differentially affect ATGL-1 activity and thus account for the accumulation and maintenance of fat stores. To meet this end we measured the total triglyceride lipase activity in extracts obtained from both AMPK and catalase-deficient AMPK mutant dauer larvae and found that it was decreased by two-fold in the *ctl*-compromised AMPK mutant dauers (Figure 2.2A). We performed *atgl-1(RNAi)* on the catalase-deficient AMPK mutant dauers to determine whether the reduction in lipase activity could be

attributed to effects on ATGL-1. The attenuated lipase activity in these catalase-deficient mutant dauers was not further affected by *atgl-1(RNAi)* suggesting that the loss of catalase function ultimately blocked ATGL-1 activity in these double mutant dauers (Figure 2.2A).

In mammalian cells ATGL is under complex regulation by CGI-58 and Perilipin, both of which reside on lipid droplets in the adipose tissue (Schweiger et al., 2008; Gruber et al., 2010). Recent data showed that the disruption of peroxisomal β-oxidation expands the size of lipid droplets and was accompanied by an increase in triglyceride levels (Zhang et al., 2010). Because changes to the lipid droplet composition or architecture could contribute to the net activity of ATGL, we wondered whether the loss of *ctl* function affects the capacity of ATGL-1 to hydrolyse the lipid reserves in AMPK mutant dauer larvae by altering the morphology of the lipid droplets. By fluorescently staining lipids and using Oil Red O, we noted a significant expansion in lipid droplet size in day 1 *ctl*-deficient AMPK mutant dauers (Figure 2.2 G-K and C-F), which was most pronounced in *ctl-3*-deficient AMPK mutant dauers. The size expansion of the lipid droplets observed in catalase mutant dauers could be beneficial at two levels: first, they could provide additional storage volume to accommodate an increased level of triglycerides in catalase-deficient AMPK mutant dauers (Figure 2.1D and E); and second, the enlarged lipid droplets could alter the enzymatic activity of ATGL-1 and thereby affect its rate of triglyceride hydrolysis.

H_2O_2 Produced from Fatty Acid β-Oxidation in the Peroxisomes Increased the Dauer Survival of AMPK CTL Mutant Dauers.

Since the major function of catalase is to convert H_2O_2 into water and oxygen, we questioned whether the accumulation of H_2O_2 caused by the loss of catalase function was responsible for the enhanced survival of AMPK mutant dauers. We therefore assessed the levels of both total ROS and H_2O_2 in catalase-deficient AMPK mutant dauers and compared the levels with AMPK mutant dauer larvae. The total ROS levels were significantly decreased in AMPK single mutants compared to control *daf-2* mutant

dauer larvae, while mutation of any individual *ctl* gene marginally increased ROS levels in AMPK mutant dauers (Figure 2.3A). In contrast, the H_2O_2 levels were markedly increased in all catalase-deficient AMPK mutant dauers, which could be reversed by treatment with the potent antioxidant N-acetylcysteine (NAC) (Figure 2.3B). This suggests that the loss of catalase contributes more significantly to the overall levels of H_2O_2 rather than other ROS species that are present in these mutant dauers. To further confirm the effect of increased H_2O_2 levels on dauer survival, we treated the catalase-deficient AMPK mutant dauers with 10mM NAC and, in parallel, we cultured AMPK mutant dauers in the presence of H_2O_2 or with paraquat (Pq), a strong ROS-generating compound, to determine their effects on dauer survival. Consistent with the idea that the increase in H_2O_2 levels confers the beneficial effect on dauer survival, treatment with 0.1% H_2O_2, but not 10µM paraquat increased the survival of AMPK mutant dauers (Figure 2.3F and G). Moreover, treatment with 10mM NAC reversed the effect associated with catalase disruption, and reduced the survival of all three strains of catalase-deficient AMPK mutant dauers (Figure 2.3C-E). These results suggest that it is the increased level of H_2O_2 that consequently led to the prolonged survival of catalase-deficient AMPK mutant dauers.

One major source of H_2O_2 production arises from fatty acid oxidation that occurs in the peroxisome. Since the increased survival of catalase-deficient AMPK mutant dauers was related to changes in the mobilization of the triglyceride stockpile, we questioned whether the elevated levels of H_2O_2 observed in the catalase-deficient dauer larvae may be produced from peroxisomal fatty acid β-oxidation. To verify this we eliminated *daf-22* gene function, which disrupts the final step in peroxisomal fatty acid β-oxidation, in both AMPK and catalase-deficient AMPK mutant dauer larvae to determine whether the increased H_2O_2 production could be reversed in the latter. Disruption of peroxisomal fatty acid β-oxidation was sufficient to reverse the observed elevated H_2O_2 levels in the catalase-deficient AMPK mutant dauers (Figure 2.3H). We further noted that the compromise of several mitochondrial genes could also extend dauer survival, potentially by increasing flux through the peroxisomal β-oxidation pathway and generating increased H_2O_2 biproducts (Figure S2.3). These candidates were not identified in our initial screen because the affected animals expire before reaching the cutoff we

established at 10 days post dauer. Since H_2O_2 is a major product of fat catabolism, the accumulation of the reaction products could potentially affect ATGL-1 activity via product inhibition (Walter and Frieden, 1963)**.**

Taken together, our results suggest that increased peroxisomal fatty acid β-oxidation results in elevated H_2O_2 levels that accumulate in catalase-deficient AMPK mutant dauers. This increase in H_2O_2, might account for the attenuated lipase activity, presumably by affecting ATGL-1, or alternatively through protecting the accumulated fat stores in the larva from rapid depletion.

Increased Survival of AMPK CTL Mutant Dauers is HIF-1-Dependent

Given that modest increases in H_2O_2 or ROS can stimulate the hypoxia-inducible transcription factor HIF-1 to activate gene expression and promote longevity (Chandel et al., 1998; Lee et al., 2010), we determined whether the increased H_2O_2 generated in catalase-deficient AMPK mutant dauers could induce HIF-1 activation to ultimately prolong survival. In order to monitor the activation of HIF-1 we introduced a HIF-1-responsive GFP reporter, *Pnhr-57::GFP*, into the catalase-deficient AMPK mutant and AMPK mutant dauer larvae and monitored GFP expression during the dauer stage (Miyabayashi et al., 1999). We observed an increase in *Pnhr-57::GFP* expression in all three of the catalase-deficient AMPK mutant dauer backgrounds (Figure 2.4A). To verify that the increased expression of the HIF sensor indeed resulted from the increased H_2O_2 levels in the various mutants, we monitored GFP reporter expression in AMPK mutant dauers harbouring the HIF-1 sensor following treatment with 0.1% H_2O_2. Indeed, the level of *Pnhr-57::GFP* was also significantly increased compared to untreated AMPK mutant dauers (Figure 2.4A and B)

HIF-1 activity is regulated predominantly by affecting its stability, which in turn is controlled by the prolyl hydoxylase (PHD)-mediated modification of the HIF-1 protein (Epstein et al., 2001; Cockman et al., 2000). Optimal PHD activity is highly dependent on O_2 levels, and its cofactors Fe II and 2-oxoglutarate (Epstein et al., 2001). Previous findings indicated that H_2O_2 may oxidize Fe II to Fe III, thereby inhibiting PHD to

ultimately stabilise HIF-1 (Gerald et al., 2004). If the increased amount of H_2O_2 observed in the catalase-deficient AMPK mutant dauer larvae affects the cellular oxidation state of Fe II, this change could result in HIF-1 stabilisation despite otherwise normoxic conditions. Our data are consistent with this since HIF-1 accumulates in the *ctl-1*, *ctl-2* and *ctl-3* mutant backgrounds to levels that are near the range of those seen with *vhl-1(RNAi),* while similar HIF-1 stabilisation is observed by treating animals with 0.1% H_2O_2 (Figure 2.4C). Somewhat unexpectedly, we did not note any effect of AMPK depletion on HIF-1 levels, contrary to findings reported in other contexts (Shackelford et al., 2009; Shaw, 2006; Brugarolas and Kaelin, 2004). We further assessed HIF-1 protein levels in catalase-deficient AMPK mutant dauers treated with 10mM NAC which resulted in a significant drop in HIF-1 levels (Figure 2.4D) that was reversed following a combined treatment of H_2O_2 and NAC (Figure S2.4). No effect was observed following a combined treatment of NAC and *vhl-1(RNAi)* (Figure S2.4). We interpret these data to indicate that the increased H_2O_2 generated in catalase-deficient AMPK mutant dauer larvae stabilises HIF-1, potentially by blocking PHD function.

To determine if the activation of HIF-1 was associated with the prolonged survival of the catalase-deficient AMPK mutant dauers, we eliminated HIF-1 activity in these dauers and assessed its effects on dauer survival. *hif-1(RNAi)* reduced dauer survival in all three catalase-deficient AMPK mutant strains (Figure 2.4E-G). Conversely, *vhl-1(RNAi)* and *egl-9(RNAi)* both extended the survival of AMPK mutant dauers (Figure 2.4H). These results suggested that the elevated H_2O_2 levels in the catalase-deficient AMPK mutant dauers activate HIF-1-dependent transcription, which consequently prolongs the survival of the AMPK mutant dauers.

HIF-1 Activates Expression of Genes Involved in Fatty Acid Biosynthesis

Because the reduction of catalase activity was sufficient to restore lipid levels to near wild type levels in AMPK mutant dauers we surmised that HIF-1 activation would have to impinge on lipid biosynthesis. We therefore analysed the fatty acid composition of AMPK and catalase-deficient AMPK mutant dauers using Gas Chromatography/Mass

Spectrometry (GC/MS) and noted that additional monomethyl branched-chain fatty acid species (C15ISO and C17ISO) and significantly more polyunsaturated long chain Fatty Acids (PUFA) were present in the AMPK mutant dauers that lacked catalase when compared to *daf-2: aak(0)* dauers (Figure 2.5A). The branched fatty acids originate almost entirely from the *de novo* synthesis pathway (Perez and Van Gilst, 2008), which may be stimulated in the dauer larvae that lack catalase. However, because of the inherent limitations in our method of analysis, we were unable to quantitatively assess the rate of *de novo* fatty acid synthesis. Nevertheless, the loss of catalase function caused a substantial increase in triglyceride levels in these dauer animals, despite the lack of dietary intake, while also affecting the accumulation of branched chain fatty acids and PUFAs.

The rate of fatty acid synthesis is under strict control by enzymes that catalyse several rate-limiting reactions and HIF-1 could affect lipid biosynthesis by increasing the expression of key enzymes involved in any one, or several of these steps. To address this possibility we analysed the expression of enzymes involved in fatty acid synthesis and noted that the expression of *fat-2*, *fat-3*, *fat-5*, *fat-6*, *fat-7*, *elo-5* and *elo-6* were all significantly increased in AMPK mutant dauers that lacked catalase, especially in those that lacked *ctl-3* (Figure 2.5B). FAT-2 is involved in the desaturation of oleate (C18:1) and FAT-3 desaturates linoleate (C18:2) and alpha-linolenate (C18:3n-3) respectively, while FAT-5 catalyzes the desaturation of palmitate (C16:0) to palmitoleate (C16:1). The FAT-6 and FAT-7 desaturases mainly affect the generation of oleate (C18:1n9) using stearate (C18:0) as a substrate, while ELO-5 and ELO-6 catalyse the formation of C15ISO and C17ISO (Reviewed by Watts, 2009). All of these enzymes catalyse rate-limiting steps in the synthesis of fatty acids in *C. elegans*, the transcript levels of which are all greatly affected by the loss of catalase activity in AMPK mutant dauers. Based on these observations, we suggest that following its activation in the animals lacking catalase, HIF-1 promotes the survival of AMPK mutant dauers by activating the transcription of enzymes involved in the rate-limiting desaturase and elongation steps during fatty acid synthesis. To test this further, we performed *hif-1(RNAi)* in catalase-deficient AMPK mutant dauers and assessed their fatty acid composition using GC/MS. By eliminating HIF-1, the additional fatty acid species observed in the catalase-deficient

AMPK mutant dauers disappeared and the overall fatty acid profile resembled that of AMPK mutant dauers (Figure 2.5C-E). To further confirm the role of HIF-1 and H_2O_2 in affecting fatty acid biosynthesis we verified whether both *hif-1(RNAi)* or 10mM NAC treatment could also reverse the observed increases in expression of the rate-limiting enzymes required for fatty acid biosynthesis. Consistent with a role for HIF-1 in activating their transcription and hence altering the fatty acid composition in catalase-deficient AMPK mutants, we found that all the gains in gene expression observed for each of these critical enzymes were suppressed following either *hif-1(RNAi)* or NAC treatment (Figure 2.5F).

Despite the fact that the dauer larva can use alternative pathways to generate macromolecular precursors (O'Riordan and Burnell, 1990; Wise et al., 2011; Metallo et al., 2011; Mullen et al., 2011), their compromise had no effect on dauer survival in the catalase-deficient AMPK mutants or the AMPK mutant dauers alone (Figure S2.5).

Taken together, our results suggest that HIF-1 activates the expression of rate-limiting enzymes that mediate desaturation and elongation during fatty acid synthesis to stimulate the production of specific fatty acid species, which finally contribute to the prolonged survival of the AMPK mutant dauers.

Differential Effects of Catalase Genes on Dauer Survival Reflect Varying Degrees of Oxidative Protein Damage, but not Lipid Depletion.

The removal of ATGL-1 suppresses the premature lethality of AMPK mutant dauers (Figure 2.6A) by slowing the rapid hydrolysis of lipid stores, presumably providing the animals with a long-term energy source. Although we observe a similar effect on lipid stores by eliminating any one of the catalase genes, we noted considerable differences in survival between each of the mutants (Figure 2.1C), while we also found that their survival could not be improved by removing ATGL-1 (Figure 2.6B-D). Furthermore, *atgl-1(RNAi)*, or *atgl-1(RNAi)* combined with a 10mM NAC treatment, prolonged survival of *ctl-1/2*; AMPK mutant dauers, but reversed the enhanced survival typical of *ctl-3*; AMPK mutant dauers (Figure 2.6B-D). These results led us to question whether the depletion

of fat stores in these mutants was indeed the primary cause for their expiration. To address this we determined the total fat content in terminally-arrested catalase-deficient AMPK mutant to find that the arrested *ctl-1;* and *ctl-2*; AMPK mutant dauers terminate prior to the exhaustion of their available fat stores (Figure 2.6E); while *ctl-3* AMPK mutant dauers were clear, indicating that their lipid stores were exhausted (Figure 2.6E). These observations suggested that the depletion of fat stores was not the primary reason for the terminal arrest of both the *ctl-1;* and *ctl-2;* AMPK mutant dauer larvae.

Since catalase enzymes are responsible for protecting the cell from oxidative damage, and the levels of ROS were significantly increased in these mutant backgrounds, it is conceivable that the catalase-deficient AMPK mutant dauers expire because of excessive oxidative damage that would normally be buffered through the protection conferred by the catalase enzymes. ROS cause damage by introducing carbonyl groups onto proteins which can be quantified using standard immunoblotting methods. *ctl-1;* and *ctl-2;* AMPK mutant dauers demonstrated significantly higher levels of carbonylated proteins, the levels of which were comparable to control dauers treated with the strong ROS generating compound 0.1mM paraquat (Figure 2.6F). On the other hand, the level of oxidative protein damage observed in *ctl-3;* AMPK mutant dauers was significantly lower than either of the two other catalase mutants suggesting that the primary cause of terminal arrest in *ctl-1/-2* AMPK mutant dauer larvae was most likely due to excessive oxidative protein/macromolecular damage, and not depletion of lipid reserves, as was the case in AMPK and *ctl-3;* AMPK mutant dauer larvae. This was further supported by our determination of catalase activity, where AMPK and *ctl-3*; AMPK mutant dauer larvae demonstrated significantly higher catalase activity compared to the other two catalase-deficient AMPK mutant dauer larvae (Figure 2.6G).

Taken together, these results suggest that a balance between HIF-1-mediated fatty acid synthesis and H_2O_2-induced oxidative damage must be achieved to maximize the survival of catalase-deficient AMPK mutant dauers. Since *ctl-3* is the least active member of the catalase family, its disruption only marginally increased the level of H_2O_2, yet nonetheless to a level sufficient to trigger a substantial beneficial effect through the activation of HIF-1, yet without generating the excessive levels of oxidative protein

damage typical of its paralogues *ctl-1/-2*. It is this fine equilibrium between HIF-1 activation and the damaging effects of ROS generation that explains the enhanced survival of *ctl-3* mutations compared to *ctl-1*, and *ctl-2* AMPK mutant dauers (Figure 2.1C).

Discussion

The *C. elegans* dauer stage represents an extraordinary example of metabolic remodelling in response to environmental stress. Since dauer larvae stop feeding yet remain motile, it is imperative that the animals derive energy from intracellular sources, but without any possibility of replenishing these resources from the external environment. This is satisfied first by accumulating fat before dauer entry and later, during dauer, by actively maintaining pathways involved in both carbohydrate and lipid synthesis/hydrolysis throughout the duration of the diapause. (Figure S2.2A; O'Riordan and Burnell, 1990; Perez and Van Gilst, 2008).

The regulation of these pathways in *C. elegans*, like in most organisms, is largely dependent on AMPK; a master regulator of metabolic homeostasis. In the dauer larva AMPK attenuates the activity of the triglyceride lipase ATGL-1 to protect long-term energy stores (Narbonne and Roy, 2009). In situations of compromised AMPK signaling, ATGL-1 activity is abnormally high, reducing the global triglyceride levels remarkably, consequently leading to premature dauer lethality. Curiously, some fatty acid species are substantially reduced in AMPK mutant dauers (Figure S2.2B), suggesting that AMPK not only regulates triglyceride hydrolysis in dauer larvae, but must also impinge on fatty acid biosynthesis, perhaps through its well-known targets *ACC1/2* (*pod-2* in *C. elegans*). Whether these fatty acid species are required to contribute to the overall lipid/energy pool or whether they may play additional roles in signaling during the dauer stage still remains to be determined. Recent data have shown that alterations in the AMPK-dependent regulation of fatty acid synthesis can have widespread positive and negative implications for cellular homeostasis suggesting that AMPK compromise may extend beyond the maintenance of the lipid pool during dauer (Jeon et al., 2012). Nevertheless, many of the metabolic changes typical of dauer development most likely involve AMPK. In the absence of AMPK, dauer larvae that are compromised for insulin signaling are incapable of re-adjusting to the physiological constraints imposed by this state and as a result expire prematurely.

Using a non-biased genome-wide survey we identified 551 RNAi clones that affect the survival of prematurely arresting AMPK mutant dauers. These gene identities will help

us to build a framework to better understand how AMPK converges on a plethora of cellular processes required to promote the typical long-term survival of the dauer larva. Among the most common groups of genes we identified in our screen were nuclear hormone receptors, ubiquitin ligases, F-box containing proteins and Zn-finger containing proteins; setting the stage for further interrogation of their individual roles in the typical metabolic remodeling that accompanies dauer development.

Our data also suggest that the peroxisome may play a central role in regulating dauer survival since peroxide consuming enzymes, such as *mlt-7*, T06D8.10 and *prdx-3*, and a gene that affects peroxisomal fatty acid oxidation encoded by ZK550.5; a peroxisomal phytanoyl-CoA hydroxylase enzyme, were also identified in our RNAi screen. Other genes that affect mitochondrial function or genes such as malate dehydrogenase (*mdh-1*), which generates NADPH to reduce peroxide levels, prolong dauer survival in the AMPK mutants (Figure S2.6), although some of these were not identified in our screen due to our cutoff criteria.

Not all gene products that alter peroxisome function or morphology are involved in this pathway: several peroxisomal genes that have been characterised for their roles in the maintenance of lipid droplet morphology were not identified as suppressors of the AMPK-dependent lethality in dauers (Zhang et al. 2010). The candidates that we identified most likely affect cellular H_2O_2 levels and it is the compromise of this function of the peroxisome that enhances the survival of AMPK mutant dauer larvae.

Because we identified both *ctl-1* and *-2* in this screen, we focused on how the loss of catalase gene function could confer organismal survival in a situation where energy resources are drastically limited; namely during the dauer diapause in *C. elegans.* The observed beneficial effect of each of the individual catalase genes on AMPK mutant dauer survival is somewhat curious based on their described expression patterns (Petriv and Rachubinski, 2004). However, each of the catalase genes is significantly upregulated in essentially all tissues in dauer larvae (Figure S2.1), suggesting that a threshold level of organismal catalase activity is required to counteract the general increase in ROS typical of dauer (Figure 2.3A). Nonetheless, in addition to their effects on premature dauer lethality, the individual compromise of these genes also blocked the

abnormally rapid hydrolysis of fat stores, while also improving the osmosensitivity of AMPK mutant dauers; essentially correcting all the AMPK-dependent metabolic defects that we have characterised in the dauer larva.

More importantly however, the loss of these gene functions allowed us to unveil a previously uncharacterised role of H_2O_2 as a major effector of lipid homeostasis during nutrient stress. In this sensitised background where H_2O_2 is allowed to accumulate, we were able to demonstrate how its increased levels can re-adjust the fatty acid biosynthetic machinery to ultimately prolong the survival of the dauer larvae, despite the metabolic challenges it must confront due to the loss of AMPK function. Curiously, the increases in H_2O_2 rescue all the metabolic defects that arise due to the disruption of AMPK by activating HIF-1 to alter gene expression to favour fatty acid biosynthesis, but also through its HIF-1-independent effects on ATGL-1 activity, the molecular basis of which is still unclear (Figure 2.2B).

Our data strongly indicate that incremental changes in H_2O_2, a major contributor to intracellular ROS levels, can extend dauer survival when supra-threshold levels activate a sensitive intracellular oxygen sensor, HIF-1. Many physiological conditions have been shown to affect HIF-1 activity and most of them do so by protecting HIF-1 from VHL-mediated degradation. Previous findings have implicated H_2O_2 in perturbing PHD function through its ability to drive the Fenton reaction to decrease the effective cellular concentrations of Fe II (Gerald et al. 2004). Whether the observed increases in H_2O_2 affect the cellular Fe II oxidation state in AMPK mutant dauers is unclear, but such changes may provide a plausible explanation for the HIF-1 accumulation. By blocking PHD function, HIF-1 accumulates, allowing this critical factor to re-adjust the entire transcriptional repertoire of the organism to better adapt to the perceived environmental stress and prolong survival in the stressed state (Figure 2.7).

Over the course of the last century ROS have been implicated in several different contexts, where they almost invariably have been shown to interrupt cellular functions by damaging macromolecules involved in key cellular/physiological processes. These negative effects of ROS have recently been critically evaluated using genetically-tractable systems (reviewed by Hekimi et al., 2011; Owusu-Ansah and Banerjee, 2009).

The outcome of this body of work is perplexing since, quite unexpectedly, low to intermediate concentrations of ROS were actually found to be beneficial for some of these processes, namely stem cell function and lifespan extension.

So how could such a vilified family of molecular intermediates act in a beneficial way? In 1943, Southam and Ehrlich described how sub-critical concentrations of toxic compounds could confer cellular benefit through a presumptive intracellular adaptation mechanism that was referred to as “hormesis”. This phenomenon has been demonstrated for many toxic compounds (Cook et al., 2006; Heinz et al., 2010) and recently, this same effect has been shown for ROS in *C. elegans* (Schulz et al., 2007; Mouchiroud et al., 2011; Lee et al., 2010).

The pro-survival benefits we describe here are entirely attributable to increases in H_2O_2 levels within the animal. These beneficial effects correspond to a limited range of H_2O_2 levels that likely approaches, but does not exceed some threshold concentration, above which results in macromolecular damage. This is best demonstrated in *ctl-1* and *-2* mutants where any benefit that these mutations confer on dauer survival through the generation of extra lipid/energy, is counterbalanced by the extensive oxidative protein damage that eventually results in terminal arrest. In contrast, loss of *ctl-3* gene increases the levels of H_2O_2 only modestly, placing it in the optimal range to activate a HIF-1-dependent transcriptional effect without the consequences of ROS-mediated macromolecular damage. Our data therefore provide a molecular basis to account for the hormesis attributed to cases of low to intermediate levels of H_2O_2 and/or ROS production.

The activation of a HIF-1-dependent transcriptional program that affects cellular energy stores is indeed critical for adapting to energy stress and prolonging the survival of these dauer larvae. These changes are typical of the metabolic adjustments that occur in cancer cells associated with the Warburg effect, where energetically sound pathways are modified to provide a novel means of satisfying the unique growth requirements of these rogue cells, while consequently compromising their energetic efficiency (Deberardinis et al. 2007).

In this light, the events that occur during the nutrient-constrained dauer stage may be representative of what occurs during tumourigenesis. The tumour environment can be very dense, and therefore the internal regions are often nutrient-depleted and largely hypoxic. This favours HIF-1 activation, which drives the transcription of numerous factors that will ultimately impinge on many angiogenic and metabolic regulators (Semenza, 2010). This is very common in rapidly growing, aggressive tumours, and is often associated with poor prognosis (reviewed by Dewhirst et al., 2008). Our data indicate that in addition to the known effects of HIF-dependent transcription on angiogenesis and cell growth, it may also dramatically alter the expression of several rate-limiting enzymes required for lipid biosynthesis. These changes in lipid synthesis may in turn directly or indirectly affect other processes that impinge on cell survival (Jeon et al., 2012).

If HIF-1 can affect the ability of the tumour cells to generate their own energy by modifying their capacity for lipid biosynthesis, its activation in the cells deep within the tumour would make them less dependent on nutrient delivery, while also releasing them from external regulatory constraints, thereby enhancing their potential for unscheduled growth. Because AMPK would normally play a protective role to block cell growth in response to poor nutrient availability or during oxidative stress, it would seem imperative to evaluate whether activation of HIF-1 is associated with the loss of LKB1 or AMPK in various tumours, or in patients with tumour predisposing syndromes such as Peutz Jeghers Disease.

Experimental Procedures

Feeding RNAi

Our feeding RNAi protocol was performed as described (Kamath et al., 2001). Briefly, L3-L4 stage hermaphrodites were transferred onto regular plates seeded with individual dsRNA-expressing bacterial clones. The animals were transferred to a new set of seeded plates after 1 day of incubation at 15°C and phenotypes were scored for the F2 generation.

Dauer Survival

Dauer survival was determined as described elsewhere (Narbonne and Roy, 2006). Briefly, dauer larvae were kept in double-distilled water or with dissolved chemicals. Survival was scored according to their appearance and moving response to a gentle tap on the plate. For H_2O_2 treatment, treated animals were protected from light with aluminium foil and were exposed to freshly prepared H_2O_2 solution daily to prevent H_2O_2 decomposition.

Oil Red O Staining of Dauer Larvae

Oil Red O staining of dauer larvae was performed as described (Soukas et al., 2009). Dauer larvae were fixed in 2% paraformaldehyde and stained with 60% Oil Red O solution. Stained dauer larvae were observed and imaged using a Zeiss Imager.21 microscope equipped with a Hamamatsu camera and DIC optics. Optical density was determined using OpenLab software (Improvision).

Worm Extract Preparation

Worm extracts were prepared by sonication and subsequent centrifugation. Protein concentration was determined using a NanoDrop 2000c spectrophotometer (Thermo Scientific).

Triglyceride Quantification

Triglyceride content was determined with a commercially available kit (Sigma-Aldrich) according to manufacturer’s recommendations. Absorbance was measured with a

NanoDrop 2000c spectrophotometer at 540 nm. All calculated triglyceride concentrations were finally normalized to protein concentration.

Osmotic Resistance Assay

Osmotic resistance of dauer larvae was performed as described (Narbonne and Roy, 2009). The survival of day 4 dauer larvae was scored after being exposed to solutions of varying NaCl concentrations for 24 hours at 25°C.

Quantification of Lipase Activity

Lipase activity for dauer animals was measured as described (Narbonne and Roy, 2009) using a commercially available QuantiChrom kit from BioAssay Systems according to manufacturer's recommendations. OD values were measured with a Varioskan Flash Multimode Reader version 3.00.7 at the wavelength of 412 nm.

C1-BODIPY-C12 Staining

C1-BODIPY-C12 staining was performed as described (Mak et al., 2006). Synchronized L1 larvae were transferred to regular plates with C1-BODIPY-C12 and grown at 25°C until they reach the dauer stage. C1-BODIPY-C12 stained dauer larvae were observed and imaged using a Zeiss Imager.21 microscope outfitted with DIC optics equipped with a Hamamatsu camera. Lipid droplet diameter was measured using Openlab software and volume was calculated using the following formula: $4/3 \times \pi \times (\text{diameter}/2)^3$.

Measurement of Reactive Oxygen Species

ROS levels were quantified as described elsewhere (Lee et al., 2010). Worm extracts were incubated with 2',7'-Dichlorofluorescein Diacetate (DCF-DA). Fluorescence intensity was measured with a Varioskan Flash Multimode Reader version 3.00.7 at the excitation wavelength of 485 nm and the emission wavelength 535 nm.

Hydrogen Peroxide Quantification

Hydrogen peroxide level was determined with a commercially available Amplex Red Hydrogen Peroxide/Peroxidase Assay Kit (Invitrogen) according to manufacturer's recommendations. The fluorescence was measured with a Varioskan Flash Multimode

Reader version 3.00.7 at the excitation wavelength of 540 nm and the emission wavelength 560 nm. The fluorescence intensity was normalized by subtracting the background fluorescence of the Amplex Red reagent/HRP working solution.

Gas Chromatography/Mass Spectrometry Analysis (GC/MS)

Fatty acids were extracted into the organic phase as described (Miquel and Browse, 1992). Gas chromatography was performed on a HP6890N instrument (Agilent) equipped with a DB-23 column (30 m × 250 µm × 0.25 µm). The column was run at a constant flow mode at 0.8ml/min. The initial oven temperature was 160°C with an initial time of 1min. It was increased to a final temperature of 240°C at a rate of 4°C/min with a final time of 10 min. The detector was at 240°C. Fatty acid (FA) species were identified by comparison with FA standards (C8-C24, Supelco) and mass spectrometric analysis.

RNA Isolation and Real Time PCR

Total RNA was extracted using Trizol (Invitrogen) as described (Burdine and Stern, 1996) and purified with the RNeasy kit (Qiagen) according to manufacturer's recommendations. RNA concentration and purity were determined by using a NanoDrop 2000c spectrophotometer. 0.5 µg of purified RNA was used to synthesize cDNA. Gene expression levels were determined by real time PCR using the SYBR® Green Supermix and BioRad iCycler Real Time PCRSystem (BioRad). Relative gene expression was normalized to *act-1* and *cdc-42* as internal loading control.

Oxidative Protein Damage Level Measurement

The level/degree of oxidative protein damage was measured using a commercially available kit (Oxyblot) as described (Yang et al., 2007). Band intensities were measured using OpenLab software and normalized to α-tubulin present in the same sample.

Statistical Analysis

Values are mean+SD. Comparison of mean values was evaluated by one-way ANOVA followed by a Tukey HSD test. A p value less than 0.05 was considered significant. In all experiments, the number of asterisks represents the following: * $P<0.05$ and ** $P<0.01$.

Acknowledgements

We thank Dr. Jo Anne Powell-Coffman for the ZG120 strain; *iaIs[Pnhr-57::GFP; unc-119(+)]* strain, and Dr. Peter J Ratcliffe for HIF-1 antibody. We also thank Tamara Western for use of the GC/MS and the *Caenorhabditis* Genetic Center for *C. elegans* strains. This work was supported by a research grant from Canadian Institutes of Health Research (CIHR).

References

Boon, E. M., Downs, A. and Marcey, D. (2007). Proposed mechanism of catalase. *Catalase Structural Tutorial*.

Brugarolas, J. and Kaelin, W. G. Jr. (2004). Dysregulation of HIF and VEGF is a unifying feature of the familial hamartoma syndromes. *Cancer Cell* **6**, 7-10.

Burdine, R. D. and Stern, M. J. (1996). Easy RNA isolation from C.elegans: A TRIZOL based method. *Worm Breeder's Gazette* **14**.

Chandel, N. S., Maltepe, E., Goldwasser, E., Mathieu, C. E., Simon, M. C. and Schumacker, P. T. (1998). Mitochondrial reactive oxygen species trigger hypoxia-induced transcription. *Proc Natl Acad Sci U S A* **95**, 11715-20.

Cockman, M. E., Masson, N., Mole, D. R., Jaakkola, P., Chang, G. W., Clifford, S. C., Maher, E. R., Pugh, C. W., Ratcliffe, P. J. and Maxwell, P. H. (2000). Hypoxia inducible factor-alpha binding and ubiquitylation by the von Hippel-Lindau tumor suppressor protein. *J Biol Chem.* **275**, 25733-41.

Cook, R. and Edward, J. C. (2006). The Importance of Hormesis to Public Health. Environmental Health Perspectives. *Environ. Health Perspect* **114**, 1631-5.

Coolon, J. D., Jones, K. L., Todd, T. C., Carr, B. C. and Herman, M. A. (2009). Caenorhabditis elegans Genomic Response to Soil Bacteria Predicts Environment-Specific Genetic Effects on Life History Traits. *PLOS Genetics* **5**, e1000503.

Deberardinis, R. J., Sayed, N., Ditsworth, D. and Thompson, C. B. (2008) Brick by brick: metabolism and tumor cell growth. *Curr Opin Genet Dev.* **18**, 54-61.

Dewhirst, M. W. (2009). Relationships between cycling hypoxia**,** HIF-1, angiogenesis and oxidative stress. *Radiat Res.***172**, 653-65.

Epstein, A. C., Gleadle, J. M., McNeill, L. A., Hewitson, K. S., O'Rourke, J., Mole, D. R., Mukherji, M., Metzen, E., Wilson, M. I., Dhanda, A., Tian, Y. M., Masson, N., Hamilton, D. L., Jaakkola, P., Barstead, R., Hodgkin, J., Maxwell, P. H., Pugh, C. W., Schofield, C. J. and Ratcliffe, P. J. (2001). C. elegans EGL-9 and mammalian homologs define a family of dioxygenases that regulate HIF by prolyl hydroxylation. *Cell* **107**, 43-54.

Gerald, D., Berra, E., Frapart, Y. M., Chan, D. A., Giaccia, A. J., Mansuy, D., Pouysségur, J., Yaniv, M. and Mechta-Grigoriou, F. (2004). JunD reduces tumor angiogenesis by protecting cells from oxidative stress. *Cell* **118**, 781-94.

Gruber, A., Cornaciu, I., Lass, A., Schweiger, M., Poeschl, M., Eder, C., Kumari, M., Schoiswohl, G., Wolinski, H., Kohlwein, S. D., Zechner, R., Zimmermann, R. and Oberer, M. (2010). The N-terminal region of comparative gene identification-58 (CGI-58) is important for lipid droplet binding and activation of adipose triglyceride lipase. *J Biol Chem.* **285**, 12289-98.

Hardie, D. G. (2007). AMP-activated /SNF1 protein kinases: Conserved guardins of cellular energy. *Nature Rev. Mol. Cell Biol.* **8**, 774-85.

Hawley, S. A., Boudeau, J., Reid, J. L., Mustard, K. J., Udd L., Makela, T. P., Alessi, D. R. and Hardie, D. G. *(*2003*).* Complexes between the LKB1 tumor suppressor, STRADa/b and MO25a/b are upstream kinases in the AMP-activated protein kinase cascade*. J. Biol.* **2***,* 28*.*

Heinz, G. H. (2010). Enhanced Reproduction in Mallards Fed a Low Level of Methylmercury: An Apparent Case of Hormesis. *Environmental Toxicology & Chemistry* **29**, 650-3.

Hekimi, S., Lapointe, J. and Wen, Y. (2011). Taking a "good" look at free radicals in the aging process. *Trends Cell Biol.* **21**, 569-76.

Holliday, R. (1989). Food, reproduction and longevity: is the extended lifespan of calorie-restricted animals an evolutionary adaptation? *Bioessays* **10**, 125-7.

Jeon, S. M., Chandel, N. S. and Hay, N. (2012). AMPK regulates NADPH homeostasis to promote tumour cell survival during energy stress. *Nature*. **485**, 661-5.

Jonkel, C. J., Jonkel, Mc. T. and Cowan, I. (1977). The black bear in the sprucefir forest. *Wildl. Monogr*. **27**, 1-57.

Kamath, R. S., Martinez-Campos, M., Zipperlen, P., Fraser, A. G. and Ahringer, J. (2001). Effectiveness of specific RNA-mediated interference through ingested double-stranded RNA in Caenorhabditis elegans. *Genome Biol*. **2**, 1-10.

Kimura, K. D., Tissenbaum, H. A., Liu, Y. and Ruvkun, G. (1997). daf-2, an insulin receptor-like gene that regulates longevity and diapause in Caenorhabditis elegans. *Science*. **277**, 942-6.

J. Kirkwood, T. B. (1977). Evolution of ageing. *Nature* **270**, 301-4.

Lee, S. J., Hwang, A. B. and Kenyon, C. (2010). Inhibition of respiration extends C. elegans life span via reactive oxygen species that increase HIF-1 activity. *Curr Biol.* **20**, 2131-6.

Mak, H. Y., Nelson, L. S., Basson, M., Johnson, C. D. and Ruvkun G. (2006). Polygenic control of Caenorhabditis elegans fat storage. *Nat Genet*. **38**, 363-8.

Miquel, M. and Browse, J. (1992). Arabidopsis mutants deficient in polyunsaturated fatty acid synthesis. *J. Biol. Chem.* **267**, 1502-9.

Miyabayashi, T., Palfreyman, M. T., Sluder, A. E., Slack, F. and Sengupta, P. (1999). Expression and function of members of a divergent nuclear receptor family in Caenorhabditis elegans. *Dev Biol*. **215**, 314-31.

Mouchiroud, L., Molin, L., Kasturi, P., Triba, M. N., Dumas, M. E., Wilson, M. C., Halestrap, A. P., Roussel, D., Masse, I., Dallière, N., Ségalat, L., Billaud, M. and Solari, F. (2011). Pyruvate imbalance mediates metabolic reprogramming and mimics lifespan extension by dietary restriction in Caenorhabditis elegans. *Aging Cell* **10**, 39-54.

Narbonne, P. and Roy, R. (2006). Inhibition of germline proliferation during C. elegans dauer development requires PTEN, LKB1 and AMPK signaling. *Development* **133**, 611-9.

Narbonne, P. and Roy, R. (2009). Caenorhabditis elegans dauers need LKB1/AMPK to ration lipid reserves and ensure long-term survival. *Nature* **457**, 210-4.

Owusu-Ansah, E. and Banerjee, U. (2009). Reactive oxygen species prime Drosophila haematopoietic progenitors for differentiation. *Nature* **461**, 537-41.

Pazdernik, N. and Schedl, T. (2013). Introduction to germ cell development in Caenorhabditis elegans. *Adv Exp Med Biol.* **757**, 1-16.

Perez, C. L. and Van Gilst, M. R. (2008). A 13C isotope labeling strategy reveals the influence of insulin signaling on lipogenesis in C. elegans. *Cell Metab*. **8**, 266-74.

Riddle, D. L. and Georgi, L. L. (1990). Advances in research on *Caenorhabditis elegans*: Application to plant parasitic nematodes. *Annu Rev Phytopathol*. **28**, 247–69.

Schweiger, M., Schoiswohl, G., Lass, A., Radner, F. P., Haemmerle, G., Malli, R., Graier, W., Cornaciu, I., Oberer, M., Salvayre, R., Fischer, J., Zechner, R. and Zimmermann, R. (2008). The C-terminal region of human adipose triglyceride lipase affects enzyme activity and lipid droplet binding. *J Biol Chem*. **283**, 17211-20.

Schulz, T. J., Zarse, K., Voigt, A., Urban, N., Birringer, M. and Ristow, M. (2007). Glucose restriction extends Caenorhabditis elegans life span by inducing mitochondrial respiration and increasing oxidative stress. *Cell Metab*. **4,** 280-93.

Selesniemi, K., Lee, H. J. and Tilly, J. L. (2008). Moderate caloric restriction initiated in rodents during adulthood sustains function of the female reproductive axis into advanced chronological age. *Aging Cell*. **7**, 622-9.

Semenza, G. L. (2010) HIF-1: upstream and downstream of cancer metabolism. *Curr Opin Genet Dev*. **20**, 51-6.

Shackelford, D. B., Vasquez, D. S., Corbeil, J., Wu, S., Leblanc, M., Wu, C. L., Vera, D. R. and Shaw, R. J. (2009). mTOR and HIF-1alpha-mediated tumor metabolism in an LKB1 mouse model of Peutz-Jeghers syndrome. *Proc Natl Acad Sci U S A*. **106**, 11137-42.

Shaw, R. J. (2006). Glucose metabolism and cancer. *Curr Opin Cell Biol.* **18**, 598-608.

Soukas, A. A., Kane, E. A., Carr, C. E., Melo, J. A. and Ruvkun, G. (2009). Rictor/TORC2 regulates fat metabolism, feeding, growth, and life span in Caenorhabditis elegans. *Genes Dev*. **23***,* 496-511.

Walter, C. and Frieden, E. (1963). The prevalence and significance of the product inhibition of enzymes. *Adv. Enzymol. Relat. Areas Mol. Biol. Advances in Enzymology - and Related Areas of Molecular Biology* 25, 167–274.

Watts, J. L. (2009). Fat synthesis and adiposity regulation in Caenorhabditis elegans. *Trends Endocrinol Metab*. **20**, 58-65.

Woods, A., Johnstone, S. R., Dickerson, K., Leiper, F. C., Fryer, L. G., Neumann, D., Schlattner, U., Wallimann, T., Carlson, M. and Carling, D. *(*2003*).* LKB1 is the upstream kinase in the AMP-activated protein kinase cascade*. Curr. Biol.* **13***,* 2004-8*.*

Yang, W., Li, J. and Hekimi, S. (2007). A Measurable increase in oxidative damage due to reduction in superoxide detoxification fails to shorten the life span of long-lived mitochondrial mutants of Caenorhabditis elegans. *Genetics* **177**, 2063-74.

Zhang, S. O., Box, A. C., Xu, N., Le, M. J., Yu, J., Guo, F., Trimble, R. and Mak, H. Y. (2010). Genetic and dietary regulation of lipid droplet expansion in Caenorhabditis elegans. *Proc Natl Acad Sci.* **107**, 4640-5.

Zimmermann, R., Strauss, J. G., Haemmerle, G., Schoiswohl, G., Birner-Gruenberger, R., Riederer, M., Lass, A., Neuberger, G., Eisenhaber, F., Hermetter, A., and Zechner, R. (2004). Fat mobilization in adipose tissue is promoted by adipose triglyceride lipase. *Science* **306**, 1383-6.

Figure 2.1 A Genome-wide RNAi Survey for suppressors of AMPK-dependent dauer lethality

(A) Following analysis of 18000 predicted genes included in the RNAi-feeding library, 551 RNAi clones were identified that extend the survival of *aak-1; aak-2* (*aak(0)*) dauer larvae that die after 10-12 days in culture. Candidate genes were assigned gene ontology terms based on information provided on WormBase (www.wormbase.org*).* Details of the individual genes are listed in Table S1.

(B) Both *ctl-1* and *ctl-2* RNAi clones were able to significantly increase the survival of *aak(0)* mutant dauer larvae. Dauer larvae were maintained at 25°C as described elsewhere (Narbonne and Roy, 2006). Raw dauer survival values are shown in Table S2.

(C) Each of the *ctl-1(ok1242), ctl-2(ok1137)* and *ctl-3(ok2042)* mutations were introduced into the *daf-2(e1370); aak-1(tm1944); aak-2(ok524)* background and their individual effects on survival, triglyceride content and osmosensitivity were assessed as in (Narbonne and Roy, 2009).

(D) Mutation of any of the three *ctl* genes protects triglyceride stores from depletion in day 4 AMPK mutant dauers. Fat storage was visualized by Oil Red O staining of day 4 dauer larvae. Arrowhead indicates the junction between the pharynx (left) and the intestine (right). Oil Red O staining intensity was evaluated by measuring optical density. Error bars indicate SD of 20 animals. * and ** indicate statistical significance ($P<0.05$ and $P<0.01$, respectively) comparing to AMPK mutant dauer larvae using one-way ANOVA followed by a Tukey HSD test. The same statistical analysis was applied for all additional experiments performed herein.

(E) Colorimetric analysis of triglyceride content in day 0 and 4 dauer larvae. Error bars indicate SD of three independent experiments.

(F) Mutation of any one of three *ctl* genes enhances the osmoresistance of day 4 AMPK mutant dauers following maintenance in varying NaCl concentrations for 24 hours at 25°C.

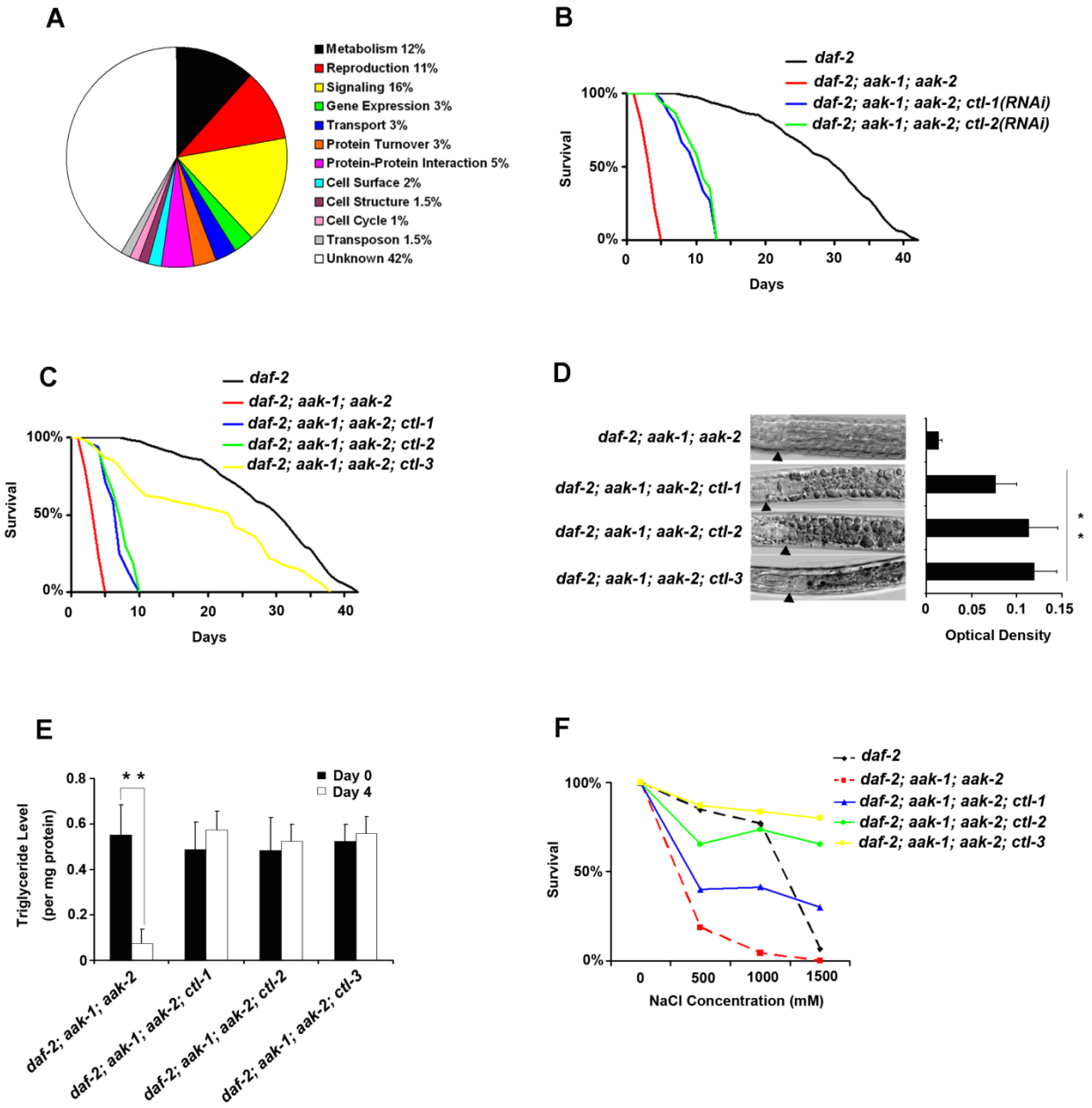
A
Metabolism 12%
Reproduction 11%
Signaling 16%
Gene Expression 3%
Transport 3%
Protein Turnover 3%
Protein-Protein Interaction 5%
Cell Surface 2%
Cell Structure 1.5%
Cell Cycle 1%
Transposon 1.5%
Unknown 42%
B
daf-2
daf-2; aak-1; aak-2
daf-2; aak-1; aak-2; ctl-1(RNAi)
daf-2; aak-1; aak-2; ctl-2(RNAi)
Survival
100%
50%
0%
0
10
20
30
40
Days
C
daf-2
daf-2; aak-1; aak-2
daf-2; aak-1; aak-2; ctl-1
daf-2; aak-1; aak-2; ctl-2
daf-2; aak-1; aak-2; ctl-3
Survival
100%
50%
0%
0
10
20
30
40
Days
D
daf-2; aak-1; aak-2
daf-2; aak-1; aak-2; ctl-1
daf-2; aak-1; aak-2; ctl-2
daf-2; aak-1; aak-2; ctl-3
0
0.05
0.1
0.15
Optical Density
E
Day 0
Day 4
Triglyceride Level (per mg protein)
0.8
0.6
0.4
0.2
0
daf-2; aak-1; aak-2
daf-2; aak-1; aak-2; ctl-1
daf-2; aak-1; aak-2; ctl-2
daf-2; aak-1; aak-2; ctl-3
F
daf-2
daf-2; aak-1; aak-2
daf-2; aak-1; aak-2; ctl-1
daf-2; aak-1; aak-2; ctl-2
daf-2; aak-1; aak-2; ctl-3
Survival
100%
50%
0%
0
500
1000
1500
NaCl Concentration (mM)

Figure 2.2 Disruption of Catalase Genes Results in the Attenuation of ATGL-1 Activity and Expansion of Lipid Droplet Size in AMPK Mutant Dauers.

(A) Total lipase activity was significantly reduced in AMPK *aak(0); ctl* mutant dauers, while *atgl-1(RNAi)* feeding was two-fold more efficient in reducing the overall lipase activity of AMPK mutant dauer larvae. *aak(0); ctl; atgl-1(RNAi)* combinations reduced lipase activity to levels typical of *atgl-1(RNAi)* alone. Error bars indicate SD of three independent experiments.

(B) Total lipase activity was significantly reduced in H_2O_2-treated AMPK *aak(0)* mutant dauers but not those subjected to *hif-1(RNAi)*. Error bars indicate SD of three independent experiments.

(C)-(F) Oil Red O staining of day 1 dauer larvae reveals an expansion in lipid droplets (arrows) in AMPK *aak(0); ctl* mutant dauers. Arrowhead indicates the junction between the pharynx (left) and the intestine (right).

(G)-(J) BODIPY-labelled day 1 dauer larvae delineates size expansion in lipid droplets (arrows) in AMPK *aak(0); ctl* mutant dauers.

(K) Volume quantification of the BODIPY-stained lipid droplet structures was performed as described elsewhere (Zhang et al. 2010) using OpenLab software (Improvision,UK). Error bars indicate SD of 20 animals.

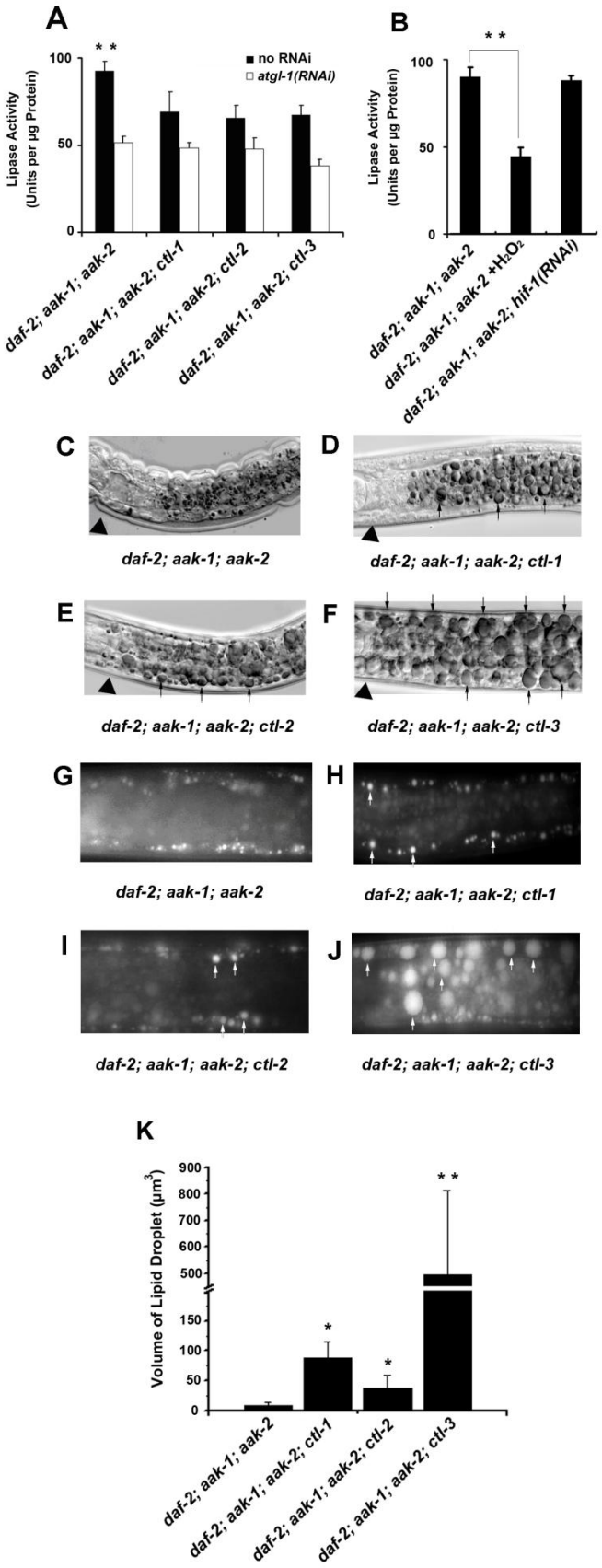
A
B
Lipase Activity (Units per µg Protein)
no RNAi
atgl-1(RNAi)
daf-2; aak-1; aak-2
daf-2; aak-1; aak-2; ctl-1
daf-2; aak-1; aak-2; ctl-2
daf-2; aak-1; aak-2; ctl-3
daf-2; aak-1; aak-2 +H2O2
daf-2; aak-1; aak-2; hif-1(RNAi)
C
D
E
F
G
H
I
J
K
Volume of Lipid Droplet (µm3)

Figure 2.3 Elevated Concentrations of H_2O_2 Enhance the Survival of AMPK Mutant Dauers.

(A) Less ROS was produced in AMPK mutant dauers (*daf-2*) as assessed using the total ROS dye indicator DCF-DA, while mutation of individual *ctl* genes only partially restored ROS levels. Error bars indicate SD of three independent experiments.

(B) Total H_2O_2 levels were significantly increased in AMPK *aak(0); ctl* mutant dauers which could be reversed by treatment with 10mM NAC. Error bars indicate SD of three independent experiments.

(C)-(E) The *ctl*-dependent enhancement of *aak(0)* dauer survival is reversed by antioxidant treatment using 10mM NAC

(F) Treatment with 0.1% and 0.01% H_2O_2 prolonged AMPK mutant dauer survival but higher concentrations of H_2O_2 were toxic. Assays were carried out under light-sensitive conditions to minimize H_2O_2 breakdown during assays.

(G) 10μM paraquat (Pq) has no effect on the survival of *aak(0)* dauers. Lower concentrations from 1-10μM did not affect dauer survival (data not shown), while higher concentrations of paraquat (0.1mM and 0.5mM) were toxic and reduced dauer survival.

(H) The increased hydrogen peroxide levels typical of *aak(0); ctl* mutant dauers are reversed following the disruption of peroxisomal fatty acid oxidation by *daf-22(RNAi).* Error bars indicate SD of three independent experiments.

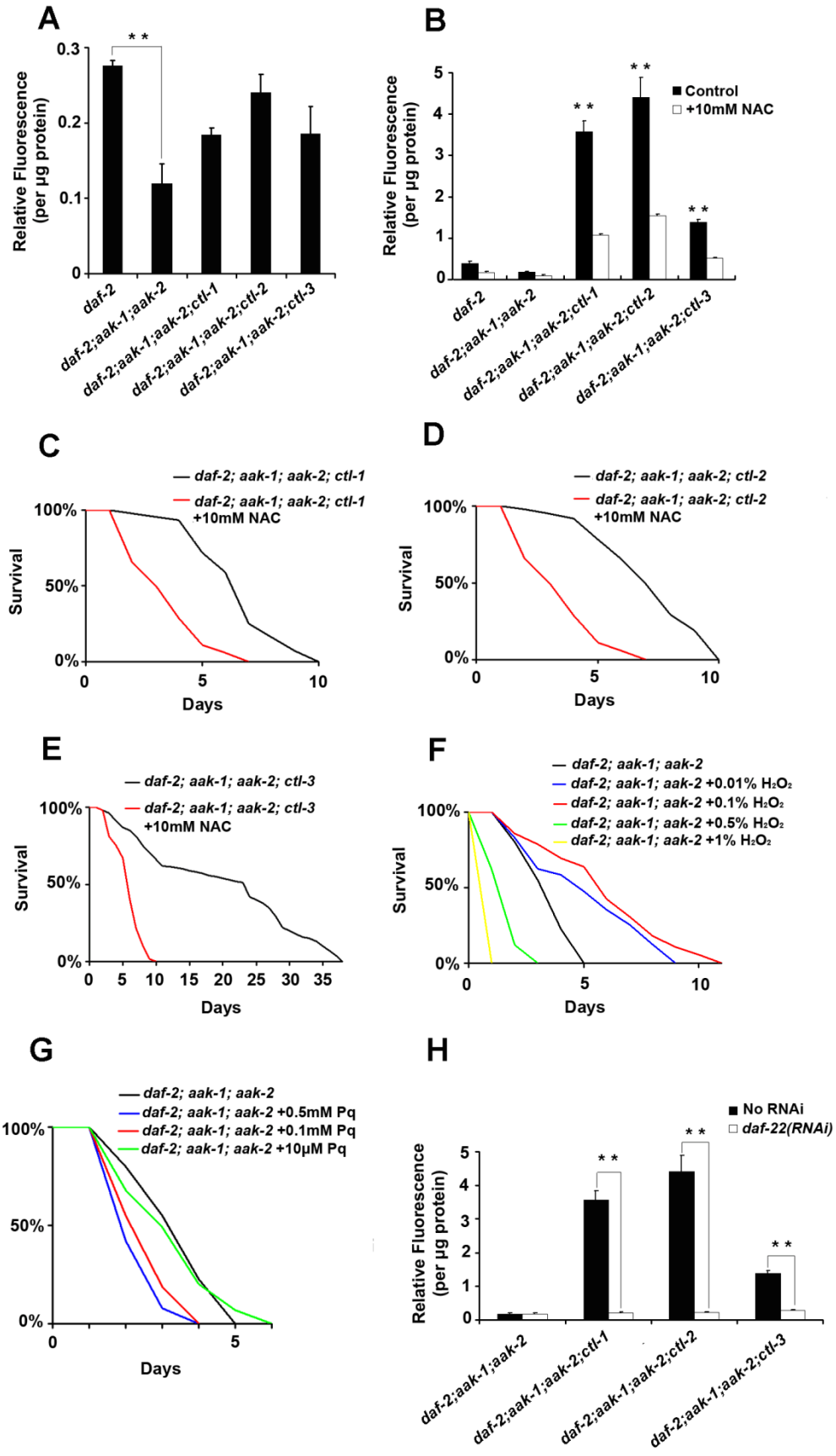
A
Relative Fluorescence (per µg protein)
0.3
0.2
0.1
0
* *
daf-2
daf-2;aak-1;aak-2
daf-2;aak-1;aak-2;ctl-1
daf-2;aak-1;aak-2;ctl-2
daf-2;aak-1;aak-2;ctl-3
B
Relative Fluorescence (per µg protein)
5
4
3
2
1
0
* *
* *
* *
Control
+10mM NAC
daf-2
daf-2;aak-1;aak-2
daf-2;aak-1;aak-2;ctl-1
daf-2;aak-1;aak-2;ctl-2
daf-2;aak-1;aak-2;ctl-3
C
daf-2; aak-1; aak-2; ctl-1
daf-2; aak-1; aak-2; ctl-1 +10mM NAC
Survival
100%
50%
0%
0
5
10
Days
D
daf-2; aak-1; aak-2; ctl-2
daf-2; aak-1; aak-2; ctl-2 +10mM NAC
Survival
100%
50%
0%
0
5
10
Days
E
daf-2; aak-1; aak-2; ctl-3
daf-2; aak-1; aak-2; ctl-3 +10mM NAC
Survival
100%
50%
0%
0 5 10 15 20 25 30 35
Days
F
daf-2; aak-1; aak-2
daf-2; aak-1; aak-2 +0.01% H2O2
daf-2; aak-1; aak-2 +0.1% H2O2
daf-2; aak-1; aak-2 +0.5% H2O2
daf-2; aak-1; aak-2 +1% H2O2
Survival
100%
50%
0%
0
5
10
Days
G
daf-2; aak-1; aak-2
daf-2; aak-1; aak-2 +0.5mM Pq
daf-2; aak-1; aak-2 +0.1mM Pq
daf-2; aak-1; aak-2 +10µM Pq
Survival
100%
50%
0%
0
5
Days
H
No RNAi
daf-22(RNAi)
Relative Fluorescence (per µg protein)
5
4
3
2
1
0
* *
* *
* *
daf-2;aak-1;aak-2
daf-2;aak-1;aak-2;ctl-1
daf-2;aak-1;aak-2;ctl-2
daf-2;aak-1;aak-2;ctl-3

Figure 2.4 The Increased Survival of Catalase-Deficient AMPK Mutant Dauer Larvae is HIF-1-dependent.

(A) AMPK mutant dauer larvae harbouring *ctl* mutations, or that were exposed to 0.1% H_2O_2 showed an elevated expression of a HIF-1-dependent GFP reporter. All animals were *daf-2; aak(0);* and carried the HIF-1 sensor transgene *Pnhr-57::GFP*. Error bars indicate SD of 20 animals.

(B) Western blot analysis of GFP levels obtained from *aak(0); ctl* mutant dauer larvae or animals cultured in 0.1% H_2O_2.

(C) Western blot analysis of HIF-1 levels obtained from control and *aak(0); ctl* mutant dauer larvae or animals fed with *vhl-1(RNAi*) or cultured in 0.1% H_2O_2.

(D) Western blot analysis of HIF-1 levels in 10mM NAC-treated *aak(0); ctl* mutant dauers.

(E)-(G) *hif-1(RNAi)* reversed the survival benefit conferred by each of the *ctl* mutations on AMPK-deficient dauer larvae.

(H) Both *vhl-1(RNAi)* and *egl-9(RNAi)* extended the survival of AMPK-deficient dauer larvae.

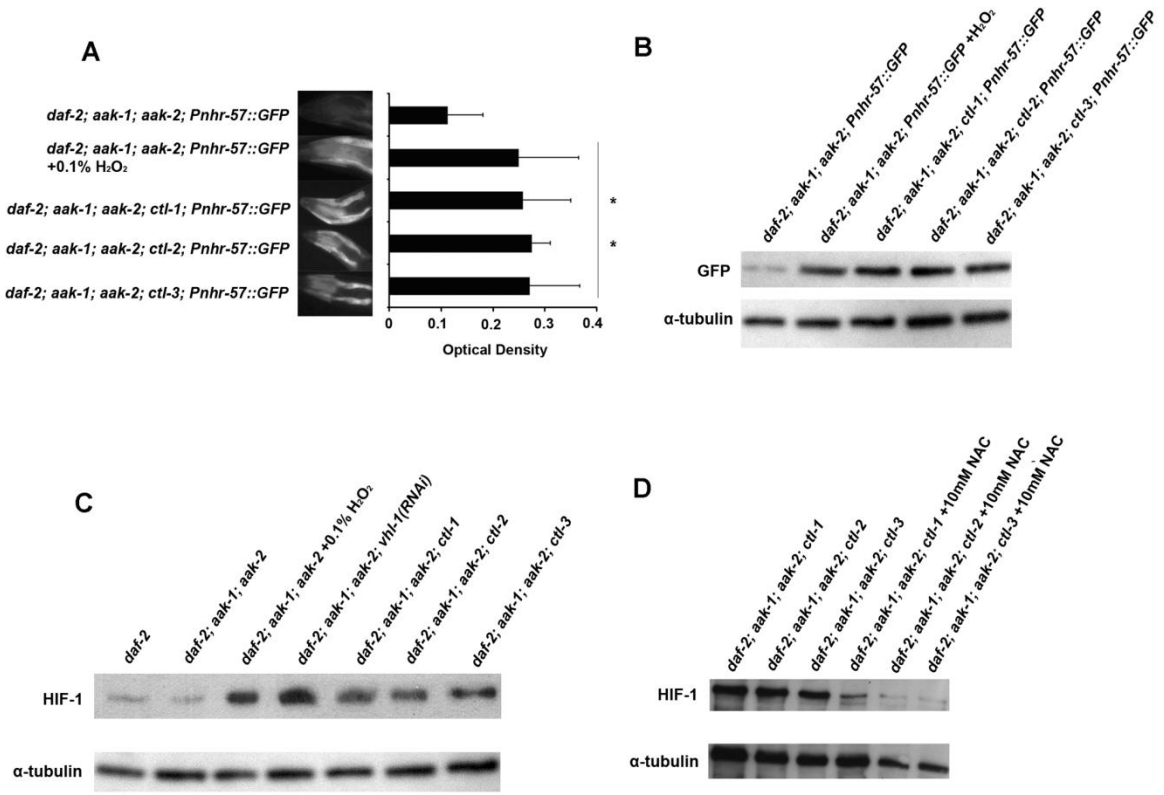
A
daf-2; aak-1; aak-2; Pnhr-57::GFP
daf-2; aak-1; aak-2; Pnhr-57::GFP +0.1% H2O2
daf-2; aak-1; aak-2; ctl-1; Pnhr-57::GFP
daf-2; aak-1; aak-2; ctl-2; Pnhr-57::GFP
daf-2; aak-1; aak-2; ctl-3; Pnhr-57::GFP
0 0.1 0.2 0.3 0.4
Optical Density
* *
B
daf-2; aak-1; aak-2; Pnhr-57::GFP
daf-2; aak-1; aak-2; Pnhr-57::GFP +H2O2
daf-2; aak-1; aak-2; ctl-1; Pnhr-57::GFP
daf-2; aak-1; aak-2; ctl-2; Pnhr-57::GFP
daf-2; aak-1; aak-2; ctl-3; Pnhr-57::GFP
GFP
α-tubulin
C
daf-2
daf-2; aak-1; aak-2
daf-2; aak-1; aak-2 +0.1% H2O2
daf-2; aak-1; aak-2; vhl-1(RNAi)
daf-2; aak-1; aak-2; ctl-1
daf-2; aak-1; aak-2; ctl-2
daf-2; aak-1; aak-2; ctl-3
HIF-1
α-tubulin
D
daf-2; aak-1; aak-2; ctl-1
daf-2; aak-1; aak-2; ctl-2
daf-2; aak-1; aak-2; ctl-3
daf-2; aak-1; aak-2; ctl-1 +10mM NAC
daf-2; aak-1; aak-2; ctl-2 +10mM NAC
daf-2; aak-1; aak-2; ctl-3 +10mM NAC
HIF-1
α-tubulin
E
daf-2; aak-1; aak-2; ctl-1
daf-2; aak-1; aak-2; ctl-1; hif-1(RNAi)
100%
50%
0%
Survival
0 5 10
Days
F
daf-2; aak-1; aak-2; ctl-2
daf-2; aak-1; aak-2; ctl-2; hif-1(RNAi)
100%
50%
0%
Survival
0 5 10
Days
G
daf-2; aak-1; aak-2; ctl-3
daf-2; aak-1; aak-2; ctl-3; hif-1(RNAi)
100%
50%
0%
Survival
0 5 10 15 20 25 30 35
Days
H
daf-2; aak-1; aak-2
daf-2; aak-1; aak-2; vhl-1(RNAi)
daf-2; aak-1; aak-2; egl-9(RNAi)
100%
50%
0%
Survival
0 4 8 12
Days

Figure 2.5 HIF-1 Activates Expression of Genes Involved in *de novo* Fatty Acid Synthesis.

(A) *aak(0); ctl* mutant dauer larvae possess additional fatty acid species that were not detected in AMPK mutant dauers. Total lipids were extracted from dauer larvae 24 hours after dauer formation and the various fatty acid species present were determined using GC/MS. Error bars indicate SD of three independent experiments in all panels.

(B) The expression levels of several genes involved in *de novo* fatty acid synthesis were upregulated in *aak(0); ctl* mutant dauers. Relative mRNA levels were analysed using quantitative real time PCR in dauer larvae 24h after dauer formation.

(C-E) The additional fatty acids detected catalase-deficient AMPK mutant dauer larvae were no longer detectable following *hif-1(RNAi)*

(F) Both *hif-1(RNAi)* and 10mM NAC treatment reversed the increased gene expression level of enzymes involved in *de novo* fatty acid synthesis in *aak(0); ctl-3* mutant dauer larvae.

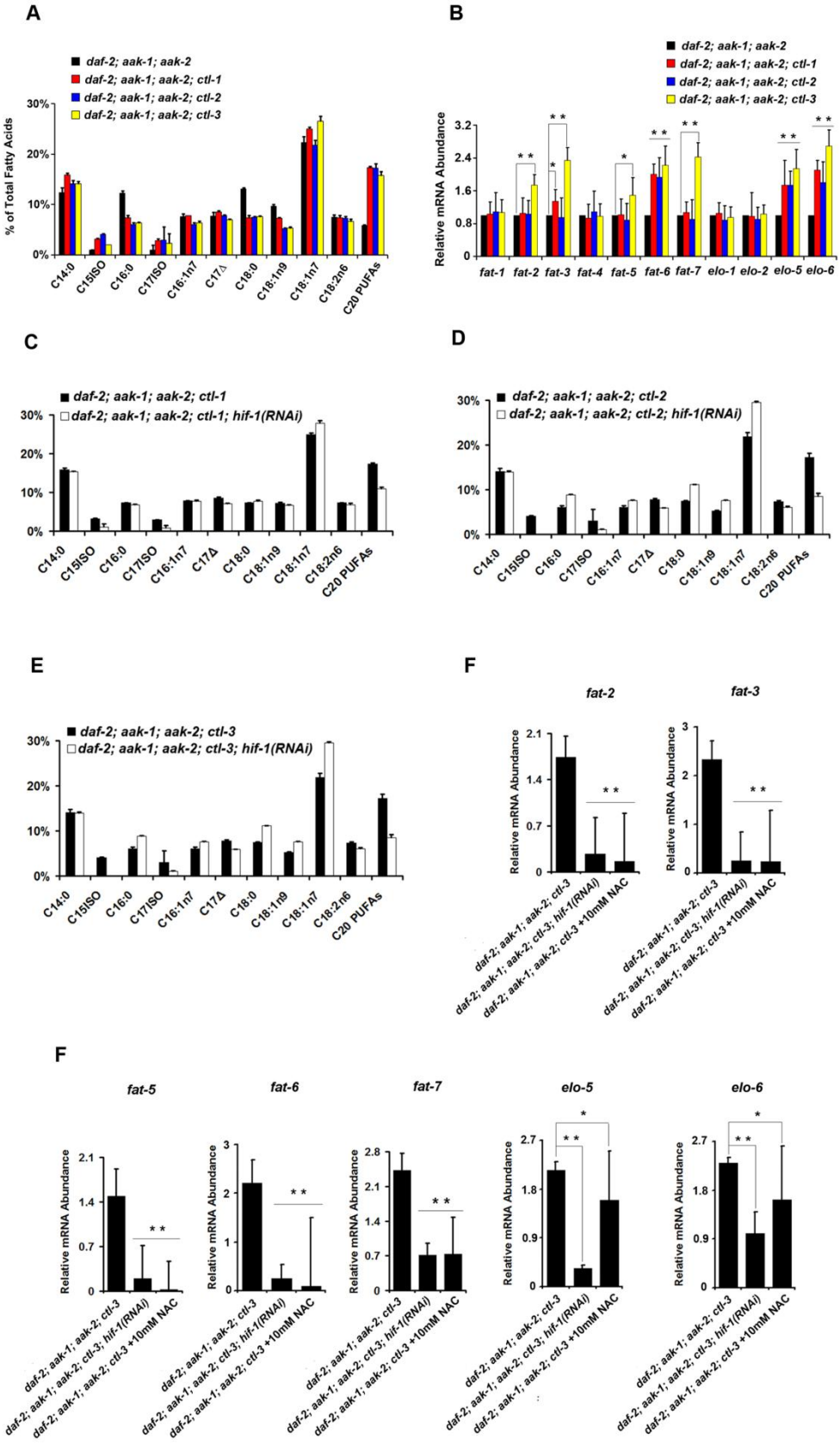
A
daf-2; aak-1; aak-2
daf-2; aak-1; aak-2; ctl-1
daf-2; aak-1; aak-2; ctl-2
daf-2; aak-1; aak-2; ctl-3
% of Total Fatty Acids
C14:0
C15ISO
C16:0
C17ISO
C16:1n7
C17Δ
C18:0
C18:1n9
C18:1n7
C18:2n6
C20 PUFAs
B
daf-2; aak-1; aak-2
daf-2; aak-1; aak-2; ctl-1
daf-2; aak-1; aak-2; ctl-2
daf-2; aak-1; aak-2; ctl-3
Relative mRNA Abundance
fat-1
fat-2
fat-3
fat-4
fat-5
fat-6
fat-7
elo-1
elo-2
elo-5
elo-6
C
daf-2; aak-1; aak-2; ctl-1
daf-2; aak-1; aak-2; ctl-1; hif-1(RNAi)
D
daf-2; aak-1; aak-2; ctl-2
daf-2; aak-1; aak-2; ctl-2; hif-1(RNAi)
E
daf-2; aak-1; aak-2; ctl-3
daf-2; aak-1; aak-2; ctl-3; hif-1(RNAi)
F
fat-2
fat-3
Relative mRNA Abundance
daf-2; aak-1; aak-2; ctl-3
daf-2; aak-1; aak-2; ctl-3; hif-1(RNAi)
daf-2; aak-1; aak-2; ctl-3 +10mM NAC
F
fat-5
fat-6
fat-7
elo-5
elo-6

Figure 2.6 An Equilibrium Between HIF-1-dependent Fatty Acid Synthesis and ROS-induced Oxidative Damage Maximizes Survival of *ctl-3*; AMPK Mutant Dauers.

(A) *atgl-1(RNAi)* increased the survival of AMPK mutant dauers by limiting unregulated triglyceride hydrolysis during dauer formation, but *atgl-1(RNAi)* had no such beneficial effect on the survival of *aak(0); ctl* mutant dauer larvae **(B-D)**. 10mM NAC treatment combined with *atgl-1(RNAi)* extended the survival of *aak(0); ctl-1/2* mutant dauers (**B** and **C**), but reduced the survival of *aak(0); ctl-3* mutant dauers (**D**).

(E) Terminally-arrested *aak(0); ctl-1 or ctl-2* larvae still stain strongly for lipids indicating that the terminal arrest of *aak(0); ctl-1* dauer larvae is unlikely to be due to premature exhaustion of lipid reserves due to misregulated *atgl-1* activity. Error bars indicate SD of 20 animals.

(F) Loss of catalase gene function results in a substantial increase in oxidative damage. *aak(0); ctl-3* mutant one day old dauer larvae have comparatively less oxidative damage at the protein level as determined by OxyBlot detection, than *aak(0); ctl-1 and aak(0); ctl-2* 24h after their switch from dauer larvae. Band intensity was quantified by measuring optical density followed by subsequent processing using Openlab software. Error bars indicate SD of three independent experiments.

(G) Catalase activity was significantly lower in both *aak(0)* and *aak(0); ctl-3* mutant dauer larvae compared to *aak(0); ctl-1* or *aak(0); ctl-2* mutant dauer larvae. Error bars indicate SD of three independent experiments.

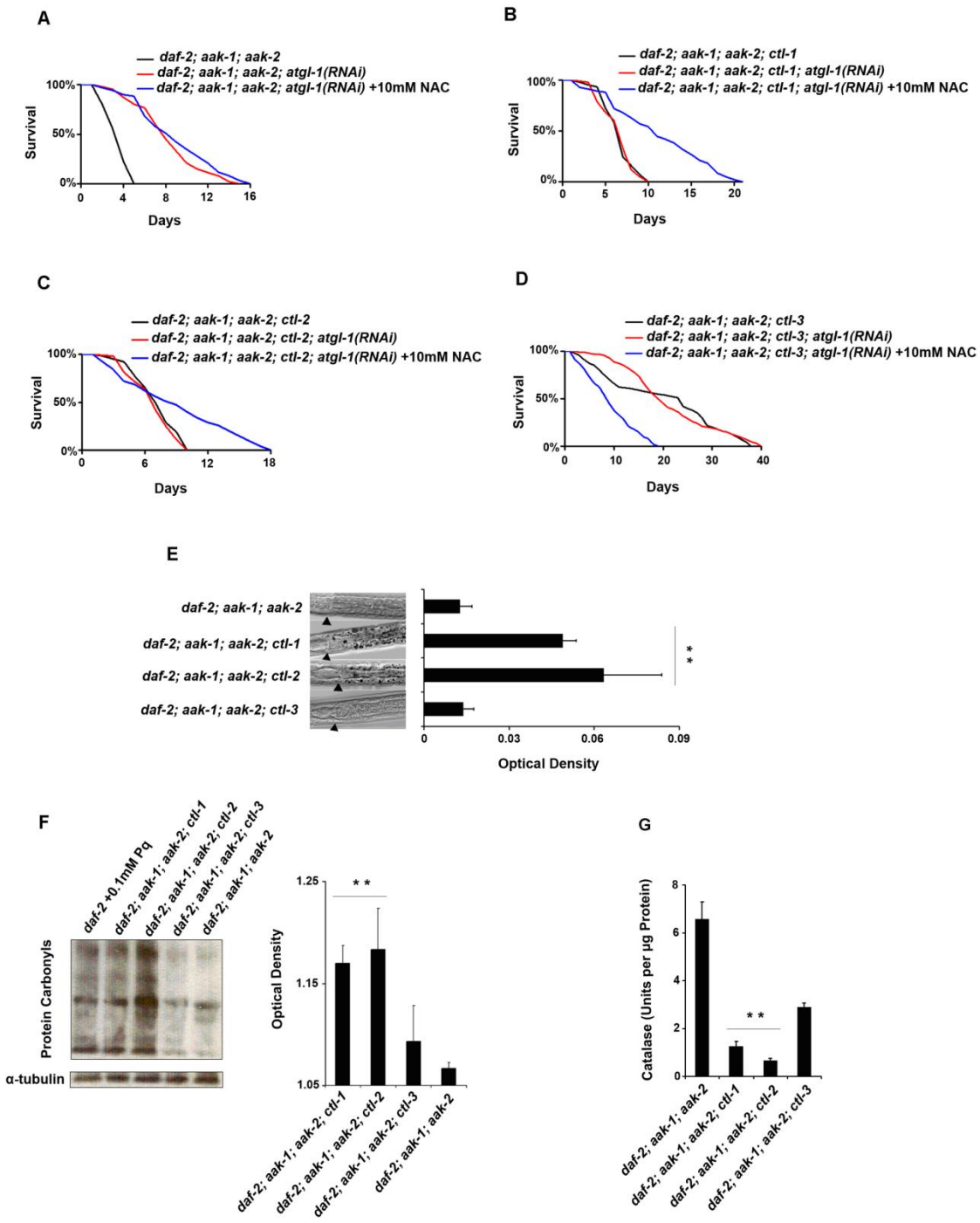
A
daf-2; aak-1; aak-2
daf-2; aak-1; aak-2; atgl-1(RNAi)
daf-2; aak-1; aak-2; atgl-1(RNAi) +10mM NAC
Survival
100%
50%
0%
0
4
8
12
16
Days
B
daf-2; aak-1; aak-2; ctl-1
daf-2; aak-1; aak-2; ctl-1; atgl-1(RNAi)
daf-2; aak-1; aak-2; ctl-1; atgl-1(RNAi) +10mM NAC
Survival
100%
50%
0%
0
5
10
15
20
Days
C
daf-2; aak-1; aak-2; ctl-2
daf-2; aak-1; aak-2; ctl-2; atgl-1(RNAi)
daf-2; aak-1; aak-2; ctl-2; atgl-1(RNAi) +10mM NAC
Survival
100%
50%
0%
0
6
12
18
Days
D
daf-2; aak-1; aak-2; ctl-3
daf-2; aak-1; aak-2; ctl-3; atgl-1(RNAi)
daf-2; aak-1; aak-2; ctl-3; atgl-1(RNAi) +10mM NAC
Survival
100%
50%
0%
0
10
20
30
40
Days
E
daf-2; aak-1; aak-2
daf-2; aak-1; aak-2; ctl-1
daf-2; aak-1; aak-2; ctl-2
daf-2; aak-1; aak-2; ctl-3
**
0
0.03
0.06
0.09
Optical Density
F
daf-2 +0.1mM Pq
daf-2; aak-1; aak-2; ctl-1
daf-2; aak-1; aak-2; ctl-2
daf-2; aak-1; aak-2; ctl-3
daf-2; aak-1; aak-2
Protein Carbonyls
α-tubulin
Optical Density
1.25
1.15
1.05
**
daf-2; aak-1; aak-2; ctl-1
daf-2; aak-1; aak-2; ctl-2
daf-2; aak-1; aak-2; ctl-3
daf-2; aak-1; aak-2
G
Catalase (Units per µg Protein)
8
6
4
2
0
**
daf-2; aak-1; aak-2
daf-2; aak-1; aak-2; ctl-1
daf-2; aak-1; aak-2; ctl-2
daf-2; aak-1; aak-2; ctl-3

Figure 2.7 H_2O_2-mediated Hormesis Prolongs Survival in AMPK mutant dauer larvae via HIF-1-Dependent and -Independent Effects on Lipid Metabolism.

Elevation of global H_2O_2 due to loss of any member of the CTL family has two beneficial effects on AMPK mutant dauer survival: expansion of lipid droplet size which may attenuate the activity of ATGL-1, while also activating HIF-1 to promote fatty acid biosynthesis; both of which act to restore fat stores for prolonged dauer survival.

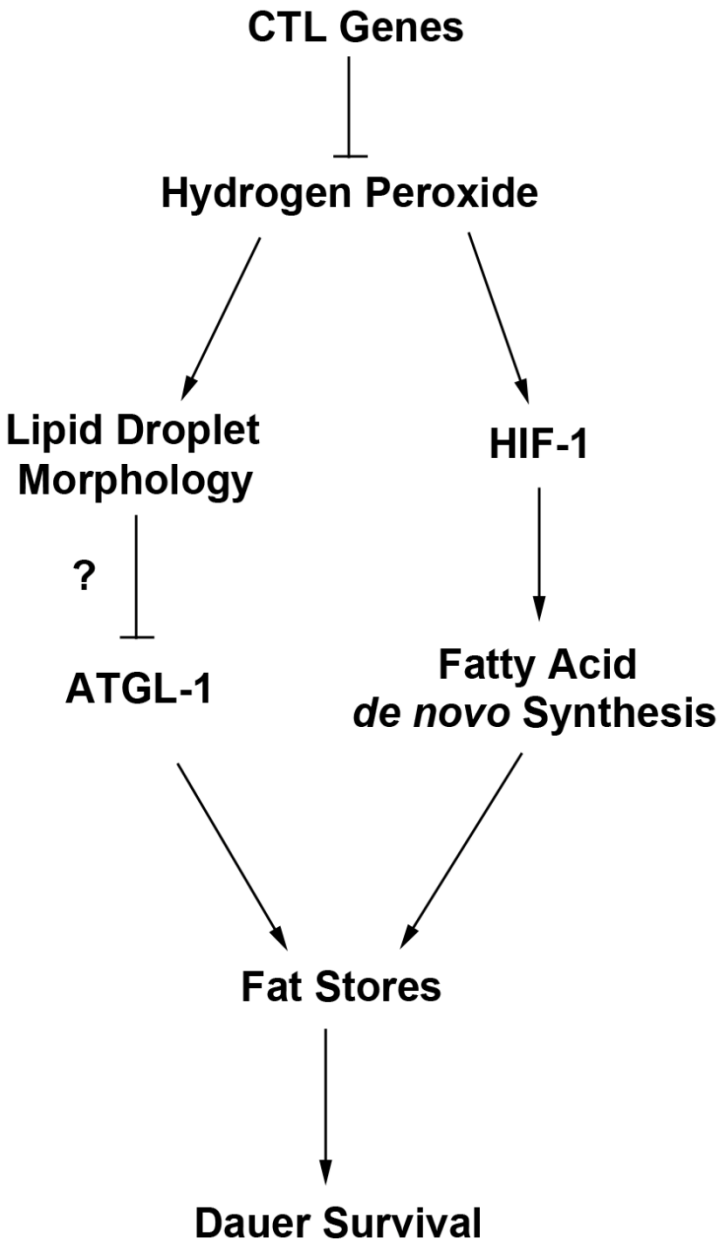

Figure S2.1 All Three *ctl* Genes were Highly Expressed during Dauer Stage Compared to the L3 Stage in Both *daf-2* and *daf-2; aak(0)* Mutant Backgrounds. Error bars indicate SD of three independent experiments.

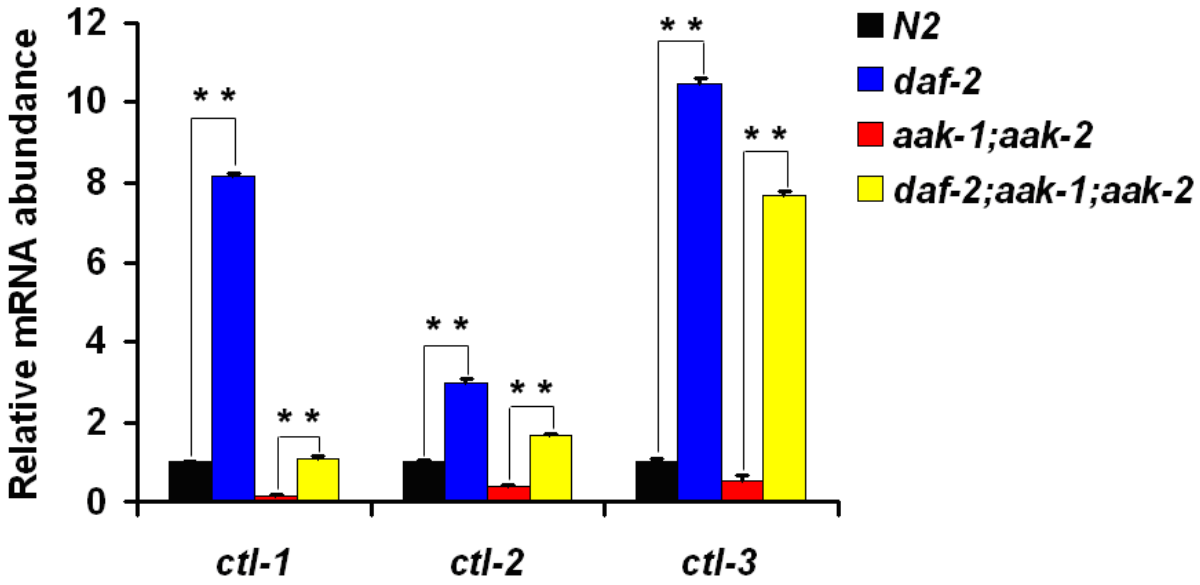

Figure S2.2 Lack of Individual Fatty Acid Species Further Contribute to the Early Expiration of AMPK Mutant Dauers.

(A) More fatty acid species were present in *daf-2* mutant dauers than wild type L3 animals. Error bars indicate SD of three independent experiments.

(B) *aak(0)* mutant dauer larvae have a reduced repertoire of fatty acid species.

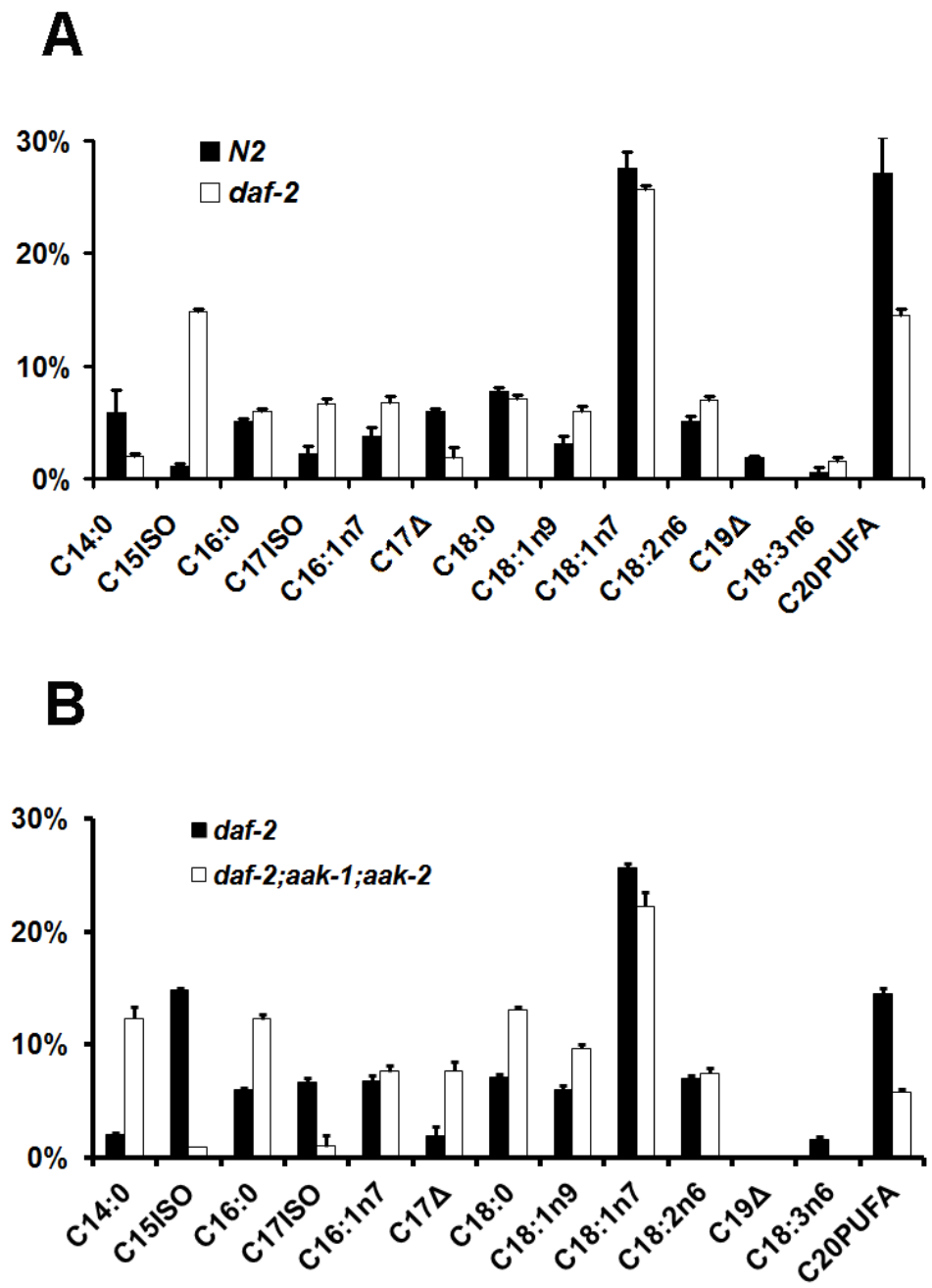

Figure S2.3 Elimination of Mitochondrial Proteins with RNAi Increased the Survival of AMPK Mutant Dauers.

All strains carry *daf-2;aak-1;aak-2* mutations.

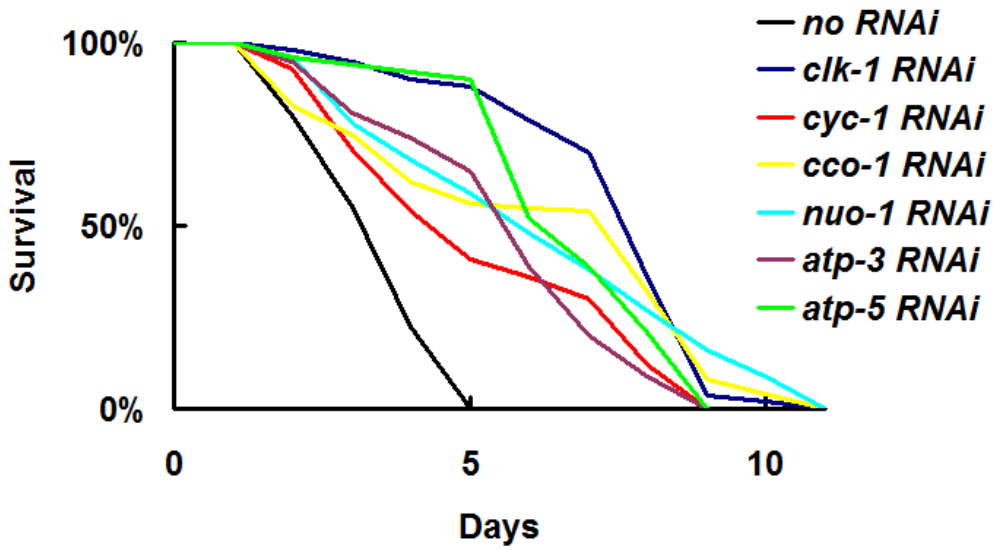

Figure S2.4 NAC Treatment Reverses H_2O_2-Induced HIF-1 Stabilisation.

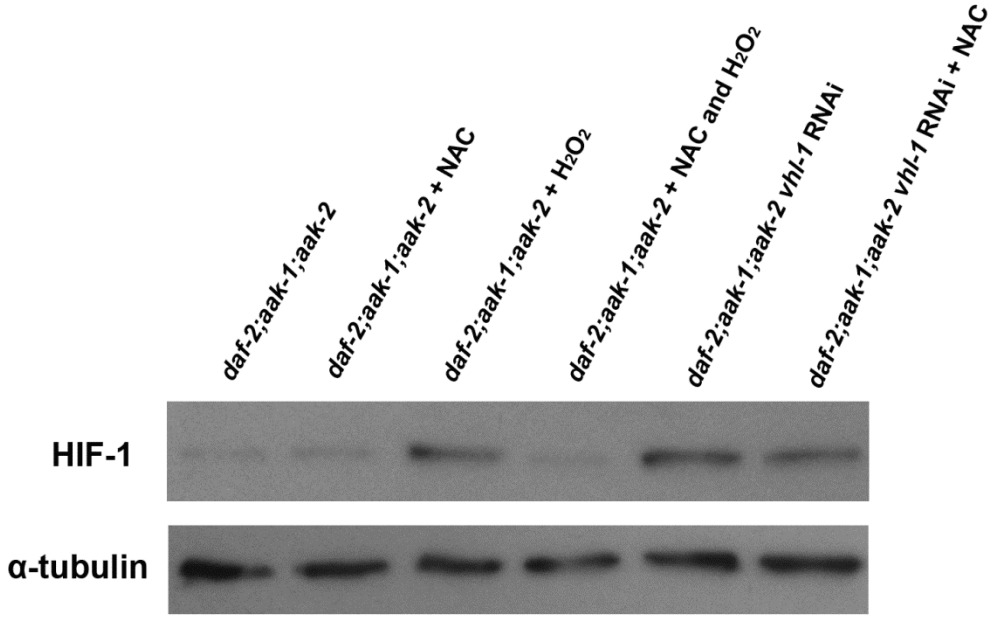

Figure S2.5 Elimination of PCK-1 and CTS-1 with RNAi Increased the Survival of AMPK Mutant Dauers but not CTL AMPK Mutant Dauers suggesting that there is no change in the glyoxylate pathway. (O'Riordan and Burnell, 1990; Metallo et al. 2011; Wise et al. 2011).

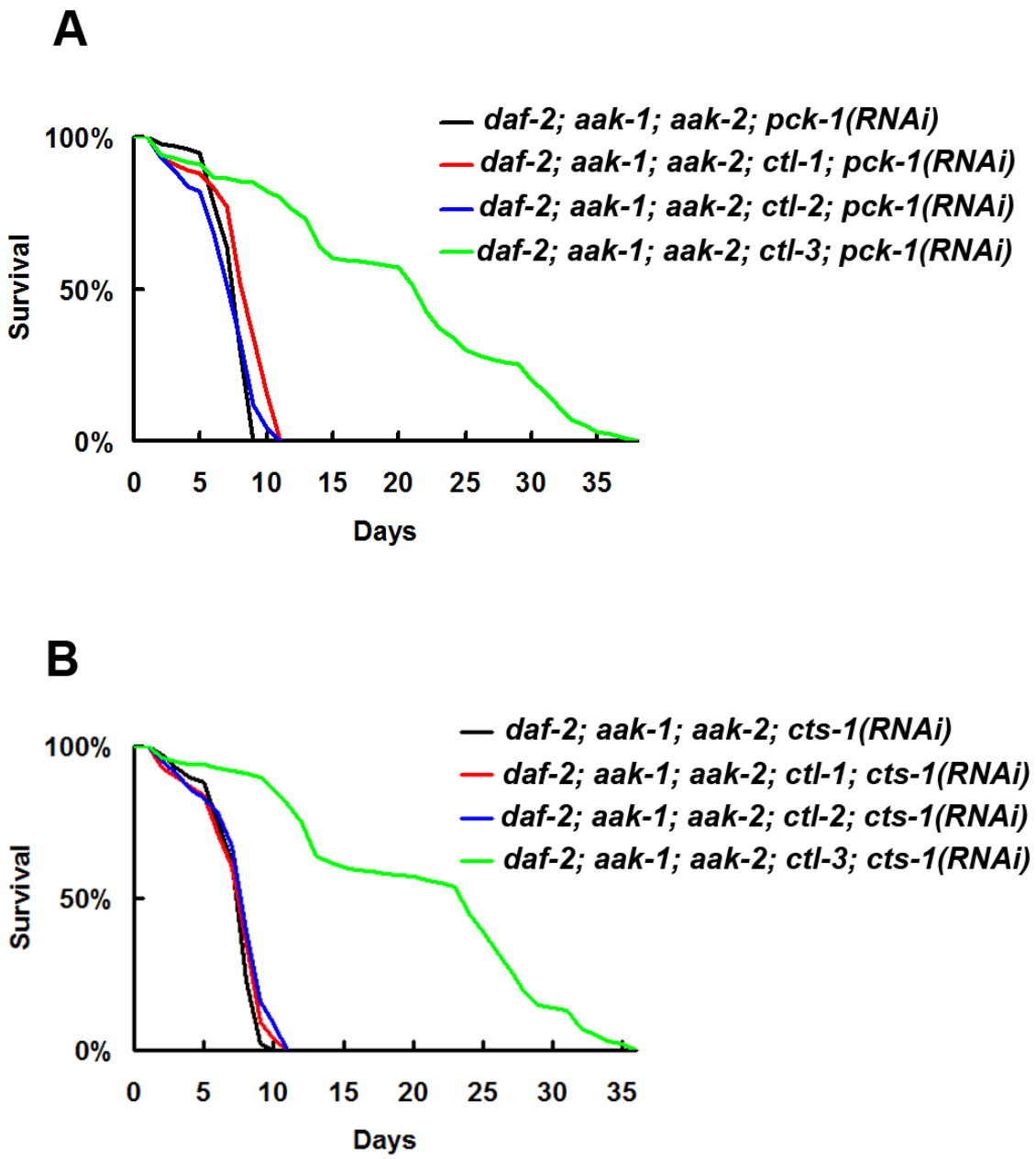

Figure S2.6 Elimination of MDH-1 with RNAi Increased both the Survival of H_2O_2 level in AMPK Mutant Dauers.

Error bars indicate SD of three independent experiments.

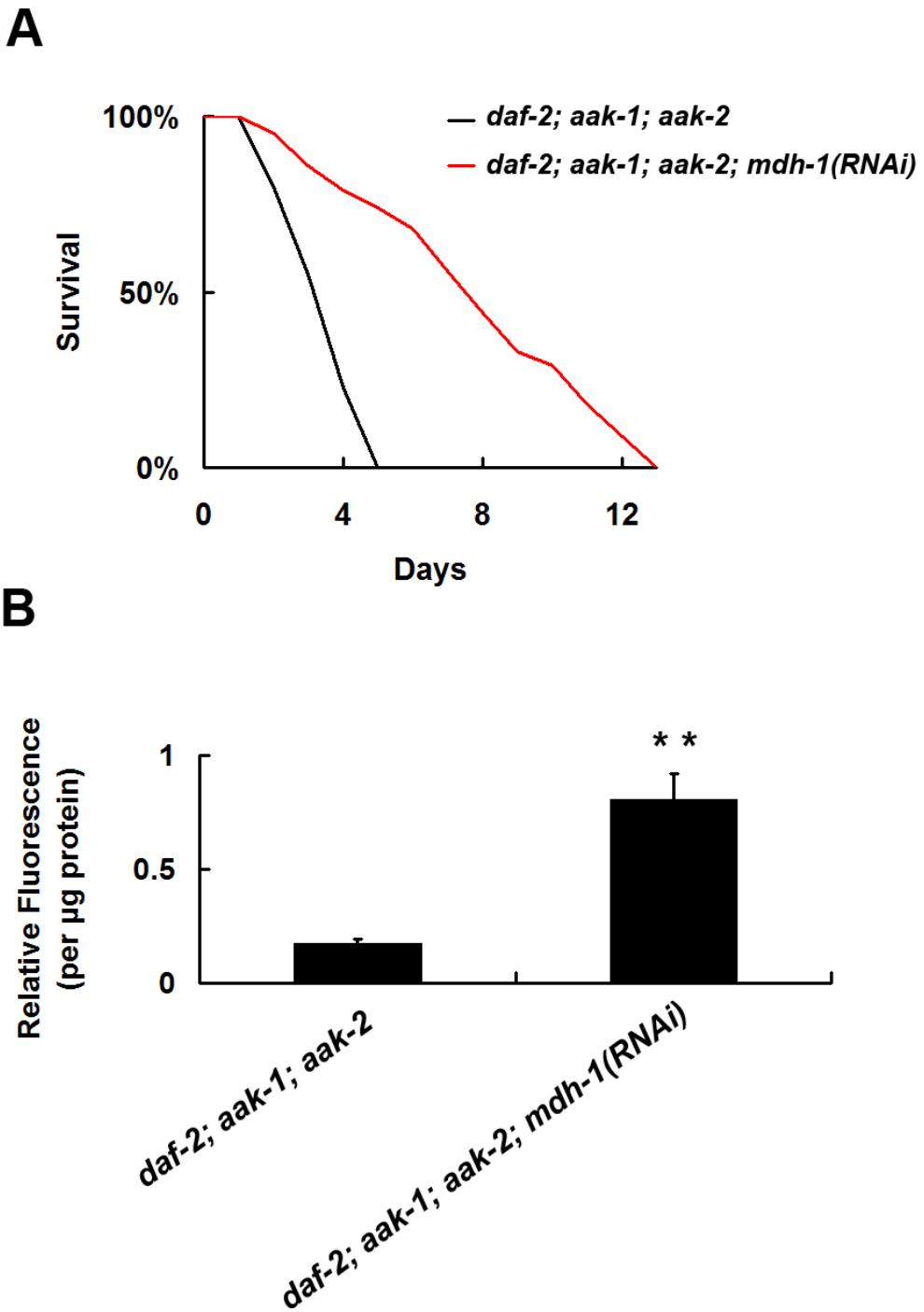

Figure S2.7 Time Course Analysis of Fatty Acid Profile in *daf-2* Dauer Larvae at 36 hours (A) and 72 hours (B) after initiation of Larval Growth at 25°C (~12h and 48h post-dauer formation, respectively).

Error bars indicate SD of three independent experiments.

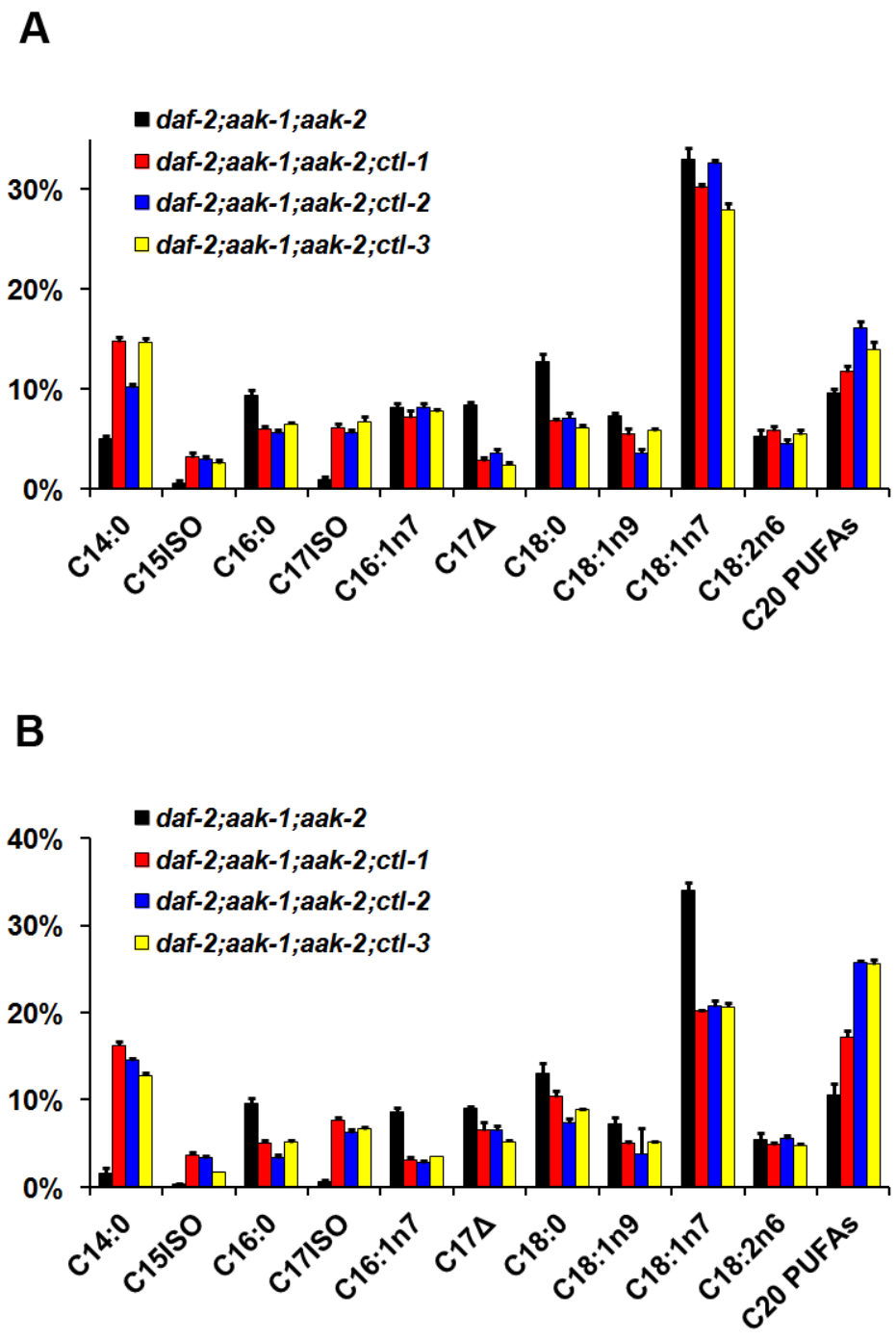

Connecting Statement: Bridging Chapter 2 and 3

Having performed a whole genome screen to search for the potential downstream protein targets that could impinge on the AMPK/ATGL pathway and revealed the role of catalase family genes in regulating lipid metabolism in AMPK-deficient dauer larvae, to further extend our understanding on regulation of the lipolysis process, I decided to investigate the detailed mechanism behind ATGL-1 phosphorylation by AMPK. To meet this end, I generated a *C. elegans* specific ATGL-1 antibody to aid the biochemical studies. Furthermore, I also performed experiments to characterize the human homologous *cgi-58* gene in *C. elegans*, which is known as a co-activator of ATGL in mammals.

Chapter 3: CGI-58 Regulates Lipolysis in an ATGL-1-Dependent and Independent Manner in *C. elegans* Dauer Larvae

Meng Xie and Richard Roy

Manuscript prepared for submission to *Cell Metabolism*

Summary

AMP-activated kinase (AMPK) is a key regulator of many mechanisms that are required by cells to aid their adjustment to stresses induced by the changing environment. In *C. elegans* dauer larvae, AMPK-null mutants expire prematurely due to hyperactive Adipose Triglyceride Lipase (ATGL) followed by rapid depletion of triglyceride stores. Using a *C. elegans* ATGL-1 specific antibody, we demonstrate that AMPK limits ATGL-1 action by signaling it for proteasome degradation and sequestering it away from cellular lipid droplets. We also provide evidence that *C. elegans* CGI-58 not only acts as a co-activator of ATGL-1 and function cooperatively to maintain regular lipid droplet structure, but also independently prevents any lipid exchange and fusion events among the lipid droplets. Our data provide a mechanistic characterization of ATGL-1 regulation by AMPK and a novel structural role of CGI-58, both of which offer indications on potential development of new treatment targeting for lipid associated diseases.

Introduction

Most, if not all, organisms possess a remarkable capacity to sense environmental variations and to modify their physiology accordingly to adapt to such changes. During periods of nutrient scarcity, animals prioritize the use of limiting macromolecules for survival benefit, even if it results in a temporary suspension of reproductive development (Jonkelet al., 1977; Holliday, 1989; Kirkwood, 1977; Selesniemi et al., 2008; Riddle and Georgi, 1990). Similarly, in the free-living nematode *C. elegans*, a highly resistant “dauer” stage provides an alternative developmental pathway that increases the animals’ fitness upon encountering suboptimal growth conditions such as resource depletion or increases in either population or growing temperature.

In *C. elegans*, parallel cross-talk among several genetic pathways determines an “all or none” dauer entry response. This developmental decision is dictated by neuronal sensing of environmental indicators followed by signal transduction in neuroendocrine cells to eventually converge on a nuclear hormone receptor-mediated transcriptional cascade (reviewed by Fielenbach and Antebi, 2008).

One of the common targets of these three genetic pathways is the AMP-activated protein kinase (AMPK) (Narbonne and Roy, 2006). Upon activation by its upstream activating protein kinase LKB1/PAR-4, AMPK will in turn phosphorylate downstream targets to promote catabolic processes while simultaneously blocking anabolic processes to restore energy homeostasis (Hawley et al., 2003; Woods et al., 2003; Hardie, 2007).

During normal growth conditions nutrient/energy is initially stored in the form of glycogen, while surplus calories are packaged into triglyceride molecules for use during situations when energy demands exceed nutrient input. The triglycerides are stockpiled in monolayer phospholipid-encapsulated organelles called lipid droplets, which serve as the major triglyceride reserves in all metazoans. Their energy-rich contents can be accessed in a regulated manner based on metabolic need.

In situations of intense energy demand, triglycerides are hydrolyzed to free fatty acids (FFAs) in a series of sequential reactions that are catalyzed by substrate-specific lipase

enzymes that each releases a single FFA. These lipases include adipose triglyceride lipase (ATGL), hormone-sensitive lipase (HSL) and monoglyceride lipase (MGL). Observation of enlarged fat deposits and triglyceride accumulation within multiple tissues in ATGL-deficient mice suggest that ATGL catalyzes the initial rate-limiting step of triglyceride breakdown to release FFA and diacylglyceride (DG) (Haemmerle et al., 2006). The latter is subsequently cleaved by HSL and MGL to generate glycerol and FFA, and the final products diffuse from the adipose tissue into the circulation.

Although ATGL possesses significant catalytic activity in vitro it is unlikely to function alone in vivo. Characterized by its presence on intracellular lipid droplets in most tissues, CGI-58 (comparative gene identification-58) is one of the major lipid droplet-associated proteins identified in mammals and is the causative gene for human Chanarin-Dorfman syndrome (CDS), (Lefèvre et al., 2001). Recent studies have revealed that CGI-58 acts as a co-activator for ATGL in mammals, by binding directly to and enhancing the hydrolase activity of ATGL (Lass et al., 2006). The interaction between CGI-58 and ATGL is necessary but not sufficient for activation of the latter, while the ability to interact with ATGL is insufficient to recruit CGI-58 to the lipid droplet. Interaction with the lipid droplet may require other proteins or regulatory mechanisms (Gruber et al., 2010).

During the dauer stage in *C. elegans* AMPK blocks the rapid hydrolysis of the accumulated triglyceride stockpiles through the phospho-inhibition of ATGL-1 (Narbonne and Roy, 2009). This phosphorylation drastically reduces its activity, although it is unclear how this occurs. To probe the regulatory inputs that control this rate-limiting step in triglyceride breakdown we generated an antibody against *C. elegans* ATGL-1 protein. Our analyses revealed that phosphorylation of ATGL-1 resulted in a change in its subcellular localization followed by its proteasome-dependent degradation, involving ubiquitylation and its prior interaction with the 14-3-3 protein. We also found that removal of the *C. elegans* homologue of human CGI-58 protein improves the survival and all metabolic defects associated with compromised AMPK function, much like ATGL-1. In addition, we provide evidence that CGI-58 physically interacts with ATGL-1 in vivo, where they act cooperatively to maintain the appropriate

morphology of the lipid droplets. Moreover, we show that CGI-58 protein plays a more comprehensive role in *C. elegans* than in human where it not only recruits and tethers ATGL-1 onto its substrate, but also functions independently of ATGL-1 as a barrier around the lipid droplet to limit collision-mediated lipid exchange to maintain lipid droplet morphology and ultimately optimize ATGL-1-dependent lipolysis.

Results

AMPK regulates the levels of ATGL-1 present on lipid droplets during the dauer stage

To understand how the initial rate-limiting step of lipolysis is regulated by AMPK during *C. elegans* dauer stage, we first questioned whether ATGL-1 protein is present on the surface of the lipid droplets during the dauer stage with and without functional AMPK. In order to do this, we introduced a fully functional ATGL-1::GFP translational fusion protein, into AMPK-sufficient (*daf-2)* and AMPK-deficient (*daf-2; aak(0))* dauer larvae to compare ATGL-1 localization with labeled lipid droplets as animals progress through the dauer stage. For comparison, we consider the first 48 hours after being shifted to non-permissive temperature as the dauer entry period, after which dauer day 0 begins. In control AMPK (+) dauer larvae, ATGL-1 was sequestered away from the lipid droplets during dauer entry (Figure 3.1A), whereas in AMPK-deficient dauers ATGL-1 began to accumulate on the surface of the lipid droplets 16 hours after being shifted to non-permissive temperature. This overlap between ATGL-1 and the lipid droplets was maintained well after the dauer entry period (Figure 3.1A and C). In addition, levels of ATGL-1 appeared significantly higher in AMPK mutant larvae suggesting that in addition to affecting localization, the levels of ATGL-1 may also be subject to AMPK-mediated regulation.

Given that ATGL-1 is directly phosphorylated and inhibited by AMPK during the dauer stage, the observed increase in ATGL-1 levels motivated us to question whether the phosphorylation of ATGL-1 by AMPK could result in a reduction of ATGL-1 protein. To address this, we first looked at the expression pattern of ATGL-1 and stained lipid droplets in control *daf-2* and AMPK-deficient dauer larvae during early dauer stage. Throughout the first 4 days of dauer the expression level of ATGL-1 was significantly higher in AMPK-deficient animals compared to control *daf-2* animals and was comparable to pre-dauer levels (Figure 3.1B and D). Using an antibody that we generated against ATGL-1 (Figure S3.1), we noted that ATGL-1 protein was significantly more abundant in AMPK-deficient dauer larvae, consistent with the GFP expression pattern, while mRNA levels were not dramatically changed (Figure 3.1E and

S3.2). Taken together, these results suggest that AMPK-mediated phosphorylation of ATGL-1 has two consequences: First, it alters the subcellular localization of ATGL-1, possibly to limit its accessibility to the lipid droplet substrates; while secondly, it reduces ATGL-1 protein abundance. Both effects eventually result in protection of the lipid reserves from premature depletion during dauer.

AMPK Regulates ATGL-1 by Altering its Subcellular Localization and Enhancing its Proteasome-Mediated Degradation

To characterize how the ATGL-1 protein levels are affected by AMPK, we first investigated whether AMPK phosphorylation targets ATGL-1 for proteasome degradation. Using RNAi, we reduced the levels of individual proteasome components in dauer larvae and compared the ATGL-1 levels with those in *daf-2* control dauer larvae. We found that RNAi of most of the proteasome components increased the amount of ATGL-1 protein in dauer larvae suggesting that ATGL-1 levels are regulated by proteasome-mediated degradation (Figure 3.2A). Given that many proteins are tagged with a polyubiquitin chain prior to proteasome degradation, we next questioned whether this might also be the case for ATGL-1. We therefore immunoprecipitated ATGL-1 protein from whole worm lysates obtained from control and AMPK-deficient dauer larvae and blotted the precipitates with anti-ubiquitin (Santa Cruz Biotechnology). When normalized for the levels of ATGL-1 protein in the immunoprecipitates, we detected more ubiquitin associated with ATGL-1 protein in *control* dauer larvae compared to AMPK-deficient animals indicating that ATGL-1 is likely ubiquitylated in an AMPK-dependent manner prior to its degradation via the proteasome (Figure 3.2B).

Many of the downstream effects of AMPK phosphorylation that have been characterized are mediated through the generation of 14-3-3 protein binding sites (Mihaylova and Shaw, 2011; Gwinn et al., 2008), Therefore, since we observed a change in the subcellular localization of ATGL-1 in the presence and absence of AMPK we questioned whether a similar mechanism might underlie the cellular relocalization of ATGL-1. We performed bioinformatic analysis of the ATGL-1 protein sequence which revealed the

presence of several regions that corresponded to potential 14-3-3 protein binding sites (data not shown). To address whether AMPK may generate 14-3-3 sites on ATGL-1 to affect its localization from the lipid droplets, we re-analyzed our ATGL-1 immunoprecipitates from control and AMPK-deficient dauers with a 14-3-3 motif antibody that was generated against peptides bearing R-X-Y/F-X-pS sequence (Cell signaling) (Figure S3.3A). Antibody staining suggested that 14-3-3 binding sites were less prominent in dauer larvae that lacked AMPK compared to control dauer larvae, consistent with a model wherein phosphorylation of ATGL-1 by AMPK generates a 14-3-3 site that affects subcellular localisation (Figure 3.2C). To directly verify the interaction between ATGL-1 and 14-3-3 protein, we performed immunoprecipitation studies on ATGL-1 and PAR-5, the major 14-3-3 protein homologue in *C. elegans*. Consistent with the observation that more 14-3-3 motifs are generated on ATGL-1 in the presence of AMPK, we found that anti-PAR-5 consistently immunoprecipitated more ATGL-1 in control AMPK (+) dauer larvae compared to AMPK-deficient larvae, while the reciprocal immunoprecipitation with our anti-ATGL-1 similarly yielded more PAR-5 in the precipitates in control dauer larvae (Figure 3.2D and Figure S3.3B). These data are consistent with an increase in 14-3-3/PAR-5 binding to ATGL-1 following phosphorylation by AMPK.

To further investigate whether the degradation of ATGL-1 and its change of subcellular localization are directly linked to AMPK phosphorylation, we compared the ATGL-1 levels and subcellular localization in *daf-2* dauer larvae containing either wild type ATGL-1 or a non-phosphorylable ATGL-1 variant (S303A) tagged with GFP (Narbonne and Roy, 2009). We found that the level of ATGL-1 expression was significantly higher in S303A variants when compared to wild type (Figure S3.4), suggesting that the major AMPK phosphorylable site S303 on ATGL-1 is critical for its proteasome-mediated degradation. Because ATGL-1 remains associated with lipid droplets and is more abundant in AMPK-deficient dauer larvae, we suggest that the phosphorylation and the increase in 14-3-3 binding are linked to the subsequent subcellular localization and degradation of ATGL-1, thus providing a switch-like mechanism that would protect the triglyceride stores for long term use during dauer.

Reducing the Levels of the *C. elegans* CGI-58 Homologue Enhances the Survival, Compromises Triglyceride Hydrolysis and Suppresses the Osmoregulatory Defects of AMPK-Deficient Dauer Larvae

Although AMPK negatively regulates ATGL-1 during the dauer stage, we and others have identified factors that enhance ATGL-1 activity (Xie and Roy, 2012; Gruber et al., 2010; Yang et al., 2010). In mammalian cells ATGL is regulated by a complex relay mechanism between lipid droplet-associated proteins such as the Perilipins, G0S2 and CGI-58. At present, no clear orthologue of G0S2, or the Perilipin protein family has been detected in the annotation of the *C. elegans* genome sequence. To further explore how ATGL-1 may be regulated during the dauer stage, we characterized the function of the *C. elegans* orthologue of mammalian CGI-58, which we identified in a genome-wide survey for genes that phenocopied *atgl-1(RNAi)* (Xie and Roy, 2012). The *C. elegans* gene locus, C37H5.3, is expressed as two alternative transcripts, both of which encode a protein that is 54% similar and 37% identical to the human CGI-58 protein (Figure 3.3A). Importantly, the N-terminal tryptophan-rich region previously shown to be critical for the correct localization and ATGL-activating function of mammalian CGI-58 is conserved in *C. elegans* (Gruber et al., 2010). Using both RNAi and an available CGI-58 mutant with a ~800bp deletion (*ok3245*), we found that elimination of CGI-58 protein significantly increased the survival of AMPK mutant dauer larvae much like *atgl-1(RNAi)* (Figure 3.3B). We also noticed that there was no difference in dauer survival when we eliminated CGI-58 and ATGL-1 together (Figure 3.3B), indicating that *C. elegans* CGI-58 protein has no ATGL-independent role in dauer survival. In addition, the *cgi-58* mutant allele partially restored the total lipid and triglyceride level, reduced ATGL-1 lipase activity and improved the osmoresistance of AMPK mutant dauer larvae when cultured in high salt conditions (Figure 3.3C-F). Consistent with the ATGL-1-dependent function of CGI-58 in dauer survival, we did not observe any apparent ATGL-independent roles of CGI-58 on total triglyceride restoration and lipase activity alteration (Figure 3.3C and E). Taken together, we conclude that the depletion of *C. elegans* CGI-58 can prolong the survival of AMPK mutant dauer larvae by reducing ATGL-1 lipase activity to conserve the lipid reserve and thereby indirectly improving

excretory/osmoregulatory function, probably through maintenance of organismal energy levels.

CGI-58 Physically Interacts with ATGL-1 in vivo and Affects ATGL-1 Localization on Lipid Droplets

To better understand the role of CGI-58 in regulating ATGL-1, we constructed a CGI-58::GFP translational fusion and introduced it into control *daf-2* animals and subsequently crossed the same array into AMPK-deficient animals. During the dauer stage, CGI-58 is expressed in both control and AMPK mutant dauer larvae mainly in the hypodermis and intestine, the two *C. elegans* tissues that have been well characterized for their role in lipid synthesis and storage (Figure 3.4A). We next compared the levels of CGI-58 in control and AMPK-deficient dauers. Similar to the ATGL-1 levels (Figure 1E), the CGI-58 protein levels were also increased in the absence of AMPK (Figure 3.4B). However, unlike ATGL-1, some GFP tagged CGI-58 proteins were expressed on the lipid droplets in control *daf-2* dauers, compared to the complete sequestration of ATGL-1 away from the lipid droplets in these animals (Figure 3.4C and 3.1A). Because the levels of ATGL-1 are regulated in an AMPK-dependent manner in dauer animals we wanted to address whether CGI-58 might contribute to the stability of ATGL-1 in this developmental context. We compared ATGL-1 levels in both AMPK-deficient control dauer larvae and in AMPK; CGI-58-deficient animals to test whether CGI-58 compromise leads to a reduction in the amount of ATGL-1 protein. We noted that overall ATGL-1 protein levels were unaffected by the elimination of CGI-58, but alternatively ATGL-1 signal was distinct from the lipid droplets at dauer day 0 in the absence of CGI-58, unlike in AMPK-deficient dauer larvae where ATGL-1 remains closely associated with the lipid droplets (Figure 3.4D and S3.5). To further confirm the role of CGI-58 in localizing ATGL-1 to the lipid droplets, we isolated lipid droplets from intact animals and determined the ATGL-1 protein levels in both control and AMPK-deficient dauer larvae that were competent or compromised for CGI-58 function. Isolated lipid droplets were verified by C_1-BODIPY-C_{12} staining, protein expression pattern and triglyceride enrichment compared to fractions carrying cytoplasm (Figure

S3.6). Following separation we observed that ATGL-1 was more abundant in the lipid droplet fraction compared to our cytoplasmic fractions in AMPK-deficient dauers, while this was completely reversed in the isolated fractions from genotypically identical animals that lacked CGI-58, suggesting that ATGL-1 associates with the lipid droplets in AMPK-deficient dauer larvae in a CGI-58-dependent manner (Figure 3.4E). This was not observed in control *daf-2* dauer larvae with mutated CGI-58, likely due to the reduced levels ATGL-1.

In mammalian cells CGI-58 was reported to bind to ATGL, which leads to its optimal activation in vitro (Schweiger et al., 2008), therefore we tested whether CGI-58 interacts with ATGL-1 in vivo, and if so, how this association is regulated. We generated a rescuing, epitope-tagged translational fusion variant of CGI-58 and incubated protein extract obtained from transgenically rescued animals with ATGL-1 antibody covalently linked to agarose beads. By probing for CGI-58 protein we noted that *C. elegans* CGI-58 also interacts with ATGL-1 protein in a mixed population of animals, consistent with observations in mammals that these proteins are associated (Figure 3.4F). To further verify their interaction during the dauer stage, we performed the same experiment on control *daf-2* and AMPK-deficient dauer animals that possessed our GFP-tagged CGI-58 transgene and we found that CGI-58 interacts with ATGL-1 during the dauer stage both in the presence and absence of AMPK (Figure 3.4G).

Taken together, *C. elegans* CGI-58 protein is mainly expressed in the hypodermis and intestine, where it interacts with ATGL-1 and tethers it to the lipid droplets in the absence of AMPK. Since the interaction of the two proteins are not affected by AMPK and ATGL-1 proteins are sequestered away from the lipid droplets and targeted for proteasome degradation, the reduced level of CGI-58 proteins observed in control animals is likely due to their co-degradation with the bounded ATGL-1 proteins. In addition, there is a second population of CGI-58 proteins remaining expressed on the lipid droplets in control animals, which are likely not bound to ATGL-1 and are therefore not degraded.

CGI-58 and ATGL-1 Cooperate to Maintain Lipid Droplet Morphology

Given that both ATGL-1 and CGI-58 are in close association with lipid droplets, we wondered whether these proteins play some structural role on the droplets in addition to their well-documented enzymatic function. It was recently shown that in late stage wild type larvae C_1-BODIPY-C_{12} labelled lysosome-related organelles (LROs) with high intensity, while lipid droplets stained with low intensity (Zhang et al., 2010). Although this may be true in L4 animals, C_1-BODIPY-C_{12} recognizes lipid droplets quite exclusively in dauer animals (Figure S3.7). Therefore, we monitored the C_1-BODIPY-C_{12}-stained lipid droplets in dauer to ascertain whether CGI-58 and ATGL-1 contribute to lipid droplet structure. We first documented the morphological changes that occur to the lipid droplets during the entire dauer entry period in control *daf-2* and AMPK-deficient animals, with or without CGI-58 function (Figure S3.8). The lipid droplet size of the AMPK; CGI-58-deficient animals was compared to those present in AMPK-deficient animals from 25 hours into the dauer entry period and thereafter, to reveal that the size of the droplets was significantly increased in the animals that lacked CGI-58 (Figure 3.5A). The difference was most pronounced 32 hours following dauer entry and was not unique to AMPK-deficient animals since similar defects were observed between control *daf-2* dauer larvae and CGI-58-deficient dauers (Figure 3.5A and B). We then tested whether the compromise of ATGL-1, CGI-58 or both mutations combined, would result in similar changes to the lipid droplets in control (*daf-2)* or AMPK-deficient dauer larvae 32 hours after dauer entry. We noticed that in both control *daf-2* and AMPK-deficient animals, elimination of either ATGL-1 or CGI-58 resulted in a slight alteration of the typical spherical morphology of the lipid droplets, while also causing an increase in lipid droplet size. However, the elimination of both genes led to a dramatic distortion of lipid droplet structure (Figure 3.5B), while these effects were also observed in isolated lipid droplets (Figure 3.5C and Figure S3.9). Notably, the removal of other lipase activities, such as hormone sensitive lipase (*hosl-1*), did not alter the lipid droplet structure in any genetic background we tested (Figure S3.10), consistent with its secondary role in lipid hydrolysis during dauer survival (Narbonne and Roy, 2009).

Since we observed a persistent increase in lipid droplet size in AMPK mutant dauers that lacked CGI-58, we questioned whether the increase resulted from an accumulation of triglycerides due to reduced hydrolytic activity. We measured the triglyceride level in isolated lipid droplets from these animals at the corresponding time points and found that the abundance of triglycerides correlated with the increase in lipid droplet size at all time points that were analysed (Figure 3.5D and E). We next questioned whether these additional triglycerides originated from synthesis in the endoplasmic reticulum (ER). To meet this end, we eliminated the genes encoding the recently identified ER resident proteins that are components of the triglyceride synthesis complex; *acs-22* and *dgat-2* (Xu et al., 2012) in AMPK; CGI-58-deficient animals to observe the effects they might cause on lipid droplet size. Indeed, elimination of either ER gene product resulted in a significant reduction in lipid droplet size in all corresponding time points except 48hr (Figure 3.5F), likely due to drop in energy production by that point. *acs-22* and *dgat-2* do not seem to genetically interact with *cgi-58*, given that the survival of AMPK and AMPK; CGI-58-deficient dauers were not affected by their compromise (Figure S3.11). The increased lipid droplet size observed in AMPK; CGI-58-deficient animals is most probably due to reduced ATGL-1 activity rather than blockage of ER flux, given that the lipid droplets of all the genotypes we tested showed an initial gradual increase in size indicating a constant deposit of synthesized lipids until about 32 hours into the dauer entry period, after which the size started to decrease, probably marking the termination of feeding and corresponding lipid synthesis (Figure 3.5A and S3.8). If ER flux was affected, the initial increase in lipid droplet size would not occur due to the impaired transport machinery. Therefore, taken together, our results suggest that the presence of the ATGL-1/CGI-58 complex is crucial for the maintenance of the normal spherical structure of lipid droplets, which is correlated with triglyceride deposition that originates from ER synthesis.

CGI-58 Prevents Lipid Droplet Fusion and Lipid Exchange

While monitoring the changes in lipid droplet morphology, we noticed that loss of CGI-58 enhanced the frequency of fusion events that occurred among individual lipid

droplets both in isolated lipid droplets (Figure 3.6A and S3.12) and live dauers monitored under real time (Figure 3.6C and S3.13). This was not observed in ATGL-1-deficient animals (data not shown), suggesting an ATGL-1 independent role of CGI-58, which is likely attributed to the population remaining on the lipid droplets that are not bound to or degraded together with ATGL-1. These fusion events occurred 2 to 6 times more frequently in the absence of CGI-58 based on quantification of over 1000 isolated lipid droplets for each genotype (Figure 3.6D). To better understand the consequences of these fusion events and how CGI-58 affected them, we differentially labeled the lipid droplets of two populations of animals with either red or green BODIPY, respectively. We then isolated the two sets of lipid droplets, co-incubated them and documented the exchange of differentially-labelled lipid constituents among the lipid droplets isolated from control or AMPK-deficient dauer larvae with and without functional CGI-58. We noticed that loss of CGI-58 resulted in an enhanced exchange of lipid content among the droplets in both control *daf-2* and AMPK-deficient animals (Figure 3.6B and E). Moreover, using FRAP assays we noted that full fluorescent signal recovered significantly less efficiently in vivo when AMPK-deficient dauer larvae possessed functional CGI-58 (Figure 3.6F and G). Taken together, these results suggest that CGI-58 acts on the surface of the lipid droplets to protect them from merging and subsequent content exchange, which ultimately affects triglyceride content, droplet size, and the overall morphology of the organelle.

Discussion

The *C. elegans* dauer stage provides the larva with a unique alternative to survive a multitude of environmental stresses, where instead of continuing the normal reproductive life cycle, larvae enter a motionless and non-feeding stage that is associated with global developmental arrest. This diapause-like stage illustrates how organisms have evolved specialized adaptations that permit them to readjust their metabolic state to respond to their variable environment. Astonishingly, dauer larvae have been documented to survive extremely low pH; desiccation; osmotic stress and they can survive months without external nutrient intake by augmenting fat accumulation during the dauer entry period and subsequent metabolic remodeling, including the activation of the glyoxylate cycle and increased fatty acid *de novo* synthesis (Riddle and Albert, 1997; Perez and Van Gilst, 2008; Xie and Roy, 2012).

Upon entry into dauer AMPK expression and activation is increased. This protein kinase acts as a “metabolic master switch” by sensing high intracellular AMP:ATP ratios to regulate a number of metabolic pathways that impact on behavior, stem cell quiescence (Narbonne and Roy, 2006)., lifespan determination (Apfeld et al., 2004; Curtis et al., 2006) and lipid metabolism. In dauer larvae, AMPK directly phosphorylates and inhibits ATGL-1 to protect the triglyceride stockpile for long-term usage (Narbonne and Roy, 2009). *daf-2* dauers with compromised AMPK function demonstrate aberrantly high ATGL-1 activity resulting in rapid exhaustion of the energy reserve and consequently premature expiration of the animals. AMPK plays an “energy protecting” role through phosphorylation of ATGL-1 in *C. elegans* dauer larvae, which we demonstrate has a two-fold effect: first, it generates a 14-3-3 protein binding sites on ATGL-1 to sequester it away from its substrate, while the same phosphorylation targets ATGL-1 for proteasome-mediated degradation. AMPK-dependent proteasome-degradation has been widely observed in skeletal muscle and myocardial cells (reviewed by Goodman et al., 2011; Baskin and Taegtmeyer, 2011), where it alters muscle contraction to cope with fluctuations in external nutrient availability. Furthermore, AMPK links cellular energy stress to growth arrest via phosphorylation of Raptor to generate a 14-3-3 protein recognition site (Gwinn et al., 2008). Similarly, during the dauer diapause AMPK

uses these two evolutionarily conserved mechanisms to safeguard the cellular energy reservoir from depletion by segregating the major lipolysis enzyme from its substrate and targeting it for degradation (Figure 3.7). It is worth mentioning that we noticed a basal level of ubiquitylation and phosphorylated 14-3-3 binding in the absence of AMPK, indicating that AMPK may not be the only enzyme that regulates ATGL in *daf-2* dauer larvae.

AMPK mutant dauer larvae die prematurely after a short period in the dauer stage, while their survival can be enhanced by removing many genes that affect lipid turnover (Xie and Roy, 2012). The triglyceride stores increase substantially in AMPK-deficient dauer larvae subjected to *atgl-1*(RNAi), while the lipid droplets acquire an abnormal morphology. The lipid droplets have long been considered as inert fat particles but are now recognized as dynamic organelles that comprise a core composed of neutral lipids surrounded by a phospholipid monolayer harbouring numerous lipophilic proteins. In mammals, a number of these lipid droplet-associated proteins have been well characterized. Among them, the Perilipin family members are considered to be the most abundant proteins present on the lipid droplet surface, presumably serving to protect the stored lipids by limiting accessibility of hydrolytic enzymes during basal conditions (reviewed by Brasaemle, 2007). In addition, the CIDE family proteins are also closely associated with lipid droplets and modulate fat storage and lipid droplet size in vertebrates (Puri et al., 2008). Intriguingly, there are no clear orthologues of these protein families in *C. elegans*, suggesting that alternative regulatory mechanisms must exist that are independent of these well-characterized proteins, or other proteins have been co-opted to carry out analogous functions in *C. elegans*.

All organisms that possess an ATGL orthologue also harbour a CGI-58-like protein that presumably functions with ATGL. Since the *C. elegans* genome does not encode regulatory molecules such as Perilipin we wondered if the interaction between ATGL-1 and CGI-58 might differ in *C. elegans*, circumventing any requirement for the Perilipin family of proteins. By characterizing the *C. elegans* orthologue of human CGI-58 protein we revealed that it affects lipid hydrolysis in an ATGL-dependent manner. Elimination of CGI-58 in AMPK-deficient dauer larvae was sufficient to prolong the survival of these

animals by correcting the associated lipolytic and osmotic defects. Consistent with its role as a co-activator of ATGL, ATGL-1 lipase activity was significantly reduced in the absence of CGI-58. Moreover, in the absence of AMPK, ATGL proteins are released from sequestration and are anew capable of binding substrate. However, this binding is mediated by CGI-58 since its elimination resulted in the clear segregation of ATGL-1 from the lipid droplets in AMPK-deficient dauer larvae (Figure 3.7). Therefore, like in mammalian cells, the activation of ATGL-1 not only requires its interaction with CGI-58, but also binding of CGI-58 to the lipid droplets (Gruber et al., 2010).

Using a novel approach based on fluorescently-labelled lipid droplet purification we revealed that in addition to its role in activating ATGL-1, CGI-58 also acts as a guardian protein at the surface of the lipid droplets to limit the expansion of the droplets from potential collision/fusion events. Such fusion events have been previously described in mammalian cells (Boström et al., 2007; Guo et al., 2008). In *Arabidopsis*, the loss of the major structural lipid droplet protein, Oleosin, resulted in apparent lipid droplet fusion, very similar to the function we ascribe to CGI-58 (Siloto et al., 2006). CGI-58 appears to have adopted dual functions throughout evolution to regulate both lipid hydrolysis and the maintenance of the lipid droplet size and morphology.

It is somewhat puzzling that the enzymatic function of CGI-58 would be linked to a role in regulating lipid droplet expansion. However, during lipolysis various lipases are recruited directly to the surface of the lipid droplet where they interact with their substrates at the interphase of surface monolayer and the neutral lipid core. The mechanism that permits these enzymes to penetrate the lipid monolayer of the lipid droplets remains unclear, as is the export of the released free fatty acid products out of the lipid droplets. Active transporters embedded in the membrane or alternative mechanisms that involve the separation of the membrane lipid constituents must be invoked. Regardless of the mechanisms, if the transporters are rate limiting, expanded lipid droplets would tend to accumulate fatty acid bi-products near the surface close to the site of catalysis, potentially limiting enzyme access to the triglyceride substrate core. This would select for an optimal lipid droplet size linked to enzymatic efficacy. Intriguingly, evidence suggests that under maximum stimulation of lipolysis, the lipid

droplets break down into smaller entities to increase the surface area for enzyme interaction (Farese and Walther, 2009). By preventing fusion of smaller lipid droplets into larger ones, CGI-58 indirectly facilitates lipolysis by enhancing the efficiency of ATGL-1. Our findings suggest that in *C. elegans* and all other nematodes that we have examined so far, the Perilipin family of proteins is absent. It is not clear why this phylum lost the Perilipin gene family, but nevertheless it strongly suggests that CGI-58 was co-opted during evolution to provide the structural supporting role of the Perilipin protein family in maintaining the regular spherical structure of the lipid droplets observed in other animals. This may provide an indication to the underlying mechanism that regulates the unique sizes of all kinds of cellular vesicles.

Mutation of the *cgi-58* gene is associated with the neutral lipid storage disease, Chanarin-Dorfman syndrome, characterized by accumulation of triglycerides in cytoplasm of multiple tissues. We have demonstrated a novel role of CGI-58 in the *C. elegans* dauer larvae where it also acts structurally to limit expansion of the lipid droplets, thereby regulating the utilization of the triglyceride energy source. Our data provide insight in the regulation of lipolysis and may provide new avenues of intervention based on modifiers of lipid droplet morphology in the treatment of Chanarin-Dorfman Syndrome or other diseases associated with impaired lipid storage and/or hydrolysis.

EXPERIMENTAL PROCEDURES

Strains, Plasmids and Transgenic Animals

C. elegans were cultured as previously described by Brenner (Brenner, 1974). The following alleles and strains were used:

The strains VS20 *hjIs67[Patgl-1::atgl-1::GFP]* (Zhang et al., 2010) and RB2386 *C37H5.3(ok3245)* were obtained from CGC and subsequently crossed into CB1370 *daf-2(e1370)* and MR1000 *daf-2(e1370); aak-1(tm1944); aak-2(ok524)* strains. *ok3245* bears a 800bp deletion that occupies almost two thirds of the gene, therefore, the allele is predicted to be null. C37H5.3 DNA and its upstream ~800bp was amplified by PCR and subsequently cloned into pPD95.77 and pMR837 vectors to generate pMR613 *(Pcgi-58::cgi-58::GFP)* and pMR612 (*Pcgi-58::cgi-58::FLAGx3)*. Extrachromosomal arrays of pMR613 and pMR612 were generated by standard microinjection into CB1370 *daf-2(e1370)* and *unc-119* animals using *unc-119* cDNA rescue fragment and *rol-6* as co-injection markers respectively. Rabbit polyclonal antibody against ATGL-1 was raised by using synthetic peptide CTKRKVPDEPTTSKR (GenScript). Anti-ubiquitin (Santa Cruz), anti-P-14-3-3 (Cell Signaling) and anti-Flag (Sigma) antibodies are available commercially.

Feeding RNAi

Our feeding RNAi protocol was performed as previously described (Kamath et al., 2001). Briefly, synchronized L1 animals were added onto regular plates seeded with individual dsRNA-expressing bacterial clones and maintained at 15°C. Phenotypes were scored subsequently.

Dauer Survival

Dauer survival was determined as described elsewhere (Narbonne and Roy, 2006). Dauer larvae were kept in double-distilled water. Survival was scored according to their appearance and moving response to a gentle tap on the plate.

Oil Red O Staining of Dauer Larvae

Oil Red O staining of dauer larvae was performed as described (Soukas et al., 2009). Dauer larvae were fixed in 2% paraformaldehyde and stained with 60% Oil Red O solution. Stained dauer larvae were observed and imaged using DIC optics on a Zeiss Imager.21 microscope equipped with a Hamamatsu camera and. Optical density was determined using OpenLab software (Improvision).

Immunoprecipitation and Western Blotting

C. elegans larvae and adults were lysed by sonication in lysis buffer (50mM Hepes pH7.5, 150mM NaCl, 10% glycerol, 1% Triton X-100, 1.5mM $MgCl_2$, 1mM EDTA and protease inhibitors) and then incubated with anti-ATGL-1 or anti-PAR-5 antibody. Immunoprecipitations were performed with Protein-A agarose followed by immunoblotting with anti-ubiquitin, anti-P-14-3-3, anti-PAR-5 or anti-ATGL-1 antibody. Protein concentration was determined using a NanoDrop 2000c spectrophotometer (Thermo Scientific).

Triglyceride Quantification

Triglyceride content was determined with a commercially available kit (Sigma-Aldrich) according to manufacturer's recommendations. Absorbance was measured with a NanoDrop 2000c spectrophotometer at 540 nm. All calculated triglyceride concentrations were finally normalized to protein concentration.

Osmotic Resistance Assay

Osmotic resistance of dauer larvae was performed as described (Narbonne and Roy, 2009). The survival of day 4 dauer larvae was scored after being exposed to solutions of varying NaCl concentrations for 24 hours at 25°C.

Quantification of Lipase Activity

Lipase activity for dauer animals was measured as described (Narbonne and Roy, 2009) using a commercially available QuantiChrom kit from BioAssay Systems according to

manufacturer's recommendations. OD values were measured with a Varioskan Flash Multimode Reader version 3.00.7 at the wavelength of 412 nm.

C1-BODIPY-C12 Staining

C1-BODIPY-C12 staining was performed as described (Mak et al., 2006). Synchronized L1 larvae were transferred to regular plates with C1-BODIPY-C12 and grown at 25°C. Images were acquired on a LSM510 confocal microscope (Zeiss) using a x40 1.3 oil objective. Lipid droplet diameter was measured using AxioVision (Zeiss) software and volume was calculated using the following formula: $4/3 \times \pi \times (\text{diameter}/2)^3$.

Lipid Droplet Isolation

Lipid droplet isolation was performed as described (Zhang et al., 2010). Animals fed with OP50/OP50+C1-BODIPY-C12 were washed with 1xPBS + 0.001% Triton X-100 and subsequently collected in Buffer A (25mM Tris pH7.6, 25mM glycine, 120mM sucrose and protease inhibitors). The mixture was placed into a metal homogenizer with a tight-fit pestle and lysed with 20 strokes. The homogenates were centrifuged at 1000g for 10 min at 4°C and the top layer containing the lipid droplets was collected and washed twice with Buffer A before analysis.

Lipid Exchange Assay

Green and red C1-BODIPY-C12 stained lipid droplets were isolated as described above. 100µl of each of the two populations of lipid droplets were added into a 1.5ml eppendorf tube and incubated at 15°C for 30min. Lipid exchange was observed using a LSM510 confocal microscope (Zeiss) with a x40 1.3 oil objective. Incubation at 4°C and 20°C was also tested and similar results were obtained. Fluorescent intensity was quantified using ImageJ software.

Lipid Droplet Fusion Live Imaging

C1-BODIPY-C12 stained animals were paralyzed in 3mM levamisol for 3 min before being transferred onto a freshly prepared 2% agarose pad. Imaging was performed on dauer larvae 32 hours after shifting to restrictive temperature using a Quorum WaveFX spinning disk confocal system, on a Leica DMI6000B inverted microscope using a

63x/1.40-0.6 oil objective and controlled by the Metamorph acquisition software. For each animal, a time series of 15 minutes was taken.

Fluorescence Recovery after Photobleaching (FRAP)

FRAP experiments were performed on dauer day 0 animals on a Quorum WaveFX spinning disk confocal system, on a Leica DMI6000B inverted microscope using a 63x/1.40-0.6 oil objective and controlled by the Metamorph acquisition software. For each animal, a time series was taken. After the tenth frame, 1000ms of photobleaching was performed using a mosaic laser at maximum power. The time series continued for 16 seconds/50 frames, immediately followed by a 5 minutes time lapse, 20 seconds per frame. Average fluorescence intensity of the bleached area was plotted against the time series. At least five photobleaching assays were performed for each strain.

Statistical Analysis

Values are mean+SD. Comparison of mean values was evaluated by one-way ANOVA followed by a Tukey HSD test. A p value less than 0.05 was considered significant. In all experiments, the number of asterisks represents the following: * $P<0.05$ and ** $P<0.01$.

Acknowledgements

We thank Dr. Andy Golden for PAR-5 antibody. We also thank the *Caenorhabditis* Genetic Center for *C. elegans* strains. This work was supported by a research grant from Canadian Institutes of Health Research (CIHR).

References

Apfeld, J., O'Connor, G., McDonagh, T., and DiStefano, P. S. and Curtis, R. (2004). The AMP-activated protein kinase AAK-2 links energy levels and insulin-like signals to lifespan in C. elegans. *Genes Dev*. **18**, 3004–9.

Baskin, K. K. and Taegtmeyer, H. (2011). An expanded role for AMP-activated protein kinase: regulator of myocardial protein degradation. *Trends Cardiovasc Med*. **21**, 124-7.

Boström, P., Andersson, L., Rutberg, M., Perman, J., Lidberg, U., Johansson, B. R., Fernandez-Rodriguez, J., Ericson, J., Nilsson, T., Borén, J. and Olofsson, S. O. (2007). SNARE proteins mediate fusion between cytosolic lipid droplets and are implicated in insulin sensitivity. *Nat Cell Biol*. **9**, 1286-93.

Brasaemle, D. L. (2007). Thematic review series: adipocyte biology. The Perilipin family of structural lipid droplet proteins: stabilization of lipid droplets and control of lipolysis. *J Lipid Res*. **48**, 2547-59.

Curtis, R., O'Connor, G. and DiStefano, P. S. (2006). Aging networks in Caenorhabditis elegans: AMP-activated protein kinase (aak-2) links multiple aging and metabolism pathways. *Aging Cell* **5**, 119–26.

Farese, R. V. Jr. and Walther, T. C. (2009). Lipid droplets finally get a little R-E-S-P-E-C-T. *Cell* **139**, 855-60.

Fielenbach, N. and Antebi, A. (2008). C. elegans dauer formation and the molecular basis of plasticity. *Genes&Development* **22**, 2149-65.

Goodman, C. A., Mayhew, D. L. and Hornberger, T. A. (2011). Recent progress toward understanding the molecular mechanisms that regulate skeletal muscle mass. *Cell Signal*. **23**, 1896-906.

Gruber, A., Cornaciu, I., Lass, A., Schweiger, M., Poeschl, M., Eder, C., Kumari, M., Schoiswohl, G., Wolinski, H., Kohlwein, S. D., Zechner, R., Zimmermann, R. and Oberer, M. (2010). The N-terminal region of comparative gene identification-58 (CGI-58)

is important for lipid droplet binding and activation of adipose triglyceride lipase. *J Biol Chem*. **285**, 12289-98.

Guo, Y., Walther, T. C., Rao, M., Stuurman, N., Goshima, G., Terayama, K., Wong, J. S., Vale, R. D., Walter, P. and Farese, R. V. (2008). Functional genomic screen reveals genes involved in lipid-droplet formation and utilization. *Nature*. **453**, 657-61.

Gwinn, D. M., Shackelford, D. B., Egan, D. F., Mihaylova, M. M., Mery, A., Vasquez, D. S., Turk, B. E. and Shaw, R. J. (2008). AMPK phosphorylation of raptor mediates a metabolic checkpoint. *Mol Cell*. **30**, 214-26.

Haemmerle, G., Lass, A., Zimmermann, R., Gorkiewicz, G., Meyer, C., Rozman, J., Heldmaier, G., Maier, R., Theussl, C., Eder, S., Kratky, D., Wagner, E. F., Klingenspor, M., Hoefler, G. and Zechner, R. (2006). Defective lipolysis and altered energy metabolism in mice lacking adipose triglyceride lipase. *Science*. **312**, 734-7.

Hardie, D. G. (2007). AMP-activated /SNF1 protein kinases: Conserved guardins of cellular energy. *Nature Rev. Mol. Cell Biol*. **8**, 774-85.

Hawley, S. A., Boudeau, J., Reid, J. L., Mustard, K. J., Udd, L., Makela, T. P., Alessi, D. R. and Hardie, D. G. (2003). Complexes between the LKB1 tumor suppressor, STRADa/b and MO25a/b are upstream kinases in the AMP-activated protein kinase cascade. *J. Biol.* **2**, 28.

Holliday, R. (1989). Food, reproduction and longevity: is the extended lifespan of calorie-restricted animals an evolutionary adaptation? *Bioessays* **10**, 125-7.

Jonkel, C. J., Jonkel, Mc. T. and Cowan, I. (1977). The black bear in the sprucefir forest. *Wildl. Monogr*. **27**, 1-57.

Kamath, R. S., Martinez-Campos, M., Zipperlen, P., Fraser, A. G. and Ahringer, J. (2001). Effectiveness of specific RNA-mediated interference through ingested double-stranded RNA in Caenorhabditis elegans. *Genome Biol.* **2**, 1-10.

J. Kirkwood, T.B. (1977). Evolution of ageing. *Nature* **270**, 301-4.

Lass, A., Zimmermann, R., Haemmerle, G., Riederer, M., Schoiswohl, G., Schweiger, M., Kienesberger, P., Strauss, J. G., Gorkiewicz, G. and Zechner, R.

(2006). Adipose triglyceride lipase-mediated lipolysis of cellular fat stores is activated by CGI-58 and defective in Chanarin-Dorfman Syndrome. *Cell Metab*. **3**, 309-19.

Lefèvre, C., Jobard, F., Caux, F., Bouadjar, B., Karaduman, A., Heilig, R., Lakhdar, H., Wollenberg, A., Verret, J. L., Weissenbach, J., Ozgüc, M., Lathrop, M., Prud'homme, J. F. and Fischer, J. (2001). Mutations in CGI-58, the gene encoding a new protein of the esterase/lipase/thioesterase subfamily, in Chanarin-Dorfman syndrome. *Am J Hum Genet*. **69**, 1002-12.

Mak, H. Y., Nelson, L. S., Basson, M., Johnson, C. D. and Ruvkun G. (2006). Polygenic control of Caenorhabditis elegans fat storage. *Nat Genet.* **38**, 363-8.

Mihaylova, M. M. and Shaw, R. J. (2011). The AMPK signalling pathway coordinates cell growth, autophagy and metabolism. *Nat Cell Biol.* **13**, 1016-23.

Narbonne, P. and Roy, R. (2006). Inhibition of germline proliferation during C. elegans dauer development requires PTEN, LKB1 and AMPK signaling. *Development* **133**, 611-9.

Narbonne, P. and Roy, R. (2009). Caenorhabditis elegans dauers need LKB1/AMPK to ration lipid reserves and ensure long-term survival. *Nature* **457**, 210-4.

Perez, C. L. and Van Gilst, M. R. (2008). A 13C isotope labeling strategy reveals the influence of insulin signaling on lipogenesis in C. elegans. *Cell Metab*. **8**, 266-74.

Puri, V., Ranjit, S., Konda, S., Nicoloro, S. M., Straubhaar, J., Chawla, A., Chouinard, M., Lin, C., Burkart, A., Corvera, S., Perugini, R. A. and Czech, M. P. (2008). Cidea is associated with lipid droplets and insulin sensitivity in humans. *PNAS* **105**, 7833-8.

Riddle, D. L. and Albert, P. S. (1997). Genetic and environmental regulation of Dauer larva development. in C elegans II, Riddle, D.L., et al. ed (Cold Spring Harbor Laboratory Press, Cold Spring Harbor, NY), pp. 739–68.

Riddle, D. L. and Georgi, L. L. (1990). Advances in research on *Caenorhabditis elegans*: Application to plant parasitic nematodes. *Annu Rev Phytopathol*. **28**, 247–69.

Schweiger, M., Schoiswohl, G., Lass, A., Radner, F. P., Haemmerle, G., Malli, R., Graier, W., Cornaciu, I., Oberer, M., Salvayre, R., Fischer, J., Zechner, R. and Zimmermann, R. (2008). The C-terminal region of human adipose triglyceride lipase affects enzyme activity and lipid droplet binding. *J Biol Chem*. **283**, 17211-20.

Selesniemi, K., Lee, H. J. and Tilly, J. L. (2008). Moderate caloric restriction initiated in rodents during adulthood sustains function of the female reproductive axis into advanced chronological age. *Aging Cell*. **7**, 622-9.

Siloto, R. M., Findlay, K., Lopez-Villalobos, A., Yeung, E. C., Nykiforuk, C. L. and Moloney, M. M. (2006). The accumulation of oleosins determines the size of seed oilbodies in Arabidopsis. *Plant Cell.* **18**, 1961-74.

Soukas, A. A., Kane, E. A., Carr, C. E., Melo, J. A. and Ruvkun, G. (2009). Rictor/TORC2 regulates fat metabolism, feeding, growth, and life span in Caenorhabditis elegans. *Genes Dev.* **23***,* 496-511.

Woods, A., Johnstone, S. R., Dickerson, K., Leiper, F. C., Fryer, L. G., Neumann, D., Schlattner, U., Wallimann, T., Carlson, M. and Carling, D. *(*2003*).* LKB1 is the upstream kinase in the AMP-activated protein kinase cascade*. Curr. Biol.* **13***,* 2004-8*.*

Xie, M. and Roy, R. (2012). Increased levels of hydrogen peroxide induce a HIF-1-dependent modification of lipid metabolism in AMPK compromised C. elegans dauer larvae. *Cell Metab*. **16**, 322-35.

Xu, N., Zhang, S. O., Cole, R. A., McKinney, S. A., Guo, F., Haas, J. T., Bobba, S., Farese, R. V. Jr. and Mak, H.Y. (2012). The FATP1-DGAT2 complex facilitates lipid droplet expansion at the ER-lipid droplet interface. *J Cell Biol*. **198**, 895-911.

Yang, X., Lu, X., Lombès, M., Rha, G. B., Chi, Y. I., Guerin, T. M., Smart, E. J. and Liu, J. (2010). The G(0)/G(1) switch gene 2 regulates adipose lipolysis through association with adipose triglyceride lipase. *Cell Metab*. **11**, 194-205.

Zhang, S. O., Trimble, R., Guo, F. and Mak, H. Y. (2010). Lipid droplets as ubiquitous fat storage organelles in C. elegans. *BMC Cell Biology* **11**, 96.

Figure 3.1. AMPK Regulates ATGL-1 Abundance and Association with Lipid Droplets

(A) ATGL-1 protein levels associated with lipid droplets were compared in *daf-2* control dauer larvae and *daf-2; aak(0)* mutant dauers. Dissociation of ATGL-1 from the lipid droplets correlates with a decreased abundance of ATGL-1 protein in *daf-2* animals as they progress through the dauer stage. These and all subsequent images were taken with a Zeiss 510 Meta Confocal Laser Microscope at x40 magnification using identical microscope settings, unless specified otherwise. Scale bar = 10µm in **(A)** and **(B)**. All strains carry *daf-2(e1370)* (control) in **(A)** to **(E)**.

(B) ATGL-1 was still highly expressed during the early dauer stage in *daf-2; aak(0)* mutants compared to *daf-2* dauer larvae.

(C)-(D) Western blot analysis of GFP levels in *daf-2* and *daf-2; aak(0)* mutant dauer larvae during dauer entry period and early dauer stage. All strains are *daf-2(e1370)* and harbor the translational fusion transgene *hjIs67[Patgl-1::atgl-1::GFP]*.

(E) Western blot analysis indicating ATGL-1 protein levels in *daf-2* and *daf-2; aak(0)* mutant dauer larvae.

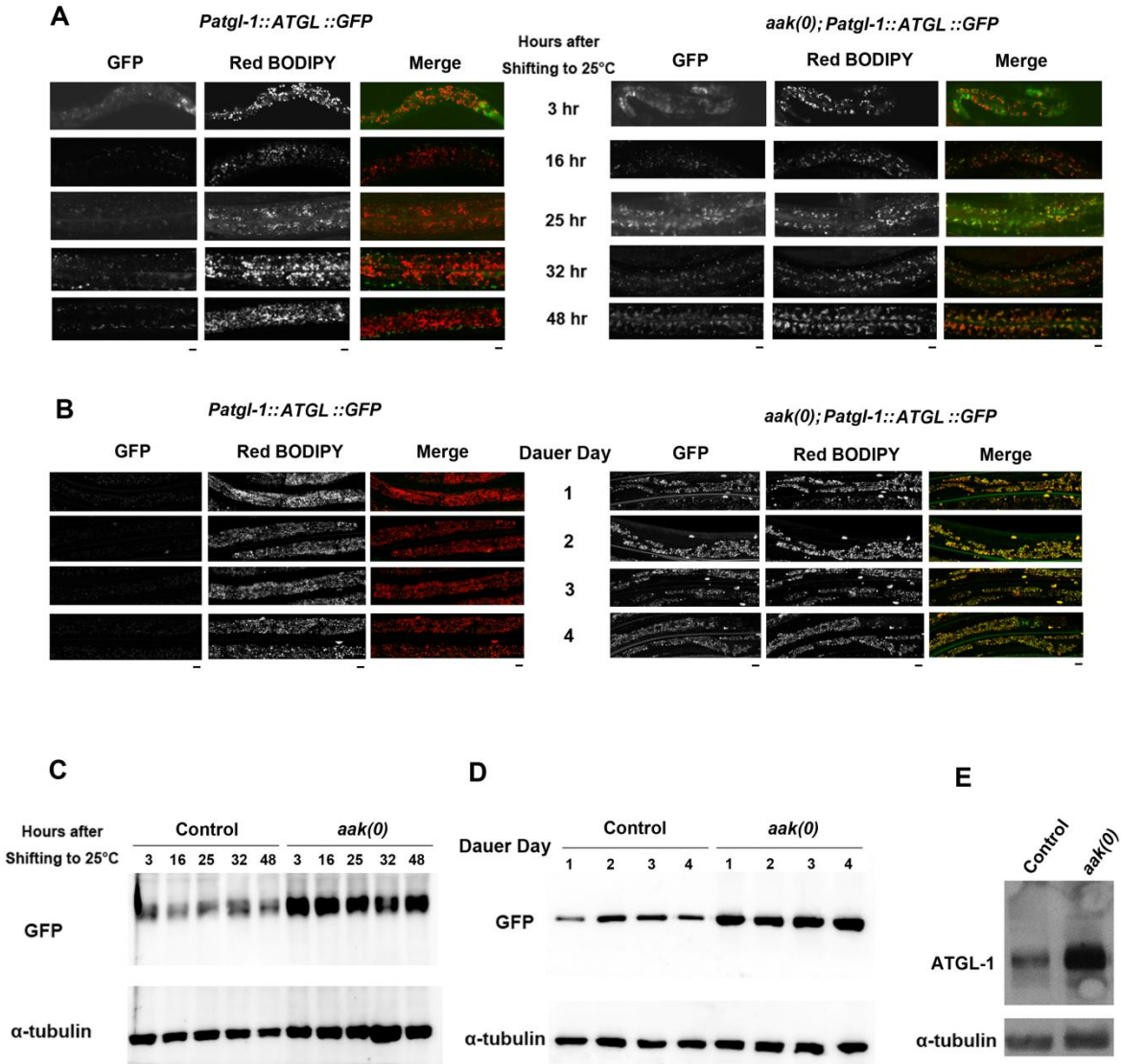
A
Patgl-1::ATGL ::GFP
aak(0); Patgl-1::ATGL ::GFP
GFP
Red BODIPY
Merge
Hours after Shifting to 25°C
3 hr
16 hr
25 hr
32 hr
48 hr
B
Patgl-1::ATGL ::GFP
aak(0); Patgl-1::ATGL ::GFP
Dauer Day
1
2
3
4
C
Hours after Shifting to 25°C
Control
aak(0)
3 16 25 32 48 3 16 25 32 48
GFP
α-tubulin
D
Dauer Day
Control
aak(0)
1 2 3 4 1 2 3 4
GFP
α-tubulin
E
Control
aak(0)
ATGL-1
α-tubulin

Figure 3.2. AMPK-Mediated Phosphorylation of ATGL-1 Enhances 14-3-3 Binding and Ubiquitin-Mediated Degradation via the Proteasome

(A) ATGL-1 protein levels are regulated by AMPK by enhancing ubiquitin-mediated proteasomal degradation. Individual proteasome components were compromised through RNAi, of which many, but not all, increase the levels of ATGL-1 in *daf-2* dauer larvae.

(B) Ubiquitylated intermediates of ATGL-1 accumulate in AMPK mutant dauer larvae. Immunoprecipitation of ATGL-1 from lysates obtained from both *daf-2* and *daf-2; aak(0)* mutant dauer larvae was analyzed by western blot analysis using anti-ubiquitin antibody. High molecular weight ubiquitin-conjugated entities are seen in immunoprecipitates obtained from *daf-2* but are more prominent in the *daf-2; aak(0)* lysates.

(C) 14-3-3 binding to ATGL-1 is AMPK-dependent. Immunoprecipitation of ATGL-1 from total lysates obtained from *daf-2* and *daf-2; aak(0)* mutant dauer larvae were immunoblotted with antisera that recognizes 14-3-3 binding sites.

(D) Immunoprecipitation of ATGL-1 or PAR-5 from protein lysates obtained from either *daf-2* or *daf-2; aak(0)* mutant dauer larvae were subjected to immunoblot analysis using PAR-5 or ATGL-1 antibody respectively.

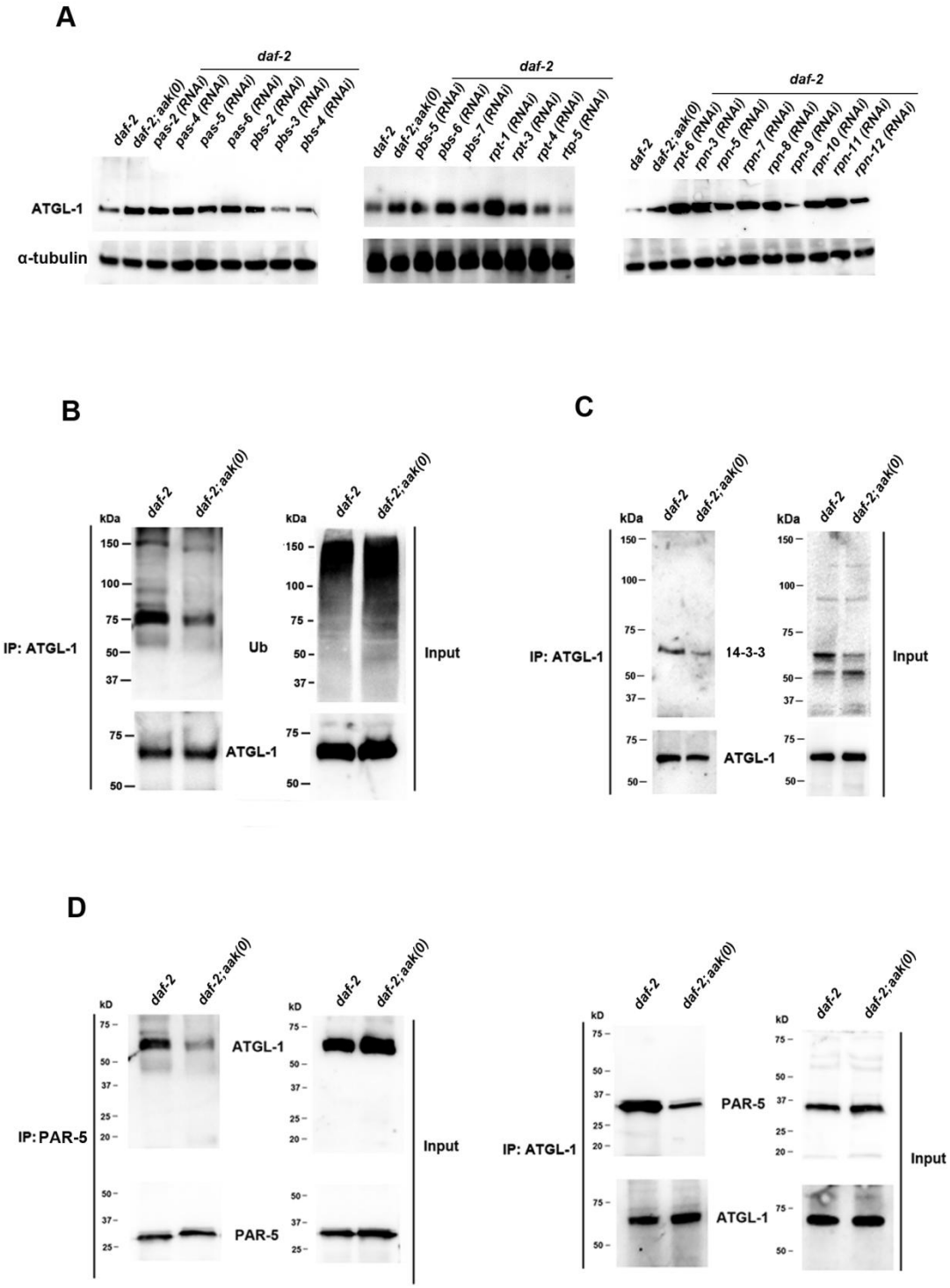
A
daf-2
daf-2;aak(0)
pas-2 (RNAi)
pas-4 (RNAi)
pas-5 (RNAi)
pas-6 (RNAi)
pbs-2 (RNAi)
pbs-3 (RNAi)
pbs-4 (RNAi)
pbs-5 (RNAi)
pbs-6 (RNAi)
pbs-7 (RNAi)
rpt-1 (RNAi)
rpt-3 (RNAi)
rpt-4 (RNAi)
rtp-5 (RNAi)
rpt-6 (RNAi)
rpn-3 (RNAi)
rpn-5 (RNAi)
rpn-7 (RNAi)
rpn-8 (RNAi)
rpn-9 (RNAi)
rpn-10 (RNAi)
rpn-11 (RNAi)
rpn-12 (RNAi)
ATGL-1
α-tubulin
B
C
D
kDa
kD
IP: ATGL-1
Ub
Input
14-3-3
IP: PAR-5
PAR-5

Figure 3.3. Elimination of CGI-58 Rescued both Triglyceride Levels and Excretory Defects in *daf-2; aak(0)* Mutant Dauer Larvae

(A) Protein alignment of the two isoforms of *C. elegans* CGI-58 (C37H5.a and C37H5.b) with human CGI-58. Conserved amino acids are highlighted in black (identical) and grey (similar).

(B) Elimination of CGI-58 significantly enhanced the survival of *daf-2; aak(0)* mutant dauer larvae to a similar degree as *atgl-1(RNAi)*. Compromise of both genes affects survival in a non-additive manner suggesting that these genes likely function in a linear pathway.

(C) CGI-58 and ATGL-1 protect the triglyceride stores from depletion in *daf-2; aak(0)* mutant dauer larvae. Colourimetric analysis of triglyceride content in day 4 dauer larvae. ** indicates statistical significance ($P<0.01$) compared to all four of the other genotypes using one-way ANOVA followed by a Tukey HSD test. The same statistical analysis was applied for all subsequent experiments performed hereafter. Error bars indicate SD of three independent experiments.

(D) Elimination of CGI-58 protects the triglyceride stockpile in *daf-2; aak(0)* mutant dauer larvae. Oil Red O staining of day 4 dauer larvae. Arrowhead indicates the junction between the pharynx (left) and the intestine (right). Oil Red O staining intensity was evaluated by measuring optical density. Error bars indicate SD of 20 animals. * and ** indicate statistical significance ($P<0.05$ and $P<0.01$, respectively) compared to *daf-2; aak(0)* mutant dauer larvae. Scale bar = 5µm.

(E) Optimal ATGL-1 lipase activity requires CGI-58. ATGL-1-dependent triglyceride hydrolysis was determined in *daf-2; aak(0)* mutant dauer larvae with wild type or compromised CGI-58 function. Error bars indicate SD of three independent experiments.

(F) Osmoregulatory defects typical of AMPK dauer larvae were corrected by reducing CGI-58 function. CGI-58 compromise restores osmoresistance of day 4 *daf-2; aak(0)* mutant dauer larvae following culture in varying NaCl concentrations for 24 hours at 25°C.

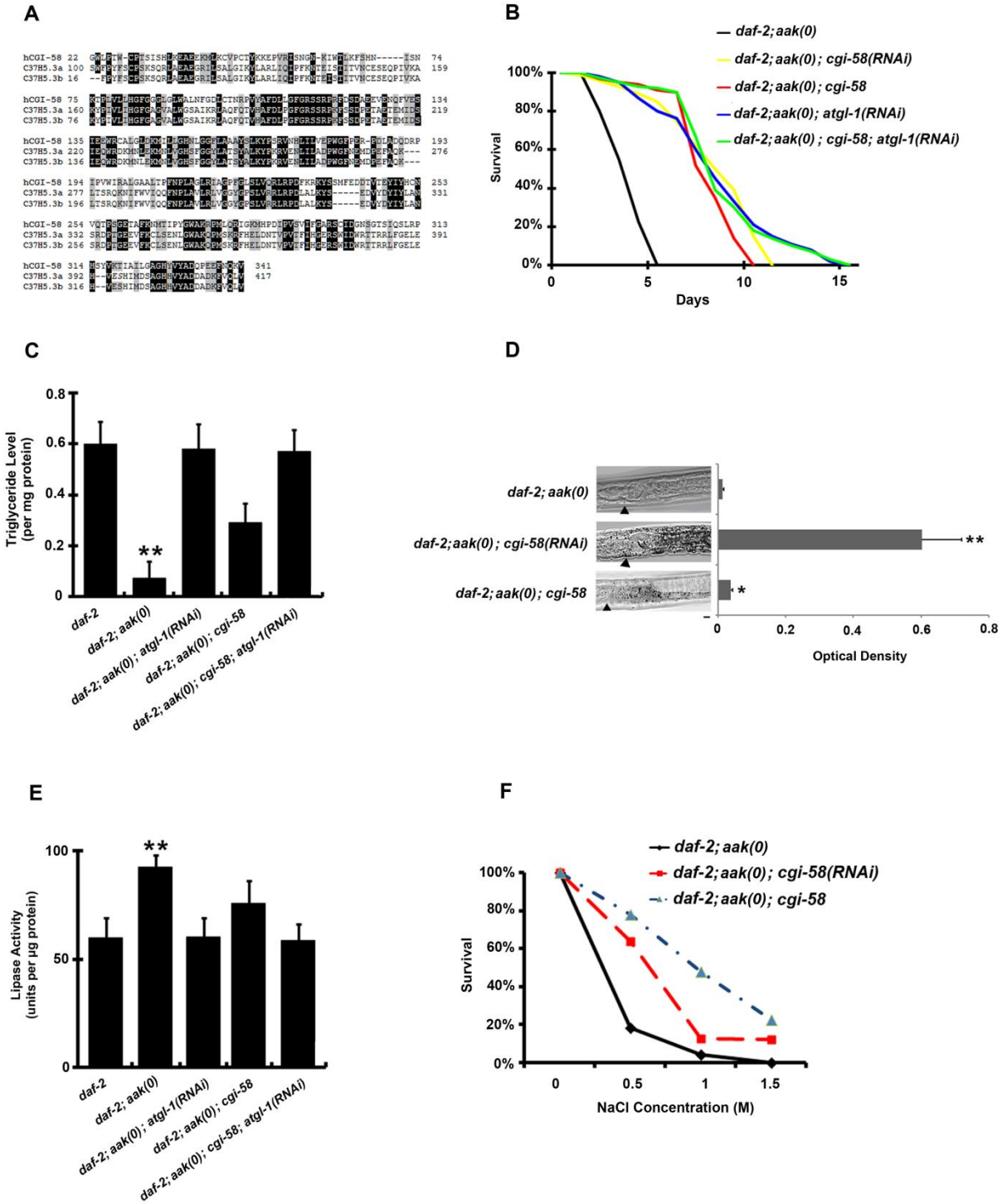
A
B
daf-2;aak(0)
daf-2;aak(0); cgi-58(RNAi)
daf-2;aak(0); cgi-58
daf-2;aak(0); atgl-1(RNAi)
daf-2;aak(0); cgi-58; atgl-1(RNAi)
Survival
Days
C
Triglyceride Level (per mg protein)
daf-2
daf-2; aak(0)
daf-2; aak(0); atgl-1(RNAi)
daf-2; aak(0); cgi-58
daf-2; aak(0); cgi-58; atgl-1(RNAi)
D
daf-2; aak(0)
daf-2;aak(0); cgi-58(RNAi)
daf-2; aak(0); cgi-58
Optical Density
E
Lipase Activity (units per µg protein)
F
NaCl Concentration (M)

Figure 3.4. CGI-58 Physically Interacts with ATGL-1 and is Required for ATGL-1 Localization to the Lipid Droplets in AMPK Mutant Dauer Larvae

(A) CGI-58::GFP was expressed in the hypodermis and the intestine and at comparable levels in both control *daf-2* and *daf-2; aak(0)* mutant dauer larvae. The indicated strains all carry *daf-2(e1370)* in **(A)**, **(B), (C), (D) (E)** and **(G)** and the *Ex[Pcgi-58::CGI-58::GFP; rol-6D]* transgenic array in **(B), (C)** and **(G)**. Scale bar = 20µm.

(B) More CGI-58 proteins are present in AMPK-sufficient day 0 dauer animals.

(C) CGI-58::GFP localized to the surface of the lipid droplets at dauer day 0 in both *daf-2* and *daf-2; aak(0)* mutant dauers. Scale bar = 10µm

(D) Elimination of *cgi-58* resulted in separation of ATGL-1 protein from the lipid droplets. All strains are *daf-2*, *aak-1(tm1944)* and *aak-2(ok524)* and carry the *hjIs67[Patgl-1::atgl-1::GFP]* transgene. Scale bar = 10µm.

(E) ATGL-1 association with the lipid droplets is dependent on appropriate CGI-58 levels. Immunoblot analysis was used to determine the levels of ATGL-1 in isolated lipid droplets (L) and cytoplasm (C) obtained from total day 0 dauer extracts of each genotype: *daf-2*, *daf-2; cgi-58, daf-2; aak(0)* and *daf-2; aak(0); cgi-58*. Protein concentration was measured and 30µg of total protein was loaded in each sample lane**.**

(F) CGI-58 and ATGL-1 exist in a ternary complex in vivo. Co-immunoprecipitations were performed using anti-ATGL-1 and a FLAG-tagged variant of CGI-58 demonstrating that ATGL-1 and CGI-58 are directly or indirectly associated in extracts obtained from a mixed worm population. CGI-58::FLAGx3 refers to animals carrying the transgenic array Ex(*Pcgi-58::cgi-58::FLAGx3; rol-6D)*

(G) Anti-ATGL-1 co-immunoprecipitations were repeated on lysates obtained from *daf-2* and *daf-2; aak(0)* day 0 dauer larvae expressing a GFP-tagged CGI-58 transgene. CGI-58::GFP refers to animals carrying the transgenic array *Ex(Pcgi-58::CGI-58::GFP; rol-6D)*.

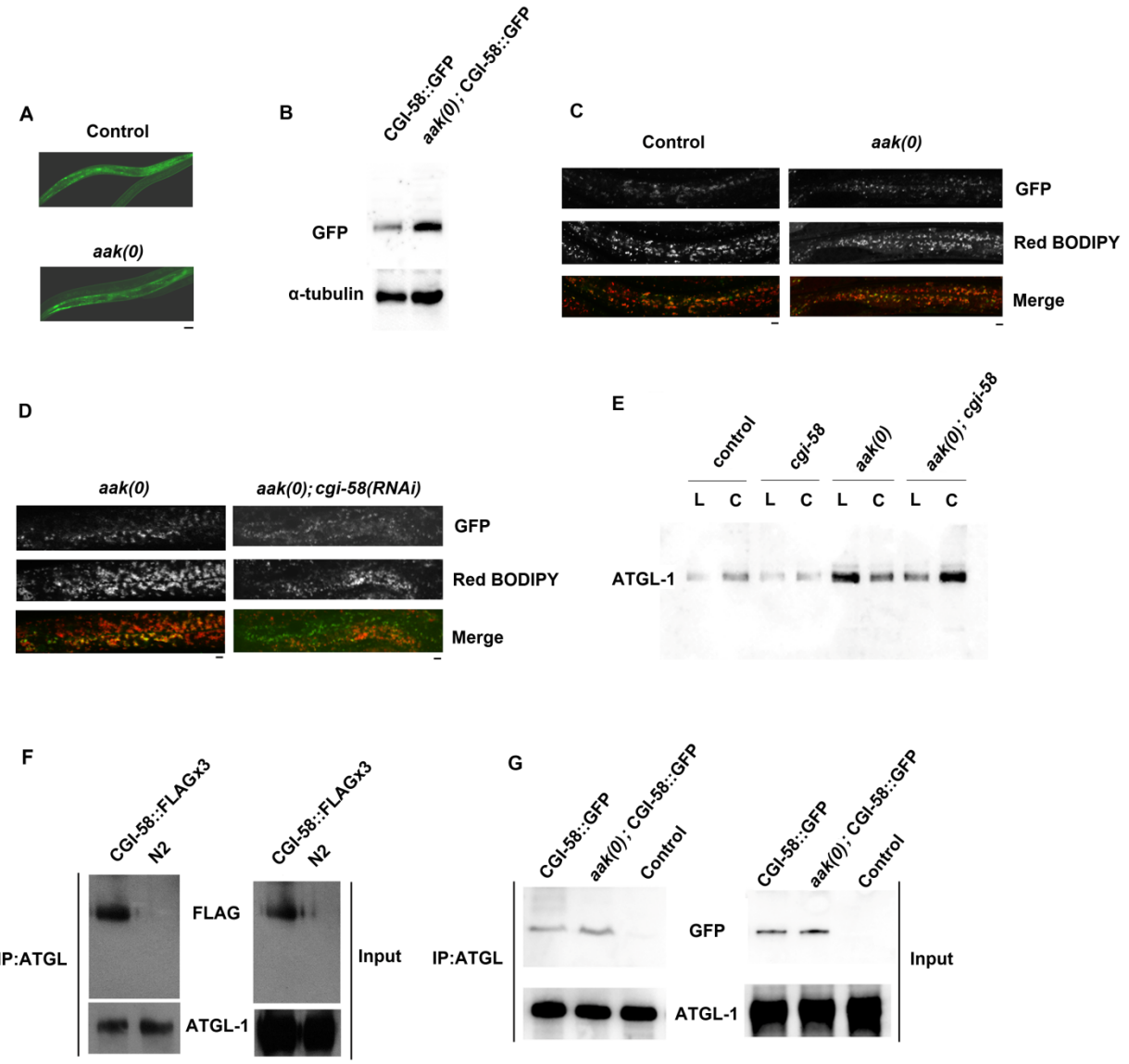
A
Control
aak(0)
B
CGI-58::GFP
aak(0); CGI-58::GFP
GFP
α-tubulin
C
Control
aak(0)
GFP
Red BODIPY
Merge
D
aak(0)
aak(0); cgi-58(RNAi)
GFP
Red BODIPY
Merge
E
control
cgi-58
aak(0)
aak(0); cgi-58
L C L C L C L C
ATGL-1
F
CGI-58::FLAGx3
N2
CGI-58::FLAGx3
N2
IP:ATGL
FLAG
ATGL-1
Input
G
CGI-58::GFP
aak(0); CGI-58::GFP
Control
CGI-58::GFP
aak(0); CGI-58::GFP
Control
IP:ATGL
GFP
ATGL-1
Input

Figure 3.5. CGI-58 and ATGL-1 Are Essential for Lipid Droplet Size and Morphology

(A) Elimination of CGI-58 in *daf-2; aak(0)* animals led to dramatic increase in lipid droplet size during the later part of dauer entry. C_1-BODIPY-C_{12} -stained lipid droplets were imaged and their dimensions were quantified using the AxioVision (Zeiss) software. All strains carry *daf-2(e1370)* (control) in **(A)** to **(F)**.

(B) Loss of ATGL-1 or CGI-58 function caused aberrations in lipid droplet structure and morphology. *atgl-1(RNAi)* and *cgi-58(ok3245)* mutant larvae were imaged using C_1-BODIPY-C_{12} to stain lipid droplets 32 hours after shifting to restrictive temperature (25˚C) to induce dauer formation. Elimination of *atgl-1* gene was performed with RNAi feeding method in **(B)** and **(C)**.

(C) C_1-BODIPY-C_{12} -stained lipid droplets isolated from lysates obtained from each genotype indicated 32 hours following shift to restrictive temperature. Scale bar = 10µm.

(D)-(E) Increased lipid droplet size correlates with triglyceride content in dauer larvae that lack CGI-58. Triglyceride levels were determined in *daf-2; aak(0)* and *daf-2; aak(0); cgi-58* animals at the later part of dauer entry.

(F) Loss of ACS-22 or DGAT-2 function reduced the lipid droplet size in *daf-2; aak(0); cgi-58* animals at the later part of dauer entry.

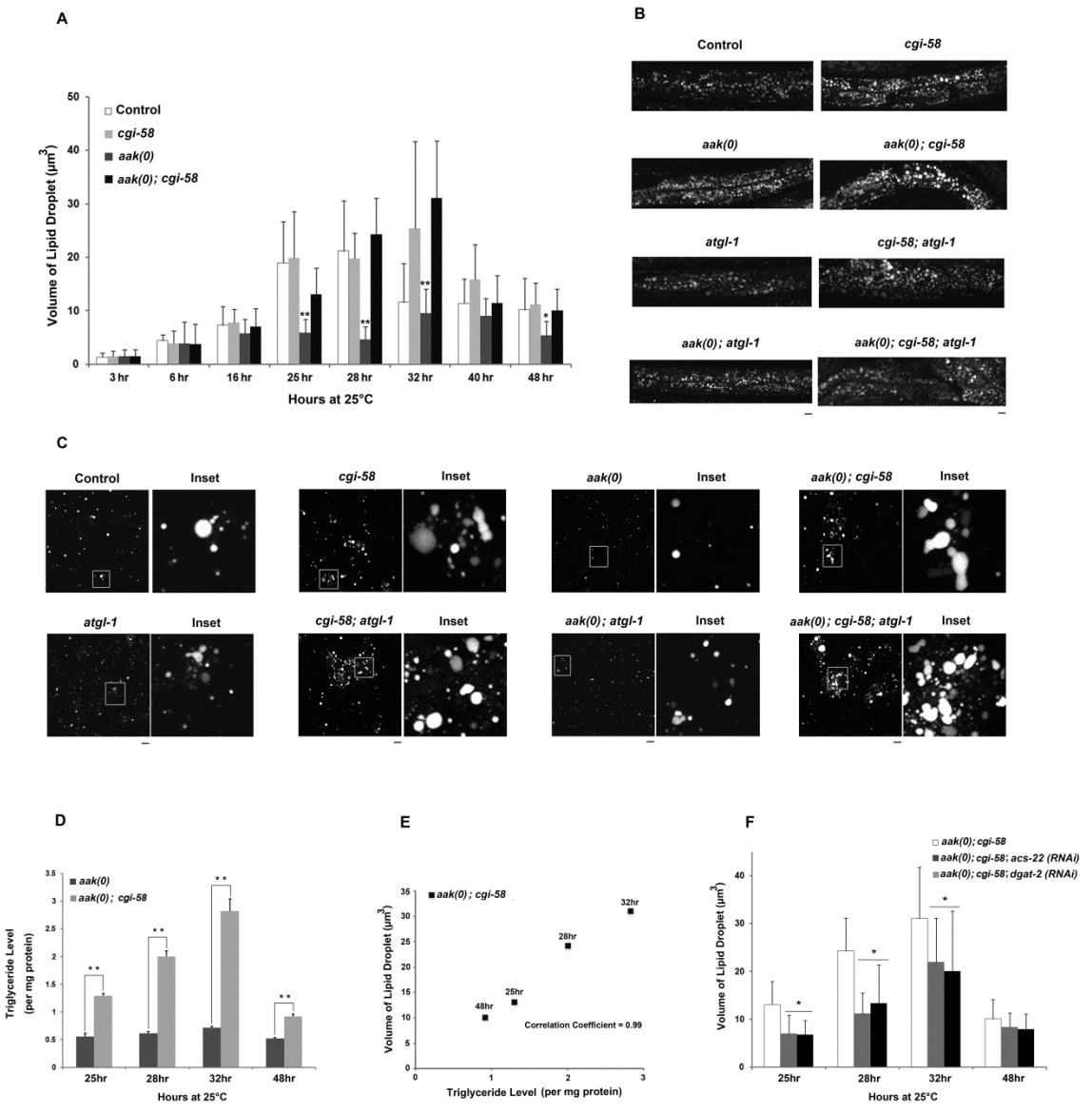
A
Control
cgi-58
aak(0)
aak(0); cgi-58
Volume of Lipid Droplet (μm3)
3 hr
6 hr
16 hr
25 hr
28 hr
32 hr
40 hr
48 hr
Hours at 25°C
B
Control
cgi-58
aak(0)
aak(0); cgi-58
atgl-1
cgi-58; atgl-1
aak(0); atgl-1
aak(0); cgi-58; atgl-1
C
Control
Inset
cgi-58
aak(0)
aak(0); cgi-58
atgl-1
cgi-58; atgl-1
aak(0); atgl-1
aak(0); cgi-58; atgl-1
D
aak(0)
aak(0); cgi-58
Triglyceride Level (per mg protein)
25hr
28hr
32hr
48hr
Hours at 25°C
E
aak(0); cgi-58
Volume of Lipid Droplet (μm3)
Correlation Coefficient = 0.99
Triglyceride Level (per mg protein)
F
aak(0); cgi-58
aak(0); cgi-58; acs-22 (RNAi)
aak(0); cgi-58; dgat-2 (RNAi)
Volume of Lipid Droplet (μm3)
Hours at 25°C

Figure 3.6. CGI-58 Regulates Lipid Droplet Fusion and Lipid Exchange

(A) CGI-58 limits the frequency of lipid droplet encounters in AMPK mutant dauer larvae. C_1-BODIPY-C_{12} stained isolated lipid droplets were obtained from lysates generated from dauer larvae 32 hours after shifting to restrictive temperature. It revealed more frequent lipid droplet encounters in the absence of CGI-58. All strains carry *daf-2(e1370)* (control) in **(A)** to **(G)**.

(B) CGI-58 limits the exchange of lipid content among isolated lipid droplets from dauer larvae 32 hours after shifting to restrictive temperature. Representative lipid droplets containing both red and green BODIPY labeled lipids are highlighted with arrowheads and the fluorescent intensity of each channel was quantified to illustrate the lipid exchange event during the 30min co-incubation excluding the possibility of fluorescence overlap. 1 and 2 represent LD1 and LD2 respectively. The line graph at the right side of each set of images represents the fluorescent intensity of Green and Red C_1-BODIPY-C_{12} labeled lipid droplets along the white arrow. The box represents the inset area.

(C) CGI-58 limits the active fusion events among lipid droplets in AMPK mutant dauer larvae. Red C_1-BODIPY-C_{12} labeled lipid droplets were imaged in real time (15 min) in live dauer larvae 32 hours after shifting to restrictive temperature.

(D) Quantification of the lipid droplet encounters described in **(A)** determined for 1000 lipid droplets analyzed for each respective genotype.

(E) Quantification of the lipid droplets containing both green and red lipid contents (both red and green fluorescent intensities are greater than 200) described in **(B)** and **Figure S** determined for 1000 lipid droplets analyzed for each respective genotype.

(F) Quantification of the intensity difference between the lipid droplets before and 5 minutes after photobleaching in *aak(0)* and *aak(0)*; *cgi-58* mutant day 0 dauer larvae as shown in **(G)**.

(G) Lipid content was more rapidly replenished in *aak(0)*; *cgi-58* animals. FRAP experiments were performed on dauer day 0 animals on a Quorum WaveFX spinning

disk confocal system, on a Leica DMI6000B inverted microscope using a 63x/1.40-0.6 oil objective and raw imaging data were obtained using Metamorph acquisition software.

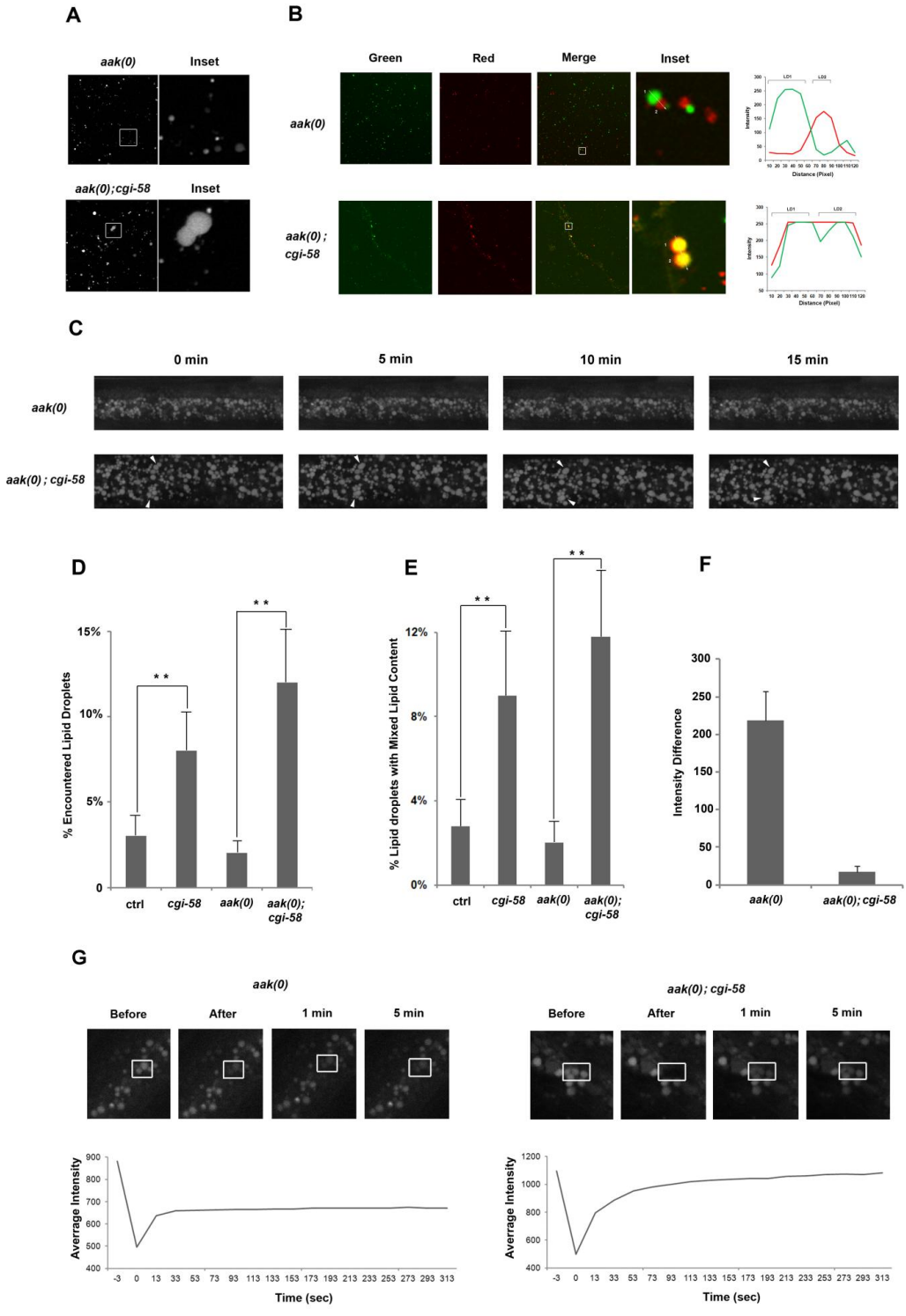

Figure 3.7. Model of Action of ATGL-1 and CGI-58 on during Dauer Lipolysis.

In control *daf-2* dauers, AMPK phosphorylation of ATGL-1 promotes its interaction with the 14-3-3 protein PAR-5 and targets it for proteasome degradation to eventually protect the triglyceride stockpile from rapid depletion. CGI-58 proteins possess dual roles on the lipid droplet surface: some of them form a barrier to prevent the expansion of the lipid droplet by lipid exchange following droplet-droplet encounters; and others interact with ATGL-1 to tether it to the lipid droplet (and degraded in complex with ATGL-1 following AMPK phosphorylation), both of which ultimately optimize ATGL-1-mediated lipolysis.

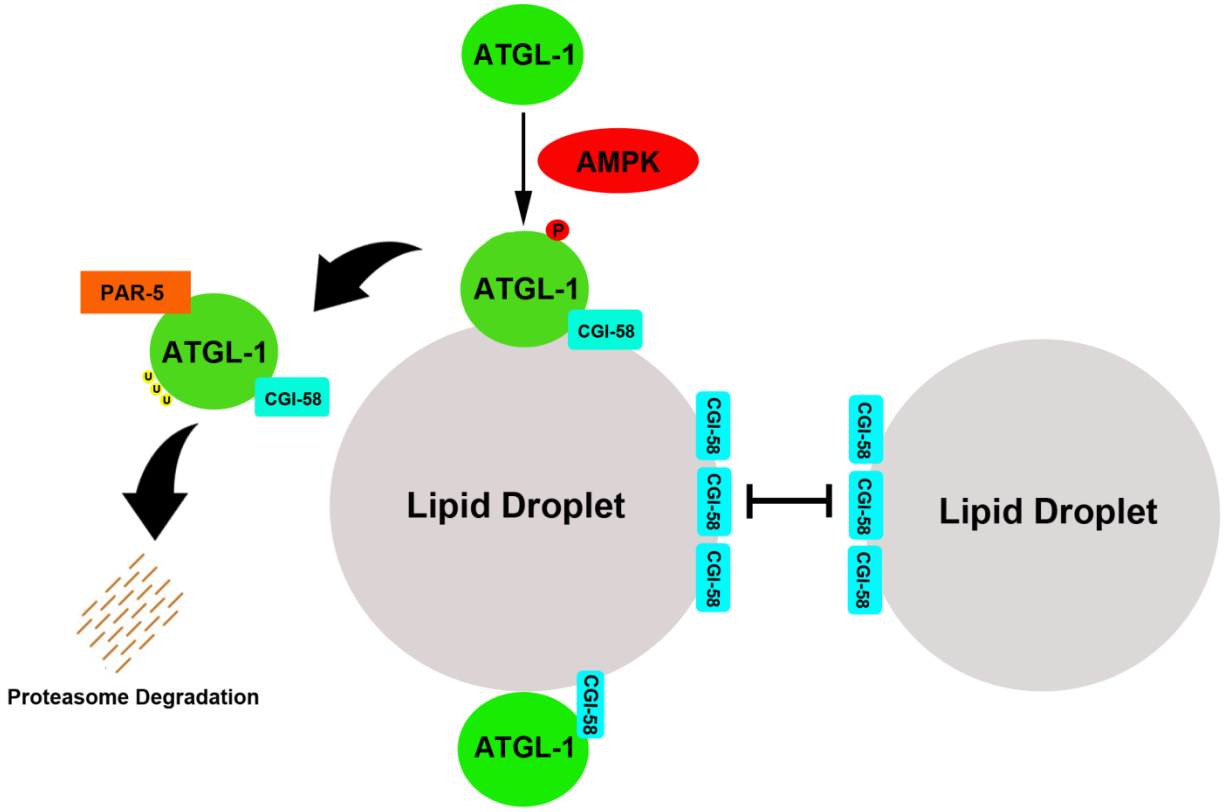

Figure S3.1. The Anti-ATGL-1 antibody is specific for ATGL-1. The ATGL-1 antisera recognizes a single band that migrates at approximately 70kD, which corresponds to the molecular weight of ATGL-1, and is reduced in *atgl-1(RNAi)* animals.

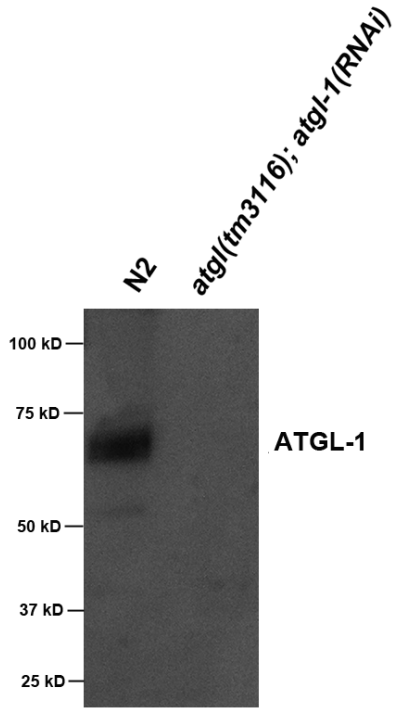

Figure S3.2. Expression Levels of ATGL-1 were similar in *daf-2* and *daf-2; aak(0)* Animals. Relative mRNA levels were Analyzed with Quantitative real-time PCR in Dauer Day 0 Animals.

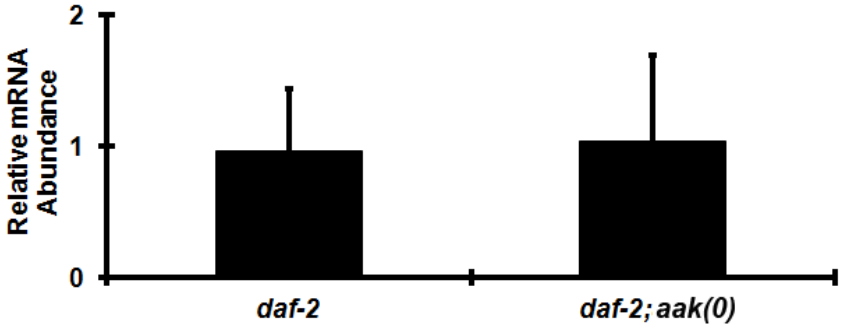

Figure S3.3. P-14-3-3 and PAR-5 Antibody Test

(A) An increase in both the abundance and the number of bands that were detected by the P-14-3-3 antibody was observed in lysates obtained from N2 animals treated with the potent phosphatase inhibitor calyculin A.

(B) The anti-PAR-5 antibody recognized a single band at approximately 30kD, corresponding to Its predicted molecular weight and which disappeared following *par-5(RNAi).*

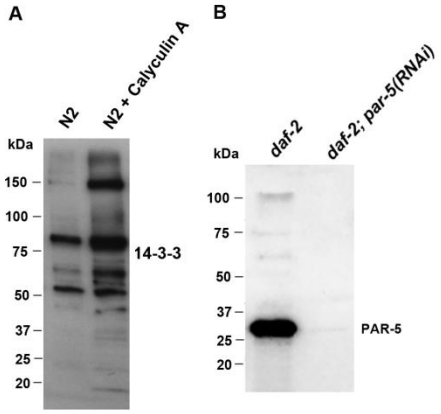

FigureS3.4. The Major AMPK Phosphorylable Site S303 on ATGL-1 is Important for Its Intestinal Expression and Proteasome Degradation.

(A) ATGL-1 was expressed in hypodermis and intestine in S303A variants.

(B) Western blot analysis of GFP levels in WT and S303A variants.

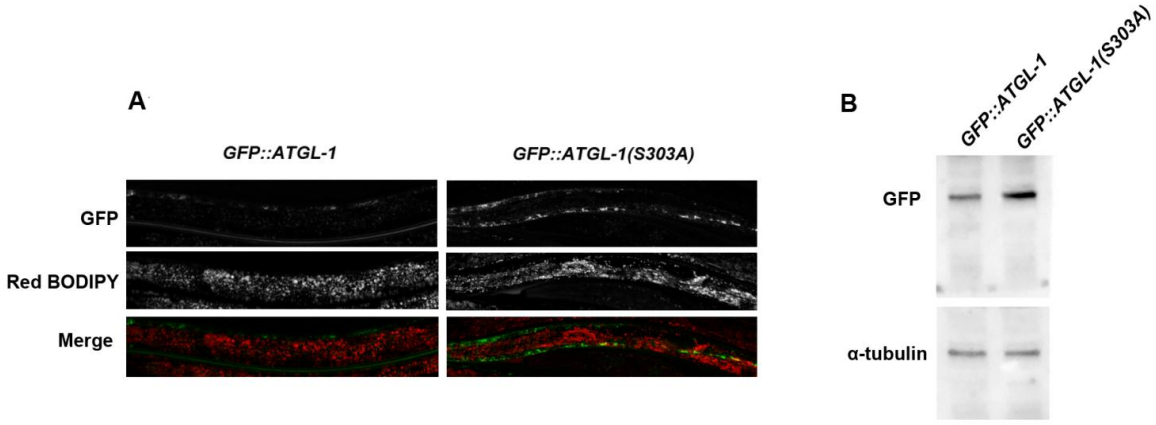

Figure S3.5. CGI-58 does not contribute to ATGL-1 stability in AMPK mutant dauers. ATGL-1 levels were determined by immunoblot using anti-ATGL-1 antisera in lysates obtained from control and *cgi-58* mutant dauer larvae with or without AMPK.

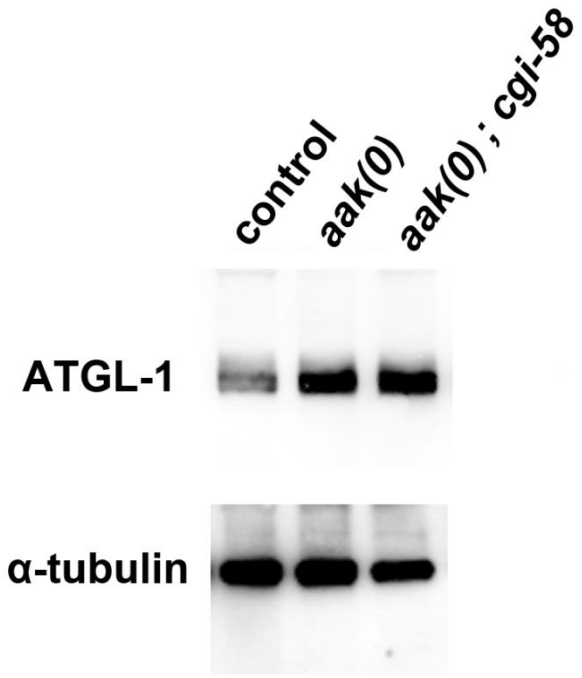

Figure S3.6. Verification of the Isolated Lipid Droplets

(A)-(B) C_1-BODIPY-C_{12} staining of isolated lipid droplets and cytoplasm (remaining portion of the total lysate) from *daf-2* day 0 dauer larvae.

(C) Associated proteins present in the isolated lipid droplets were clearly distinct from that of the supernatant and the cellular debris fractions.

(D) Triglyceride was enriched several-fold in the isolated lipid droplets.

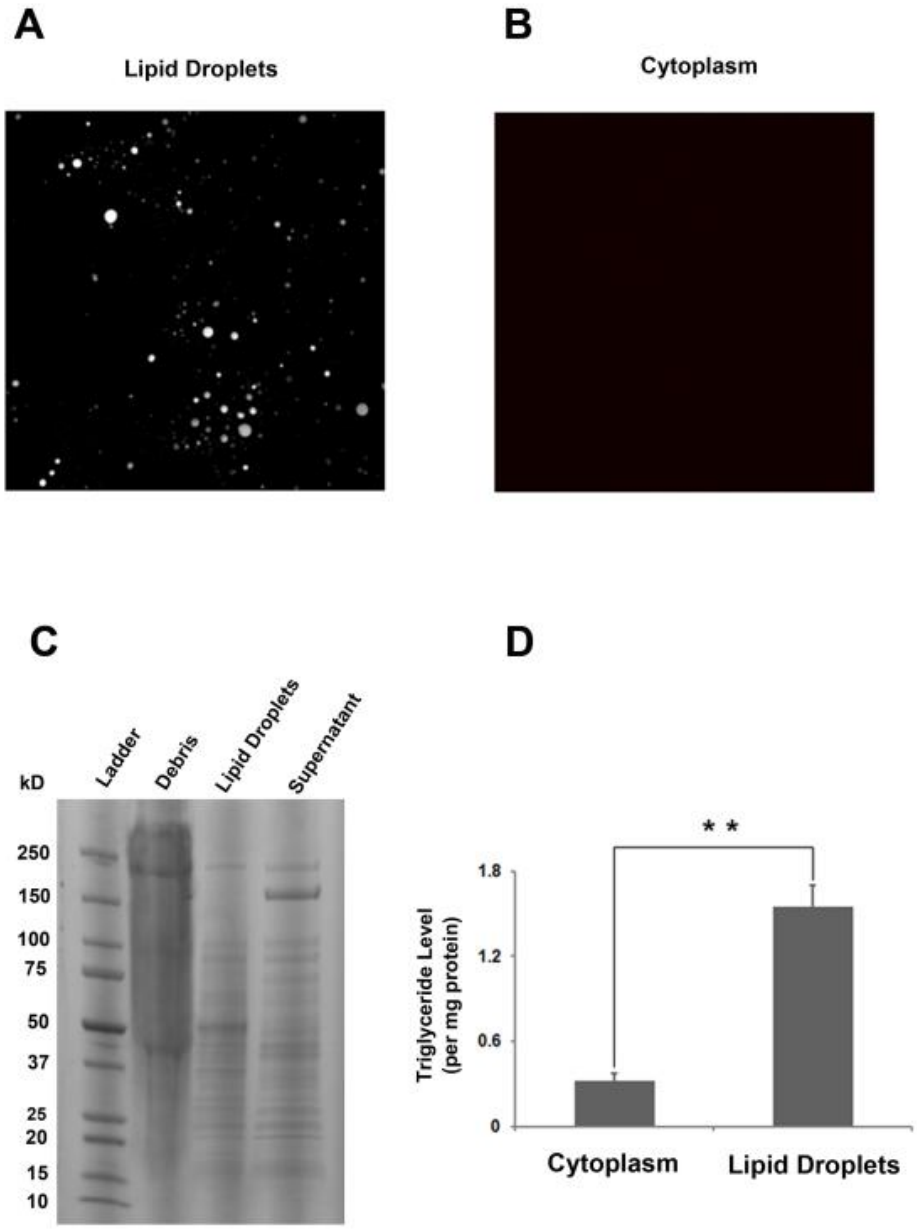

Figure S3.7. C_1-BODIPY-C_{12} Staining of Lipid Droplets Demonstrated a Similar Staining Pattern in *daf-2* and *daf-2; glo-4* Day 0 Dauer Larvae.

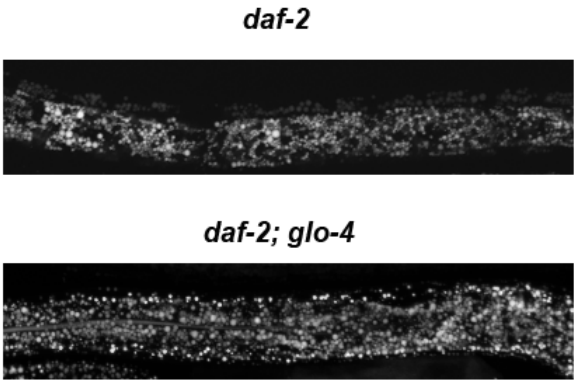

Figure S3.8. C_1-BODIPY-C_{12} Staining of Lipid Droplets during the Entire Dauer Entry Period.

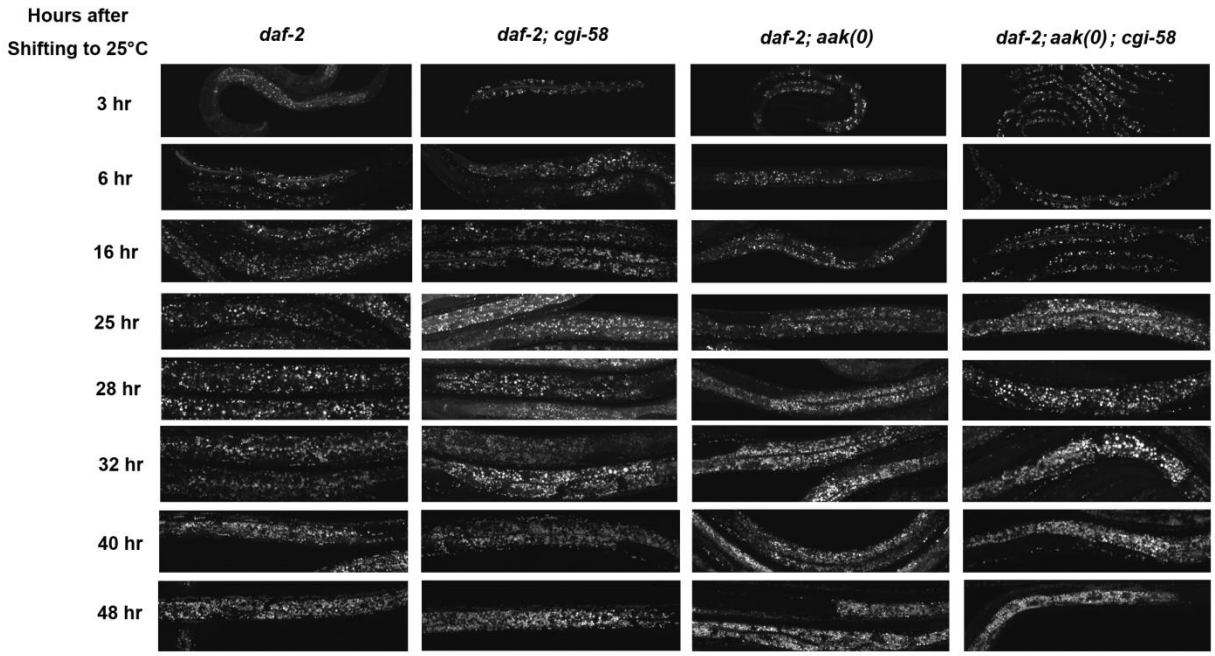

Figure S3.9. C_1-BODIPY-C_{12} Staining of Isolated Lipid Droplets in *daf-2* and *daf-2; aak(0)* Animals Fed with *cgi-58* RNAi.

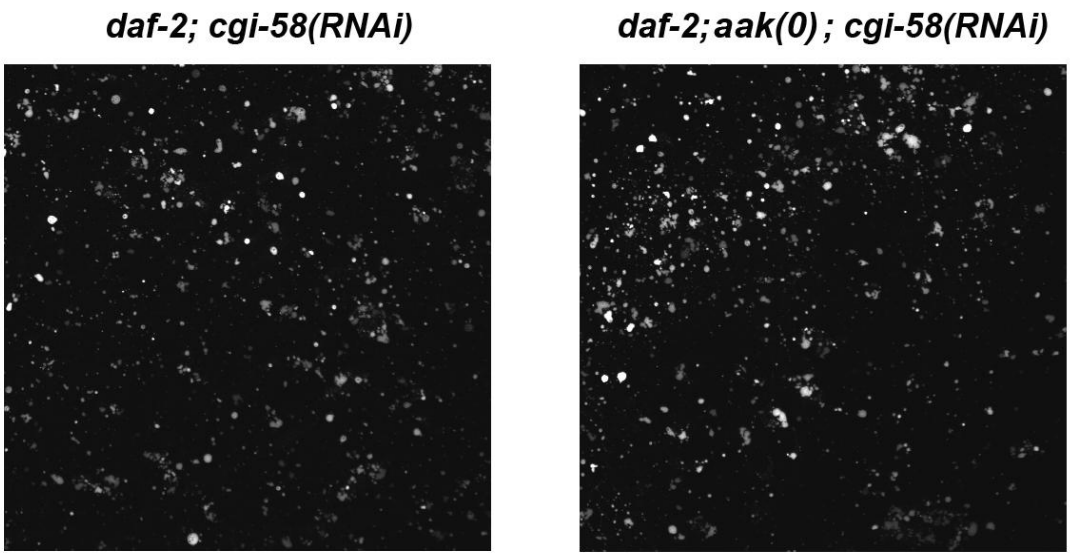

Figure S3.10. Elimination of Hormone Sensitive Lipase Does Not Affect Lipid Droplet Morphology.

All strains carry *daf-2* mutations.

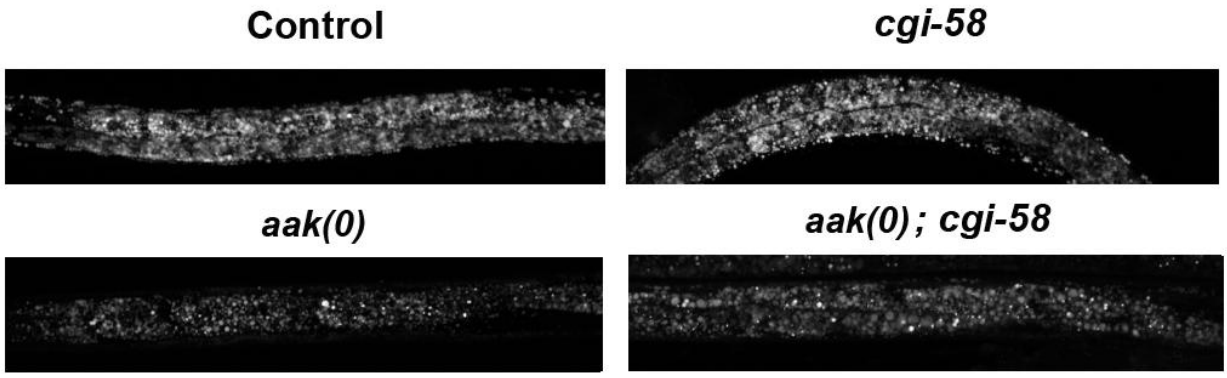

Figure S3.11. Elimination of either *acs-22* or *dgat-2* Does Not Affect the Survival of AMPK (A) and AMPK; CGI-58 (B)-Deficient Dauers.

All strains carry *daf-2* mutations.

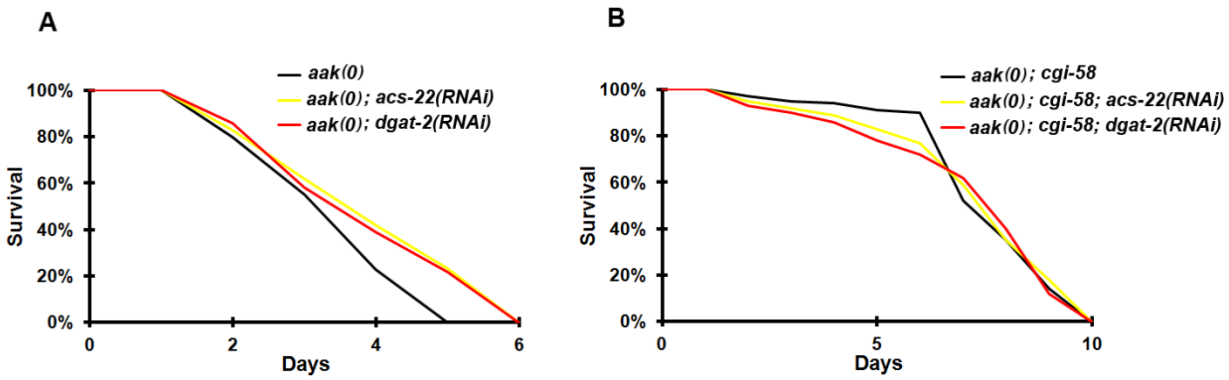

Figure S3.12. CGI-58 limits the frequency of lipid droplet encounters.

C_1-BODIPY-C_{12} stained isolated lipid droplets were obtained from lysates generated from dauer larvae 28 and 32 hours after shifting to restrictive temperature. It revealed more frequent lipid droplet encounters in the absence of CGI-58. All strains carry *daf-2* mutations.

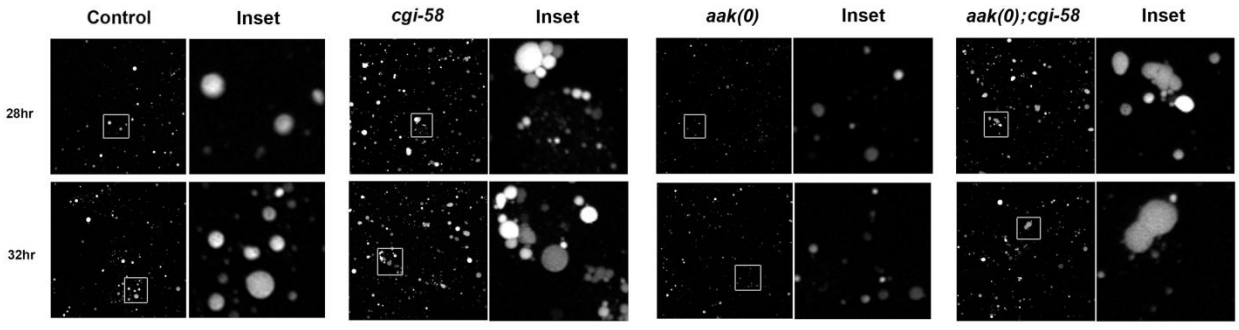

Figure S3.13. CGI-58 limits the active fusion events among lipid droplets in control dauer larvae.

Red C_1-BODIPY-C_{12} labeled lipid droplets were imaged in real time (15 min) in live dauer larvae 32 hours after shifting to restrictive temperature. All strains carry *daf-2* mutations.

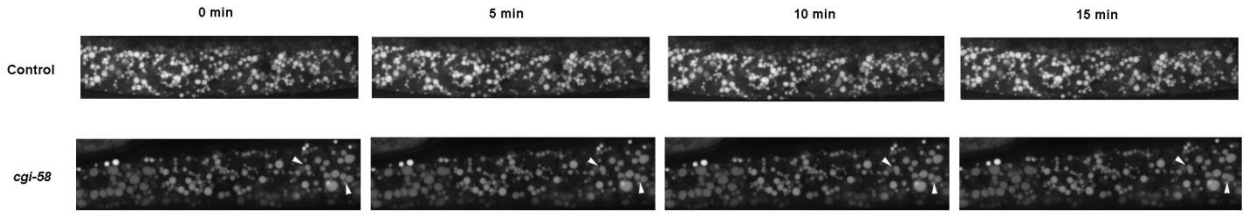

Chapter 4: Discussion

C. elegans dauer larvae demonstrate an excellent example of how animals adjust their metabolic profile to adapt to the changing environment. The dauer larvae can live up to 120 days, 4 to 8 times longer than the normal 20 day life span. There is only a certain amount of energy available to support all the animal's activities during this time. To maximize their survival, the dauer larvae must sacrifice their reproduction and mobility, both of which presumably minimize the use of limited energy sources to favor their long-term survival. Another unique feature of dauer animals is that they do not feed once entering the dauer stage. Limiting the feeding behavior also seems to contribute to their long-term survival. Since the dauer larvae only feed during the dauer entry period, which is less than 1% of their total life span, the animals must possess a tightly regulated energy expenditure process to avoid any unnecessary consumption. This provides a unique model to investigate the regulatory pathways associated with catabolic processes, such as lipolysis and fatty acid oxidation. One good example of this is that, in *daf-2* dauer larvae, the "metabolic master switch" protein AMPK regulates the first step of lipolysis by direct phosphorylation and inhibition of the responsible enzyme, ATGL-1 (Narbonne and Roy, 2009). Loss of AMPK led to premature expiration of the animals at early dauer stage as a result of energy depletion. Based on that, I performed a whole genome survey on AMPK-deficient dauer larvae to identify genes that when compromised, could prolong survival. By doing so, I established a basic framework of gene activities that can be further studied for their potential interaction with AMPK in dauer survival.

By further analysing one of these gene families identified in our survey, the catalase genes, I discovered a hormetic effect of a generally toxic compound, hydrogen peroxide, where optimal increase of its levels could benefit the survival of AMPK-deficient dauers by stimulating fatty acid *de novo* synthesis via the transcription factor, HIF-1 (Xie and Roy, 2012). The nutrient-constrained *daf-2* dauers probably recapitulate a similar environment to the hypoxic and energy-depleted internal environment of growing tumors, which favors the activation of HIF-1. As a cluster of abnormally grown neoplastic cells, tumors are often isolated from the entire body and require extra nutrient supply to support their own growth. The fact that activated HIF-1 stimulates the transcription of genes encoding the enzymes responsible for fatty acid *de novo* synthesis could be one

mechanism employed by the tumor cells to sustain their own growth and propagation. With the aid of their own energy power house, the tumor cells could potentially become independent from the rest of the body and possibly possess a greater potential of malignancy. Therefore, the HIF-1-fatty acid synthesis pathway might be a fruitful model to identify novel anticancer therapeutics.

ATGL-1 catalyzes the initial and rate limiting step of the lipolysis process. In mammals, it is tightly regulated by a number of proteins at both the transcriptional and translational level. In *C. elegans* dauer larvae, ATGL-1 is directly phosphorylated and inhibited by AMPK to preserve the energy depot for long term usage (Narbonne and Roy, 2009). Such phosphorylation led to sequestration of ATGL-1 away from its substrate and subsequent proteasome degradation. ATGL-1 seems to be the major lipase that responds to AMPK regulation during the dauer stage since elimination of other lipases, such as HSL, did not affect the survival of AMPK-deficient dauer larvae (Narbonne and Roy, 2009). Therefore, by separating ATGL-1 away from the lipid droplets and promoting its degradation, the animals can minimize the breakdown of the triglyceride reservoir. The AMPK-ATGL-1 regulation mechanism has not been observed in non-dauer animals; in contrast, mutation of ATGL-1 in normal *C. elegans* led to premature lethality. Such phenotypic differences could be explained by the differential energy demands between the normal and dauer animals. Animals following the reproductive life cycle require extra energy to support their feeding, mobility, mating and reproductive behaviors, which are not observed in dauer animals at all. Therefore, loss of ATGL-1 function leads to insufficient energy supply in adult animals and consequently early expiration. Such mutation would not shorten the survival of dauer animals due to the minimal energy requirement to support their limited behaviors; and in addition, it could benefit the survival of AMPK-deficient dauers by reducing energy production/consumption rates. The distinct effects of ATGL-1 compromise observed in adult and dauer animals demonstrate a differential requirement of protein function under different energy demanding conditions. This may be useful for the development of novel approaches to ameliorate the condition of individuals that suffer from lipid disorders.

In mammals, lipid droplets are decorated by a number of proteins including lipases and their regulatory proteins (ATGL-1, HSL, CGI-58 and G0S2), lipid synthesizing enzymes (CCT and FATP-1/DGAT-2 complex), structural proteins (Perilipin family proteins) and vesicular trafficking proteins (Rab-18). Due to technical limitations of the large scale proteomic studies in *C. elegans*, many of these proteins have not been identified or characterized yet. By studying the homologous gene of human CGI-58 in *C. elegans*, I identified a more comprehensive role of CGI-58 in *C. elegans* compared to other studies performed with mammalian models and showed that it not only acts as a co-activator of ATGL-1, but also provides a structural support to the lipid droplets to maintain their regular spherical shape and prevent them from coalescence with other lipid droplets. The latter strongly supports that a new pathway must be in place to modulate the lipolysis process from the substrate perspective. In the absence of CGI-58, lipid droplets tend to merge into bigger ones to limit the access of ATGL-1, likely by accumulating the hydrolyzed fatty acids that are not yet transported at the periphery of the lipid droplets. Therefore, by preventing them from doing so, CGI-58 further enhances the action of ATGL-1. CGI-58 may ultimately maximize the interaction surface between the substrate at the droplet core and the hydrolytic enzymes at the periphery to enhance enzyme/substrate accessibility critical for the efficient regulation of lipolysis.

Final Statement and Perspective

Overall, my work has uncovered two important mechanisms that are involved in rationing of the energy depot in *C. elegans* dauer larvae: first, I revealed a hormetic effect of low levels hydrogen peroxide to stimulate the fatty acid synthesizing ability in energy deprived animals to prolong survival., We also observed enlarged lipid droplets in catalse deficient AMPK mutant animals, however the underlying mechanism is not clear. Future work could focus on how the lipid droplet size is affected in those animals, whether it is due to increased level of H_2O_2 or feedback mechanisms via product inhibition. In addition, studies in mammalian system should be performed to extend our understanding of such *hif-1* dependent regulation of lipid metabolism. For example, *hif-1* gene activity and fatty acid synthesis rate could be assessed in carcinoma cells to test

whether HIF-1 is the key gene that regulates energy supply to the isolated tumour cells. If HIF-1 can produce similar effect as observed in *C. elegans* dauer larvae to stimulate the expression of fatty acid synthetic enzymes in carcinoma cells, novel cancer therapies could be developed for the purpose of altering the *hif-1* gene activity to cut off the energy supply to the tumours.

Second, I dissected the consequent mechanisms of ATGL-1 following AMPK phosphorylation and characterized a comprehensive role of the *C. elegans* orthologue of the human CGI-58 protein. To further investigate such ATGL independent role of CGI-58, lipid droplet fusion and content exchange could be monitored in the CGI-58-/- mouse embryonic fibroblast cells to see whether similar phenomenon can be observed. If that is the case, it may shed light on the mechanism underlying the Chanarin-Dorfman syndrome. Then, therapies to prevent formation of large lipid droplet can be developed to treat the syndrome.

Results of my studies extend beyond the *C. elegans* dauer larvae and provide implications on how we should perceive the regulation of lipolysis in all organisms. To conclude, animals only possess a certain amount of energy to support all their living activities; to live longer, they have to either sacrifice some of the activities or find ways to prolong their available energy depot by stimulating all the biosynthetic reactions while limiting their ultimate breakdown.

References

Aebersold, D. M., Burri, P., Beer, K. T., Laissue, J., Djonov, V., Greiner, R. H. and Semenza, G. L. (2001). Expression of hypoxia-inducible factor-1alpha: a novel predictive and prognostic parameter in the radiotherapy of oropharyngeal cancer. *Cancer Res.* **61**, 2911-6.

Hockel, M. and Vaupel, P. (2001). Tumor hypoxia: definitions and current clinical, biologic, and molecular aspects. *J. Natl Cancer Inst.* **93**, 266–76.

Narbonne, P. and Roy, R. (2009). Caenorhabditis elegans dauers need LKB1/AMPK to ration lipid reserves and ensure long-term survival. *Nature* **457**, 210–4.

Unruh, A., Ressel, A., Mohamed, H. G., Johnson, R. S., Nadrowitz, R., Richter, E., Katschinski, D. M. and Wenger, R. H. (2003). The hypoxia-inducible factor-1 alpha is a negative factor for tumor therapy. *Oncogene.* **22**, 3213-20.

Xie, M. and Roy, R. (2012). Increased levels of hydrogen peroxide induce a HIF-1-dependent modification of lipid metabolism in AMPK compromised C. elegans dauer larvae. *Cell Metab.* **16**, 322-35.

Xu, N., Zhang, S. O., Cole, R. A., McKinney, S. A., Guo, F., Haas, J. T., Bobba, S., Farese, R. V. Jr. and Mak, H. Y. (2012). The FATP1-DGAT2 complex facilitates lipid droplet expansion at the ER-lipid droplet interface. *J Cell Biol.* **198**, 895-911.